Thermal simulation of Passive Downdraught Evaporative Cooling (PDEC) in non-domestic buildings

David Martinez

Thermal Simulation of Passive Downdraught Evaporative Cooling (PDEC) in non-domestic buildings

David Martinez Ing. Ind.(elec) MCITI

A thesis submitted in partial fulfilment of the requirements of the De Montfort University for the degree of Doctor of Philosophy

July 2000

Institute of Energy and Sustainable Development
De Montfort University Leicester

To my parents, for their encouragement and support during these four years

Abstract

Sustainable development has been established as a goal in many countries. The use of fossil fuels is resulting in pollution of the atmosphere. Energy demand has increased in recent years with a resultant increase in the need to produce energy. Several things can be done including producing cleaner energy or using less energy or even both. Ventilation and air conditioning systems consume 30% of all the energy consumed in Europe. Naturally ventilated buildings have been successfully developed and could significantly reduce environmental emissions. One of these strategies is Passive Downdraught Evaporative Cooling (PDEC). This system is based on the evaporative cooling effect achieved when evaporating microscopic droplets into an air stream of dry hot air. It has been demonstrated that PDEC works. In order to promote and increase its use, however, PDEC must be supported by adjusting some factor in the results equation, such as climate selection or targeted comfort levels.

This research has aimed to evaluate strategies for modelling and controlling PDEC using thermal simulation programs. It has established the outdoor conditions for which the PDEC system is able to maintain acceptable indoor thermal conditions. The potential of other low energy cooling techniques was investigated and the local thermal comfort conditions in PDEC buildings were assessed.

The research reported here has focused on different fields including psychrometry to verify chart and formulae and climate to analyse what has been done and what can be done. The graphical and analytical study developed by counting the number of hours per year in the different psychrometric zones, together with the new developed comfort envelopes, resulted in renewed research opportunities for the study. It has been demonstrated that buildings have different behaviours which can affect the cooling technique selected. Therefore, people have to be educated if comfort levels are to be maintained in buildings.

The thermal modelling studies were considered in two stages: an initial simplified model and then a more complex model based on the conclusions obtained from the first model. These models were applied over a range of different cooling scenarios. The simplified model represented a slice of a typical PDEC building. It did not have an associated air flow network and the ventilation rates were fixed. The scenario simulated was night cooling with natural ventilation during the day and the coupling of the PDEC cooling device when required. This model produced results that showed that the graphical and analytical study developed made sense. The second, more complex, model analysed three scenarios: natural ventilation, natural ventilation plus night cooling and then the addition of PDEC. It also included a heat and mass flow network. The results from this model allowed an estimate of the cooling boundaries depending on the internal gains and the building mass chosen.

The main results from the research are that the use of a simplified psychrometric chart to plot climatic data is an improvement over traditional cartesian plots. Extended comfort envelopes have been established. By considering the adaptive behaviour of occupants, these new extended comfort envelopes can be enlarged further, sometimes by as much as 2K. PDEC is greatly influenced by air speed and this in turn affects thermal comfort. This also affects the balance between PDEC and non-PDEC operation in a building. If the implementation of PDEC into a building is not effectively controlled, occupant comfort levels could move outside the comfort envelope. This is an important consideration.

The thesis shows that PDEC is a natural cooling technique which works effectively. If the results of the research can be formulated into a simple analysis tool, perhaps the use of PDEC systems will become a standard consideration at the design stage of a building. The new boundaries for natural cooling techniques developed are also an important factor to consider for early stage design.

Acknowledgements

This research was financed by an EPSRC studentship and supported in its last year by the Research Unit and the Institute of Energy and Sustainable Development (IESD) at De Montfort University in Leicester.

I would like to thank my director of studies, Prof. Kevin Lomas for his support and guidance, to my early supervisor who helped me during the first stages of this research, Mr. Herbert Eppel, and to those who supervised the work until the completion of this thesis, Dr. Darren Robinson and especially Dr. Malcolm Cook.

I would like to thank all the staff at the IESD (especially Dr. Dusan Fiala, Dr. John Mardaljevic, Mr. Paul Cropper and Mr. Stuart Gadsden) for their support encouragement and assistance with various issues.

I could not forget to thank Prof. Neil Bowman who sadly passed away during the preparation of this thesis.

Nomenclature

p_{ws} = saturation pressure [Pa]

T = absolute temperature [°K]

p_{ss} = saturated vapour pressure [kPa]

t = temperature [$°C$]

g_{ss} = (moisture content of a mixture of air and saturated water) vapour [kg/kg]

f_s = enhancement factor [-]

p_{ss} = saturation vapour pressure of water vapour in the mixture [kPa]

ϕ = Relative Humidity [%]

p_s = partial vapour pressure of water vapour in moist air [kPa]

p_{ss} = partial pressure of saturated water vapour [kPa]

p_s = partial pressure of water vapour mixed with dry air [kPa]

p'_{ss} = saturated vapour pressure at wet bulb temperature [kPa]

p = barometric pressure of an air water vapour mixture [kPa]

A = constant depending on measuring method and temperature [K^{-1}]

t = dry bulb temperature [°C]

t' = wet bulb temperature [°C]

M = metabolic rate [W]

C_v = convection heat loss [W]

C_d = conduction heat loss [W]

E = evaporation heat loss [W]

ΔS = change in heat stored [W]

E_{diff} = due to vapour diffusion through the skin [W]

E_{rsw} = due to evaporation of regulatory sweating from the skin [W]

E_{resp} = respiration latent heat loss [W]

ρ_a = vapour pressure of ambient air [Pa]

t_a = Ambient temperature [$°C$]

h_r = radiation conductance (from surface to MRT)[W/m^{2}K]

h_c = convection conductance (from surface to air)[W/m^{2}K]

h_{cl} = clothing conductance [W/m^{2}K]

h_e = evaporation heat loss conductance [W/m^{2}kPa]

ρ_{sk} = saturation vapour pressure at mean skin temperature [kPa]

ρ_a = vapour pressure of ambient air [kPa]

F_{pcl} = vapour permeation efficiency from skin through clothing [-]

f_{cl} = the fraction of body clothed [-]

F_{cl} = insulation value of clothing= $(1/(1 + 0.155hI_{cl}))$

L = dry respiration loss [W]

K = heat transfer from skin to clothing surface [W]

R = radiation loss [W]

C = convection loss [W]

λ = latent heat of evaporation of water [575 kcal/kg]

m = permeance of skin [6.1x10^{-4}kg/h m^{2}mmHg]

ρ_s = saturation vapour pressure at skin temperature [mmHg]

ρ_a = vapour pressure of ambient air [mmHg]

V = pulmonary ventilation rate, (found as 0.006 M)

RH_{ex} = humidity ratio of air as exhaled [-]

RH_{in} = humidity ratio of air as inhaled [-]

λ = latent heat of evaporation of water [J/Kg]

I_{cl} = insulation of clothing [clo]

t_s = skin temperature [K]

t_{cl} = clothing surface temperature [K]

ε = emmitance of outer surface of clothing [-]

σ = the Stefan-Bolzmann constant [W/m^{2}K^4]

t_{cl} = temperature of outer surface of clothing [K]

t_r = mean radiant temperature [K]

q''_{evap} = latent energy lost by evaporation [W]

q''_{conv} = sensible energy from the gas by convection [W]

q''_{add} = energy added by other means [W]

ρ_a = air density $[kg/m^3]$

ρ_w = water density $[kg/m^3]$

g = gravity acceleration $[m/s^2]$

f = friction factor [-]

v = relative velocity drop air $[m/s]$

R = drop radius $[m]$

C_{pw} = specific heat of water at constant pressure $[J/kg \cdot °K]$

T = temperature $[°K]$

T_d = drop temperature $[°K]$

T_∞ = ambient temperature $(°K)$

h = convective heat tranfer coefficient $[W/m^2]$

h_{fg} = latent heat of vaporisation $[J/kg]$

Acronyms

ASHRAE	American Society of Heating and Air Conditioning Engineers
MC	Mechanical Cooling
NC	Night Cooling
NV	Natural Ventilation
PDEC	Passive Downdraught Evaporative Cooling
NV+ Lat.	Natural Ventilation plus latent (dry the air)
MC+ Lat.	Mechanical Cooling plus latent (dry the air)

Contents

Figures

Chapter 2. *Psychrometry*

Chapter 3. *Climate Analysis*

Chapter 4. *Thermal Comfort*

Chapter 5. *Passive Downdraught Evaporative Cooling*

Chapter 6. *Thermal Simulation Analysis. Model I*

Chapter 7. *Thermal Simulation Analysis. Model II*

Chapter 8. *Discussions of results and suggestions for further work*

Tables

Chapter 2. *Psychrometry*

Chapter 3. *Climate Analysis*

Chapter

1 *Introduction*

"Each problem that I solved became a rule which served afterwards to solve other problems."

RENE DESCARTES

1.1 Background

Sustainable development has been formally established as a policy goal at international levels. Environmental degradation has been increasing over the past 40 years (Pepper, 1985). Buildings contribute to approximately one third of CO_2 emissions (Roodman & Lenssen, 1995). A survey of over 1000 public and commercial buildings in Greece (Santamouris, 1992) has shown that typical annual energy consumption in non air conditioned buildings is up to 44% lower than in the air conditioned ones (from 140 kWh/m^2 to 226-250 kWh/m^2 respectively). Similar trends could be expected for other countries with similar climates. Assuming that electricity is the predominant energy source for air conditioning, which in primary energy terms is far more environmentally significant than direct fossil fuel combustion, the application of passive cooling techniques is a significant vehicle for reducing environmental emissions.

This reduction will help within the accepted plans of the United Nations (Agenda 21), the European Union (the Fifth Environment Action Plan: Towards Sustainability) and the EC's White Paper on Economic Growth, Employment and Competitiveness.

Passive Downdraught Evaporative Cooling (PDEC) is an energy efficient system which can be used to ventilate and cool buildings in hot, dry climates. It combines the benefits of a natural ventilation strategy with a passive cooling technique. Natural ventilation relies on existing air forces and density differences to move air through the building (Bahadori, 1985), and can contribute to a sustainable environment by reducing the electrical energy used in buildings. It not only reduces (or eliminates) the need for electrical energy to operate chillers, but even more significantly, it reduces the need for electricity to drive fans and pumps. Most naturally ventilated buildings imply narrower plans allowing the utilisation of daylight, thereby also reducing electrical demand for lighting (Hastings, 1994). The passive cooling effect is achieved by evaporating microscopic drops of water into a hot, dry airstream using micronisers (Rodriguez et al., 1991). Due to the absorption of the water drops by the air, the relative humidity and density increase and the dry-bulb temperature is reduced (Alvarez et al., 1991).

The experimental demonstration of the technical feasibility of PDEC (Cunningham & Thompson, 1986) in Arizona, and subsequent verification of consistent results (Givoni, 1991) has revealed both technical benefits (avoidance of fans, chillers, duct work, etc.) and some of the limitations (large supply and exit shafts, open interior of building) of PDEC. Further investigations (Alvarez, 1992) for Expo'92 has led to development of simulation tools to model aspects of PDEC. A concise summary of previous work is contained in a recent paper by Ford and Hewitt (1996).

1.2 The PDEC project

In 1996, De Montfort University with some other European partners embarked on a three year EC-funded project. Under the JOULE framework (component of the Research Technological Development, RTD, Non-Nuclear Energy programme, NNE) the Institute of Energy and Sustainable Development (IESD), initiated a project entitled "The application of Passive Downdraught Evaporative Cooling in non-domestic buildings" (Bowman et al., 2000). Some of the key aims of this project were (i) illustrate the energy and environmental benefit of PDEC designs for Southern Europe and adjacent regions, (ii) quantify and compare the overall energy demands of PDEC and non-PDEC buildings, (iii) assess the local thermal comfort conditions in PDEC buildings.

The research reported in this thesis was undertaken in parallel with the PDEC project but followed a somewhat different path based on sucessive findings.

1.3 Aims of this research

PDEC environments are characterised by high relative humidities, increased air speeds and, due to the free running nature of passively controlled buildings, a range of temperature fluctuations (Fiala, et al., 1999). In order to determine whether a building with PDEC will be comfortable, four issues need to be considered: (i) the local climate conditions, (ii) the thermal behaviour of the building and PDEC system, (iii) the resultant effect on indoor climate conditions, and (iv) the behaviour of the occupants (Martinez et al., 2000).

The main aims of this research were as follows:

- To evaluate strategies for modelling and controlling PDEC using thermal simulation programs.

- To establish the outdoor conditions, for which the PDEC system is able to maintain acceptable indoor thermal conditions, based on the interaction of a climate-based assessment strategy, new comfort envelopes, and the building performance.
- By using the new analysis method, to establish the potential of other low energy cooling techniques, or combinations of techniques, developed in this research.
- To assess the local thermal comfort conditions in PDEC buildings.

Although the research will focus on the PDEC system and its suitability in hot and dry climates, the results can also be used to analyse the possibilities of using other low energy techniques in locations with less severe climatology.

1.4 Thesis contents

The thermal studies of this research are supported by solid foundations in the fields of psychrometry, climate analysis and thermal comfort. Graphical analysis of climate and comfort conditions can be studied by representing the data on a psychrometric chart. Each one of these has been allocated a separate chapter, in which the individual findings are documented.

The psychrometry issues are outlined in Chapter 2. Here the validation of a simplified psychrometric chart based on the CIBSE formulation is presented. This cartesian chart is going to be the main tool used to plot most of the simulation results. The need for accuracy is essential. It is shown that the simplified chart is sufficiently accurate in the region of interest in this study. The conversion programs developed to deal with the data from the simulation results and climatic data are also validated.

A climate analysis study was carried out and is shown in Chapter 3. This ranged from the very basic analysis of climate with monthly averages, to developing cumulative frequency and frequency distribution graphs for hourly data. It was found that by plotting climate data on the psychrometric

chart (hourly values) a very accurate analysis could be carried out. This method also facilitates a study of the interaction between different elements such as dry bulb temperature and relative humidity. The definition of boundaries that describe different cooling techniques could lead to, by counting the number of hours per envelope, the most suitable technique or combination of techniques suitable for a certain location. This count of the number of hours could be compared with factors such as the overheating design criteria which allows a certain number of overheating hours per year, which benefits the passive cooling technique.

It is the aim to maintain indoor climate conditions within certain thermal comfort boundaries. Comfort envelopes are the main technique for architects and designers to measure the success of certain ventilation and/ or cooling systems. Free-running buildings, such as naturally cooled/ ventilated ones, are subject to a wide range of internal variations, depending on external conditions. Using existing comfort envelopes to examine a PDEC building will almost certainly lead to discomfort predictions. The need for revised comfort envelopes is therefore investigated in Chapter 4.

A state-of-the-art thermal simulation model has been used to develop new comfort envelopes, based on the well-documented adaptive behaviour theory (Baker & Standeven, 1996). The effect of increasing local air speeds by switching on small fans is investigated. Also, the variation in clothing levels, maintaining summer customs, but changing fabrics or garments has been taken into account. User-controlled shading devices such as blinds or louvres which allow regulating the amount of radiation filtered into the occupied zones have also been considered. Extended comfort envelopes have been derived based on this study, showing comfortable environment for a larger range of conditions.

Chapter 5 collects the material related to the PDEC building itself. It presents the literature review carried out for this research, and explains the main concerns about the system. It describes the physical basis such as heat and mass transfer and the evaporative cooling effect. It presents the PDEC building and its operational modes along with some of the findings of the PDEC project.

The thermal studies have been divided into two chapters: an initial simplified model and a more complex model which was developed based on the conclusions obtained from the previous model. The first thermal model and its results are outlined in Chapter 6. This model represents a slice of a typical PDEC building. It does not have an associated air flow network, and the ventilation rates are fixed. The scenario simulated is night cooling with natural ventilation during the day, and the coupling of the PDEC cooling device when needed. This cooling device, was accomplished by fixing a zone temperature with the equivalent to the 70% wet bulb temperature depression of the external dry bulb temperature via a boundary file. This emulates the temperature reduction achieved by the evaporative cooling process. The model behaviour has been studied by analysing several combination of internal gains with building mass values. This simple model, served to establish the basis of a more complex model. It also gave an orientation of the location of the psychrometric boundary that separates PDEC from mechanical cooling, along to the wet bulb temperature axis. It raised the need for studying the different cooling scenarios separately.

Chapter 7 is dedicated to the second thermal model. This is a significantly more complex approach, even thought it only represents a slice of a PDEC building. It is modelled to produce the natural ventilation effect and generate the airflows required, this is reflected in the new geometry. There is also a larger number of zones. This second model has a heat and mass flow network implemented, and a control system that facilitates the operation of the different scenarios: natural ventilation, natural ventilation with night cooling and natural ventilation plus night cooling with PDEC for

the warmer hours of the day. The model still emulates the cooling effect by linking one zone to the 70% wet bulb temperature depression of the outside dry bulb temperature. Results of this chapter led to a estimate of the position of the cooling boundaries depending on the internal gains and building mass.

Chapter 8 outlines the suggestions and further work and Chapter 9 summarises the conclusions derived from the study.

Chapter

2 *Psychrometry*

"Truly great madness can not be achieved without significant intelligence"

HENRIK TIKKANEN

2.1 Preamble

This chapter deals with psychrometry issues. It outlines the different methods and strategies for determining the psychrometric expressions and presents the formulae used in this research. It gives the CIBSE (Chartered Institution of Building Service Engineers) and ASHRAE (American Society of Heating, Refrigeration and Air conditioning Engineers) psychrometric charts and presents their differences. The chapter also explains the assumptions made for generating the simplified psychrometric chart which was used for displaying the data in this study. The chapter ends with the measurements taken that validate the new chart and formulae used.

2.2 Basic psychrometry

Psychrometry (from the Greek "psychros" [cold] and "metro" [measure] is the study of the mixture of air and water vapour in the atmosphere. *Atmospheric air* contains a large number of gaseous constituents, as well as water vapour

and miscellaneous contaminants i.e. smoke, pollen, gaseous pollutants, etc. *Dry air* exists when all water vapour and contaminates have been removed from atmospheric air. Extensive measurements have shown that the composition of dry air is relatively constant (Goff, 1949; Chaddock, 1965), but small variations in the amounts of individual components occur with time, geographical location and altitude. *Moist air* is defined as a binary mixture of dry air and water vapour. The amount of water vapour in moist air varies from zero (dry air) to a maximum which depends on temperature and pressure. All psychrometric properties are expressed at a particular barometric pressure. Temperature and barometric pressure of atmospheric air vary considerably with altitude as well as with geographical and weather conditions. The standard barometric pressure, by international agreement, is 101.325 kPa. This value is used by the Chartered Institution of Building Service Engineers (CIBSE), the American Society of Heating, Refrigeration and Air conditioning Engineers (ASHRAE) and most of the other major authorities.

2.3 The psychrometric chart

A psychrometric chart is a graphical representation of the thermodynamic properties of moist air. The chart is of practical value in solving problems concerned with thermodynamic processes.

The choice of coordinates for a psychrometric chart is arbitrary. Every condition can be uniquely represented by two parameters, from which any other variable can be obtained. Different formulation of the measured psychrometric conditions exists. There are also different techniques for generating the psychrometric chart.

2.3.1 Psychometric parameters

The different parameters that are present in the psychrometric chart are introduced next. Note that for the *partial pressure*, both formulating

techniques, CIBSE and ASHRAE are included to illustrate the differences mentioned above.

2.3.1.1 Partial pressure of water vapour

The partial pressure of water vapour (vapour pressure) in the atmosphere is linearly related to absolute humidity (*AH*). The vapour pressure is shown in a scale alongside the *AH* scale. This term depends on temperature alone. Formulation of this parameter differs from ASHRAE (Eq 2-1,Eq 2-2) and CIBSE (Eq 2-4, Eq 2-3). Note that even the nomenclature changes: p_{ws} for ASHRAE and p_{ss} for CIBSE.

For ASHRAE, the saturation vapour pressure over ice for the temperate range of -100 °C (-148F) to 0°C (32F) is given by

$$\ln(p_{ws}) = C_1/T + C_2 + C_3T + C_4T^2 + C_5T^3 + C_6T^4 + C_7\ln(T) \qquad \textbf{(2-1)}$$

where:

C_1 = −5674.5359

C_2 = 6.3925247

C_3 = −0.9677843 x 10^{-2}

C_4 = 0.62215701 x 10^{-6}

C_5 = 0.20747825 x 10^{-8}

C_6 = −0.9484024 x 10^{-12}

C_7 = 4.1635019

The saturation vapour pressure over liquid water for the temperature range of 0°C (32F) to 200°C (392F) is given by:

$$\ln(p_{ws}) = C_8/T + C_9 + C_{10}T + C_{11}T^2 + C_{12}T^3 + C_{13}\ln(T) \qquad \textbf{(2-2)}$$

where

$C_8 = -5800.2206$

$C_9 = 1.3914993$

$C_{10} = -0.04860239$

$C_{11} = 0.41764768 \times 10^{-4}$

$C_{12} = -0.14452093 \times 10^{-7}$

$C_{13} = 6.5459673$

In both equations, 2-1and 2-2,

p_{ws} = saturation pressure (Pa)

T = absolute temperature (°K)

These expressions are based on equations calculated by Hyland & Wexler (1983) which were developed to give a close agreement with the experimental results obtained by Stimson (1969) and Guildner et. al. (1976).

For CIBSE, the value of the saturation pressure over ice is given by data obtained by the National Bureau of Standards (NBS), (1955) and can be expressed as:

$$\log p_{ss} = 12.5380997 - 266391/(t + 273.15) \quad \textbf{(2-3)}$$

For Eq 2-4 and Eq 2-3

p_{ss} = saturated vapour pressure (kPa)

t = temperature ($°C$)

The value of the saturation pressure over liquid water is based on empirical work by the National Engineering Laboratory (NEL), (1964) and is:[1]

$$\log p_{ss} = 30.59051 - 8.2\log(t + 173.16) + 0.0024804(t + 273.16) - 3142.31(t + 273.16)^{-1} \quad \textbf{(2-4)}$$

1. The NEL equation is expressed in relation to the triple point of water (+0.01°C), not 0°C.

Note that from now on, only the CIBSE equations will be presented, since they are the ones used for further calculations.

2.3.1.2 Moisture content

The horizontal axis of the psychrometric chart is *dbt* (dry bulb temperature) measured in °C, and the vertical axis is moisture content or *AH* (Absolute Humidity), measured in g/Kg, i.e. grams of moisture (water vapour) per Kg of dry air. Some graphs show this quantity expressed as an Humidity Ratio (*HR*), a non-dimensional parameter (kg/kg). The equation that describes it is:

$$g_{ss} = \frac{0.62197 f_s p_{ss}}{101.325 - f_s p_{ss}} \qquad \textbf{(2-5)}$$

where

g_{ss} = (moisture content of a mixture of air and saturated water) vapour (kg/kg)

f_s = enhancement factor (-)

p_{ss} = saturation vapou pressure of the water vapour in the mixture (kPa)

The values used for f_s used in CIBSE psychrometric tables (CIBSE, 1975) are based on the following three equations developed by Goff (1949)

$$\begin{aligned} t < 11° \qquad & f_s = -0.0000073t + 1.00444 \\ 11° \le t < 26° \qquad & f_s = 0.0000132t + 1.004205 \\ 26° \le t \le 60° \qquad & f_s = 0.0000405t + 1.003497 \end{aligned} \qquad \textbf{(2-6)}$$

where

t = temperature (°C)

2.3.1.3 Relative humidity

At any temperature the air can support only a given amount of water vapour. This, represented as the top curve of the chart despicts the saturation humidity. It also corresponds with the 100% relative humidity curve. Relative humidity (*RH*) is commonly defined as the ratio of the

partial pressure of superheated water vapour in moist air at a certain temperature to the partial pressure of saturated water vapour at the same temperature:

$$\phi = \frac{p_s}{p_{ss}} \times 100 \qquad \textbf{(2-7)}$$

where

ϕ = Relative Humidity (%)
p_s = partial vapour pressure of water vapour in moist air (kPa)
p_{ss} = partial pressure of saturated water vapour (kPa)

RH curves follow a hyperbolic shape between the *dbt* (dry bulb temperature) axis and the *mc*, usually in 10% steps.

2.3.1.4 Wet bulb temperature

Wet bulb temperature (*wbt*) is empirically determined by using a temperature sensitive element covered with a wetted sleeve (preferably with distilled water) and insulated from solar radiation. Two methods are adopted for measuring the *wbt*, one using some form of mechanical aspiration to achieve the air velocity over the sleeve and other using natural air movement. The barometric pressure, dbt and wbt are related by Apjhon (1838), the equation is shown in Eq 2-8.

$$p_s = p'_{ss} - pA(t - t') \qquad \textbf{(2-8)}$$

where

p_s = partial pressure of water vapour mixed with dry air (kPa)
p'_{ss} = saturated vapour pressure at wet bulb temperature (kPa)
p = barometric pressure of an air water vapour mixture (kPa)
A = constant depending on measuring method and temperature(K^{-1})
t = dry bulb temperature (°C)
t' = wet bulb temperature (°C)

In saturated air no evaporation occurs. The dry bulb temperature and the wet bulb temperature readings are identical. They meet at the 100%

relative humidity curve (saturation curve). The wet bulb temperature lines have a slope given by:

$$\frac{\Delta AH}{\Delta t} = \frac{-1000}{2501 + 1.805t + 4.186t'} \quad \textbf{(2-9)}$$

2.3.1.5 Specific volume

The specific volume (v) of the air water mixture, measured in m^3/Kg is the reciprocal of the density. It is indicated by another set of slightly sloping lines on the psychrometric chart. This value is useful for the conversion of volumetric flow quantities into mass flow rates, but not relevant to this study.

2.3.1.6 Specific enthalpy

Enthalpy (h) is the heat content of unit mass of the atmosphere, in KJ/ kg, relative to the heat content of 0^oC dry air. It has two components, sensible heat (due to the temperature) and latent heat due to the presence of water vapour in the air. The enthalpy lines in the psychrometric chart have a gradient very close to wet bulb temperature slope, Eq 2-10.

$$\frac{\Delta AH}{\Delta t} = \frac{-1000}{2501 + 1.805t} \quad \textbf{(2-10)}$$

2.4 ASHRAE Psychrometric Charts

These charts are based on Mollier (1954) studies. He was the first in using coordinates of enthalpy (h) and humidity ratio (W). This chart provides convenient graphical solutions to many moist air problems with minimum thermodynamic approximations. ASHRAE developed five Mollier-type psychrometric charts. The first three for sea level pressure and the others for 5000 and 7500 ft altitude. All charts use oblique angle coordinates of enthalpy and humidity ratio and are consistent with the properties computation methods of Goff & Gratch (1945). Figure 2-1 shows the psychrometric chart numbered as 1, where temperature covers a range from 32 F to 120 F.

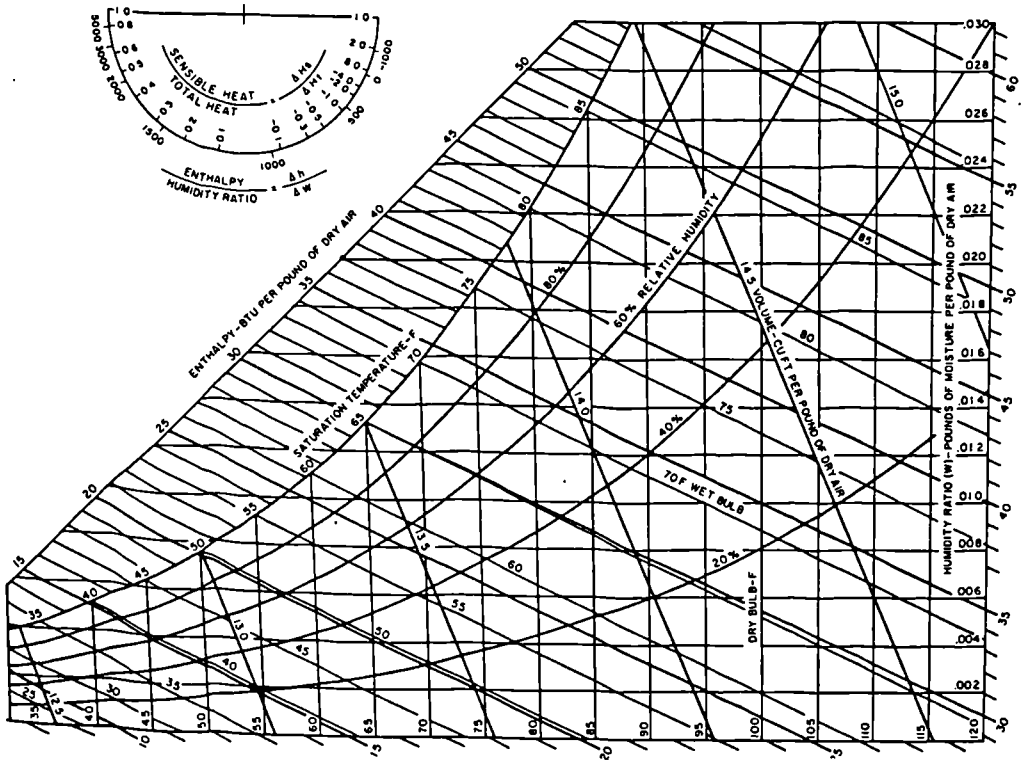

Figure 2-1. ASHRAE psychrometric chart number 1.

After ASHRAE 1981 Fundamentals

These graphs were initially developed for conventional U.S. units. Charts based on SI metric units appeared afterwards.

2.5 CIBSE Psychrometric Charts

These charts has been constructed using specific enthalpy (h) and moisture content (g_{ss}) as the coordinate system. The 30°C dry bulb line has been constructed at right angles to the lines of constant moisture content and the scale of specific enthalpy inclined obliquely to the vertical scale of moisture content. In this way, lines of constant dbt are approximately vertical, diverging slightly each side of 30°C.

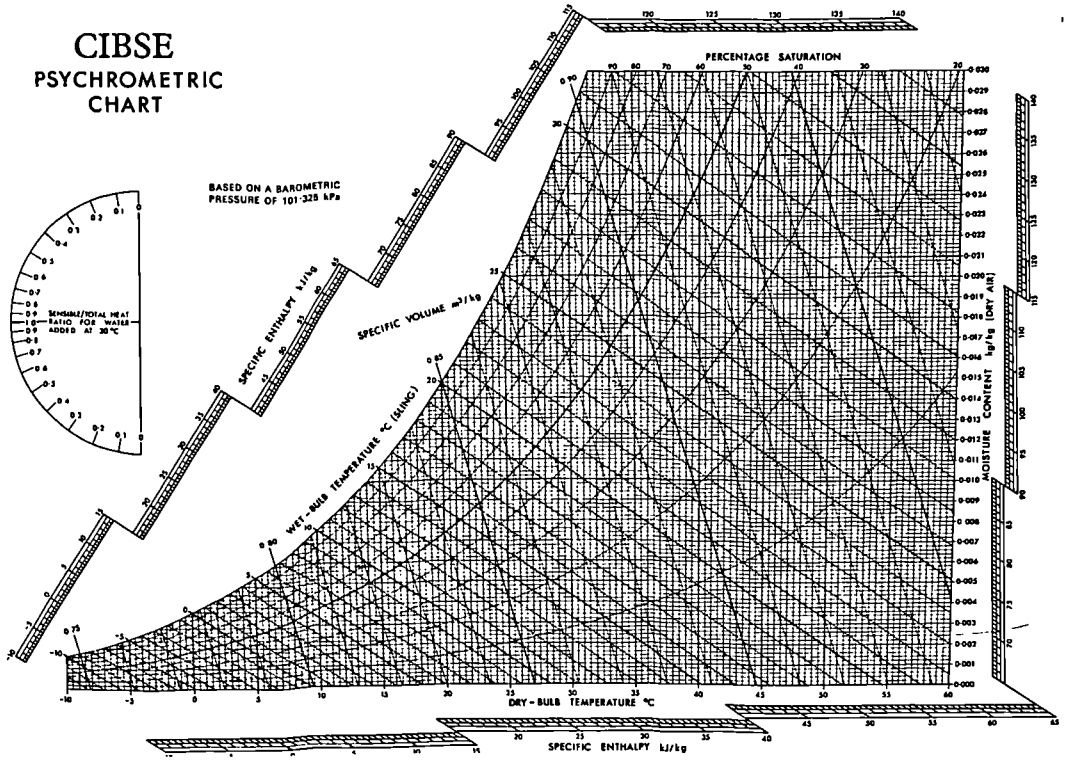

Figure 2-2. CIBSE psychrometric chart (-10°C to 60°C)

After CIBSE Guide C

The wet bulb temperature values plotted correspond to those read from a sling (or ventilated) psychrometer. Lines of percentage saturation are plotted instead of relative humidity. The data used were calculated from the tables following methods of Goff and Gratch (1945).

In the central zone there are some differences between percentage saturation and relative humidity, these differences diminishes for more saturated or dry states.

2.6 Simplified psychrometric chart

A simplified psychrometric chart has been produced at the IESD (Institute of Energy and Sustainable Development, Cook and Cropper) to plot climate data as well as results obtained from thermal simulations. It is based on CIBSE psychrometric data and equations, Goff (1949). Only some of the parameters lines have been plotted i.e. dry bulb temperature, moisture content, wet bulb temperature and relative humidity.

The chart was constructed using dry bulb temperature and moisture content as horizontal and vertical axis respectively. This differs from the pure CIBSE chart, since temperature is not a perpendicular line. The process calculates p_{ss}, from Eq 2-4 and Eq 2-3, then calculates g_{ss} with Eq 2-5 and Eq 2-6 for different relative humidities. Wet bulb temperature has been obtained using Eq 2-7 and plotted for the limits of the saturation curve, resulting in a simplified graph (Figure 2-3).

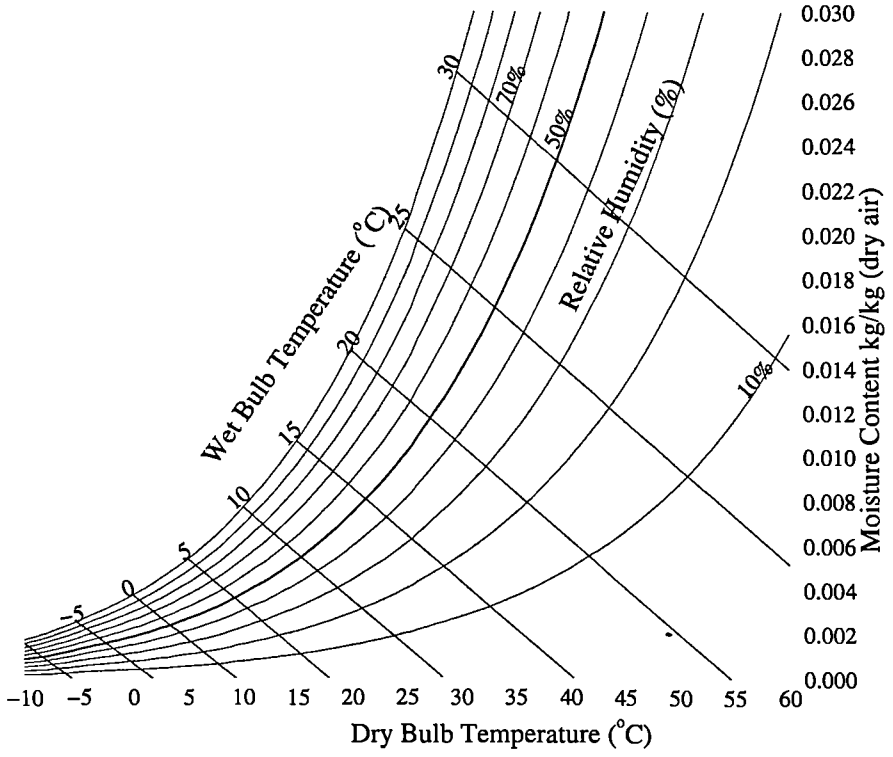

Figure 2-3. Simplified psychrometric chart

Developed at the IESD, De Montfort University

The simplified chart has been tested to determine its validity to display psychrometric data. It has been compared with the equivalent (-10°C-60°C) original CIBSE chart. Data of moisture content for different dbt's and relative humidities were measured in both cases. In Table 2-1 these values are shown.

Table 2-1. Moisture content measurement comparison between CIBSE and simplified psychrometric charts for given dbt's and relative humidities.

dbt (°C)	RH (%)	mc (CIBSE)	mc (simplified)	difference
15	30	0.0032	0.0032	0
	50	0.0054	0.0053	0.0001
	90	0.0096	0.0095	0.0001
30	30	0.0082	0.0082	0
	50	0.0137	0.0137	0
	90	0.0246	0.0246	0
40	30	0.0148	0.0148	0
	50	0.0246	0.0247	0.0001
55	20	0.0230	0.0232	0.0002

No differences are encountered for the central zone of the psychrometric chart. When moving away from the 30°C dbt line, and for high relative humidity values, some differences appear. This is due to the non-parallelism in the dbt lines in the original CIBSE chart. Nevertheless, the maximum difference observed of 0.0002 in moisture content was considered acceptable. This difference only appears with temperatures above 40°C, which infrequently happen in this study.

These findings confirmed that the simplified psychrometric chart, with dry bulb temperature lines perpendicular to the x-axis and moisture content lines perpendicular to the y-axis, was sufficiently accurate to plot the analysed data.

2.6.1 Formulae validation

The climatic and simulations result data used in this study has to had been transformed. The units in which the data was obtained were different to the ones required to plot the data. Complementary data had

to be calculated from the existing data. Because this, several FORTRAN programs where developed to carry out these tasks. All these programs, engaged the same formulae used to create the simplified psychrometric chart. Since the process and equations used for developing this chart have been satisfactory tested, is assumed that the formulae used in the FORTRAN programs are also corroborated.

2.7 Summary

Psychrometry is not a 100% accurate science. There are different mathematical approaches and different results depending on the method used (i.e. CIBSE, ASHRAE). Although these methods obtain close results, they are not identical, deriving in small differences in the generated charts.

The new simplified psychrometric chart developed has been tested. The comparison with its equivalent CIBSE chart shown that the new chart is accurate enough to serve the purposes. Maximum differences of 0.0002 Kg/Kg (less than 0.5% error) in moisture content serves to prove the validation. A series of new FORTRAN programs which deal with psychrometric issues have been developed and also validated.

Chapter

3 *Climate Analysis*

"Not everything that can be counted counts, and not everything that counts can be counted"

ALBERT EINSTEIN

3.1 Preamble

This chapter presents the work carried out related to climate analysis. It briefly describes climate and its elements and includes some guidelines to climate classification. It presents the analytical and graphical methods used to analyse climate. The chapter explains a method for subdividing the psychrometric chart into "cooling-techniques regions". It also includes a map of Southern Europe with the results obtained from processing the climate of several cities using this method.

3.2 Climate basis

Earth must remain in thermal equilibrium. The energy input provided by solar radiation is matched by the emission of low temperature radiation towards space. If this emission mechanism is impaired, such as by the effect of CO_2 and other "greenhouse" gases, the Earth's temperature will increase,

increasing the radiant emission, until a new equilibrium is established with that higher temperature.

Solar radiation is higher in equatorial regions than in polar regions due to (i) the fact that oblique incidence of a beam of radiation spread over a larger area results in a reduction in intensity, and (ii) the path of the solar radiation beam is longer at higher latitudes, most of it being absorbed by the atmosphere before reaching the surface. These are not the only factors that influence a certain climate, other include air mass flows, wind fronts, gravitational forces etc. together with location, proximity to the sea, rivers, mountains, and altitude constitute the basis of a location climate.

Climate can be defined as "the conditions of temperature, humidity, etc., prevailing in a region" (Oxford Dictionary). If weather is the particular state of the atmospheric conditions, climate is the integration in time of those conditions, representative of a certain location.

3.2.1 Elements of a climate

The climate of a given location is depicted by climatic data. These are measured values of climatic elements over a long period of time (10 years or more). Several variables are measured. Some such as barometric pressure are vital for meteorologists but irrelevant for other studies. For building design and human comfort, subjects of this research study, other variables are important, i.e. temperature, humidity, wind, solar radiation, etc.

Temperature: This is usually given as the dry bulb or "true air" temperature. Various sensors can be used with automatic data-logging equipment, but the most accurate is still the mercury in glass thermometer.

Humidity: This is most often expressed as relative humidity. Atmospheric humidity, which is the amount of water vapour or moisture in the air, is another leading climatic element, as is precipitation. All forms of precipitation, including drizzle, rain, snow, ice crystals, and hail, are produced as a result of the condensation of atmospheric moisture to form

clouds in which some of the particles, by growth and aggregation, attain sufficient size to fall from the clouds and reach the ground. The most reliable instruments to measure humidity are the wet and dry bulb thermometers.

Wind: Winds are available not only in terms of speed, but also in direction. Wind velocity is usually recorded in open, flat country at a height of 10 m (e.g. at airports). In urban areas the 10 m should be taken above the intermediate level of obstructions. Velocities near the ground (within the boundary layer), are lower than the free wind velocity. They depend on the depth of the boundary layer, which is a function of the terrain characteristics.

Solar Radiation: This is a very important parameter in climatic data. Most surfaces are not perpendicular to the Sun, and the energy they receive depends on the solar elevation angle (90º when the sun is directly overhead). This angle changes systematically with latitude, the time of year, and the time of day. Different components of the solar radiation might be used (the direct beam and the diffuse beam component) depending on the application for which the climate data is to be used

3.3 Climate classification

There is an almost unlimited number of different climates on Earth. Various attempts have been made to classify the climates of the earth into climatic regions. One notable example, is that of Aristotle's temperate, torrid and frigid zones[1]. However, the 20th century classification developed by German climatologist and amateur botanist Wladimir Köppen (1846-1940) continues to be the authoritative map of the world climates in use today.

1. In one of the first attempts at climate classification, the ancient Greek scholar Aristotle hypothesized that the earth was divided into three types of climatic zones, each based on distance from the equator.

3.3.1 Köppen-Geiger climate classification

Introduced in 1928 as a wall map (see Figure 3-1) and co-authored with student Rudolph Geiger, the Köppen system of classification was not updated and modified until his death. Since that time, it has been modified

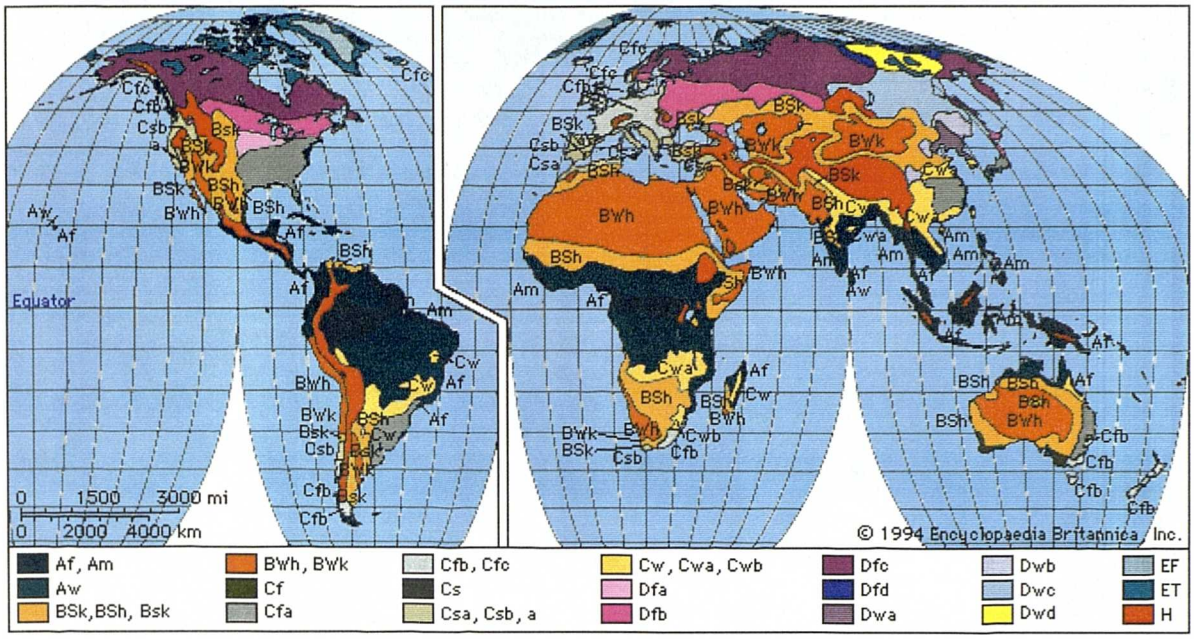

Figure 3-1. Köppen-Geiger climatic zones map.

(The legend is given by Table 3.1)

by several geographers. The most common modification of the Köppen system today is that of the late University of Wisconsin geographer Glen Trewartha. The modified Köppen classification uses six letters to divide the world into six major climate regions, based on average annual precipitation, average monthly precipitation, and average monthly temperature. Each category is further divided into sub-categories based on temperature and precipitation. For instance, the U.S. states located along the Gulf of Mexico are designated as "Cfa." The "C" represents the "mild mid-latitude" category, the second letter "f" stands for the German word *feucht* or "moist," and the third letter "a" indicates that the average temperature of the warmest month is above 22°C. Thus, "Cfa" gives us a good indication of the climate of this region, a mild mid-latitude climate with no dry season and a hot summer.

Table 3-1. Legend of the Köppen-Geiger system

A	**Tropical humid**	Af	Tropical wet	No dry season
		Am	Tropical monsoonal	Short dry season; heavy monsoonal rains in other months
		Aw	Tropical savanna	Winter dry season
B	**Dry**	BWh	Subtropical desert	Low-latitude desert
		BSh	Subtropical steppe	Low-latitude dry
		BWk	Mid-latitude desert	Mid-latitude desert
		BSk	Mid-latitude steppe	Mid-latitude dry
C	**Mild Mid-latitude**	Csa	Mediterranean	Mild with dry, hot summer
		Csb	Mediterranean	Mild with dry, warm summer
		Cfa	Humid subtropical	Mild with no dry season, hot summer
		Cwa	Humid subtropical	Mild with dry winter, hot summer
		Cfb	Marine west coast	Mild with no dry season, warm summer
		Cfc	Marine west coast	Mild with no dry season, cool summer
D	**Severe Mid latitude**	Dfa	Humid continental	Humid with severe winter, no dry season, hot summer
		Dfb	Humid continental	Humid with severe winter, no dry season, warm summer
		Dwa	Humid continental	Humid with severe, dry winter, hot summer
		Dwb	Humid continental	Humid with severe, dry winter, warm summer
		Dfc	Subarctic	Severe winter, no dry season, cool summer
		Dfd	Subarctic	Severe, very cold winter, no dry season, cool summer
		Dwc	Subarctic	Severe, dry winter, cool summer
		Dwd	Subarctic	Severe, very cold and dry winter, cool summer
E	**Polar**	ET	Tundra	Polar tundra, no true summer
		EF	Ice Cap	Perennial ice
H	**Highland**			

While the Köppen system does not take such things as temperature extremes, average cloud cover, number of days with sunshine, or wind into account, it is a good representation of the Earth's climate. With only 24 different sub classifications, grouped into the six categories, the system is easy to comprehend.

3.4 Climatic data

One of the problems with the large amount of information collected at meteorological stations is its interpretation and presentation for further analysis. Which data to select from several decades collected and how to present it: monthly averaged, daily or in an hourly basis, are common questions raised.

Initially, the intended use of the data must be established. For example, this may be (i) data to create a qualitative understanding of the climate, (ii) data to use with simple computer programs or for manual calculations, or (iii) detailed data to perform complex simulations.

3.4.1 Data for qualitative understanding

Graphic representations are particularly useful for this purpose. The "climate graph" developed by Koenigsberger in 1974 gives an idea of the climate at a glance, especially when comparing such graphs. These included monthly averages for rainfall, temperature, radiation and sunshine.

In an initial attempt to find correlations between climates (different climates and the different elements within one climate), similar graphs to the "climate graph" mentioned above were generated. Climatic data from the PASCOOL[2] project (Santamouris, 1997) of 18 Southern European capitals was used. Monthly averages for dry bulb temperature, relative humidity, and solar radiation, were plotted together for each location. An example of four of these graphs is shown in Figure 3-2.

By observing these graphs, can be outlined that the relative humidity tends to follow a negative sine-shape (Madrid, Geneva and many others not shown here) or a pseudo-flat line (Cagliari). This means that for these regions, in summer (Jun-Aug) the climate is drier than in winter, or about the same,

2. The PASCOOL project was a European founded project within the frame of the Joule II research programme. The main goal were to develop techniques, tools and guidelines to promote the use of passive cooling techniques in buildings and reduce the energy consumption for cooling purposes.

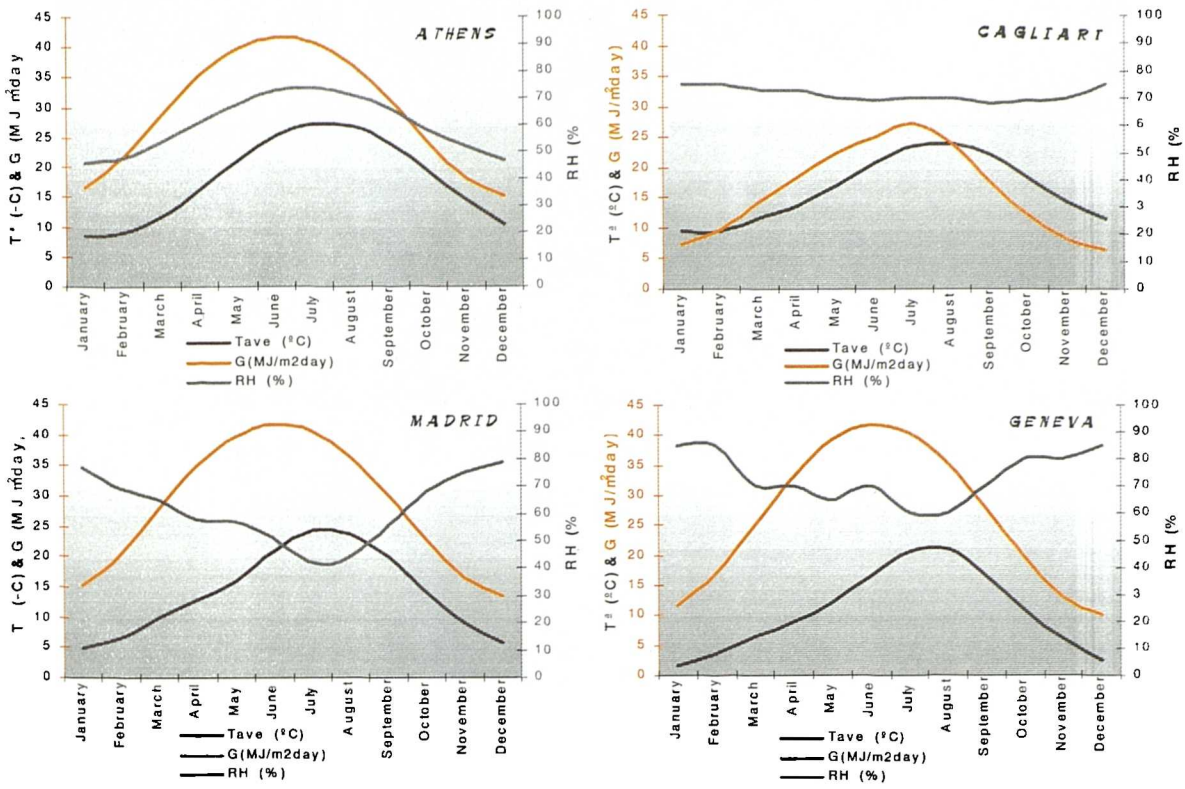

Figure 3-2. Monthly averages of four Southern European capitals

respectively. But looking at Athens, it is observed that its shape is not negative but positive, which means that summer is more humid than winter, which is unlikely to happen in a Mediterranean climate.

In order to find out the real shape of the relative humidity curve for Athens, the study was extended, and hourly data for the whole year was analysed. Using a more powerful plotting tool, two new graphs for Athens were produced: one for 24 hours data and another for the period 7am-7pm (daylight hours). The latter is reproduced in Figure 3-3. It is observed the expected negative sine-shape for relative humidity. The daily data was summarised using fourth degree regressions to get more easy-to-read lines. This lead to the conclusion that monthly averages were not reliable enough for this study.

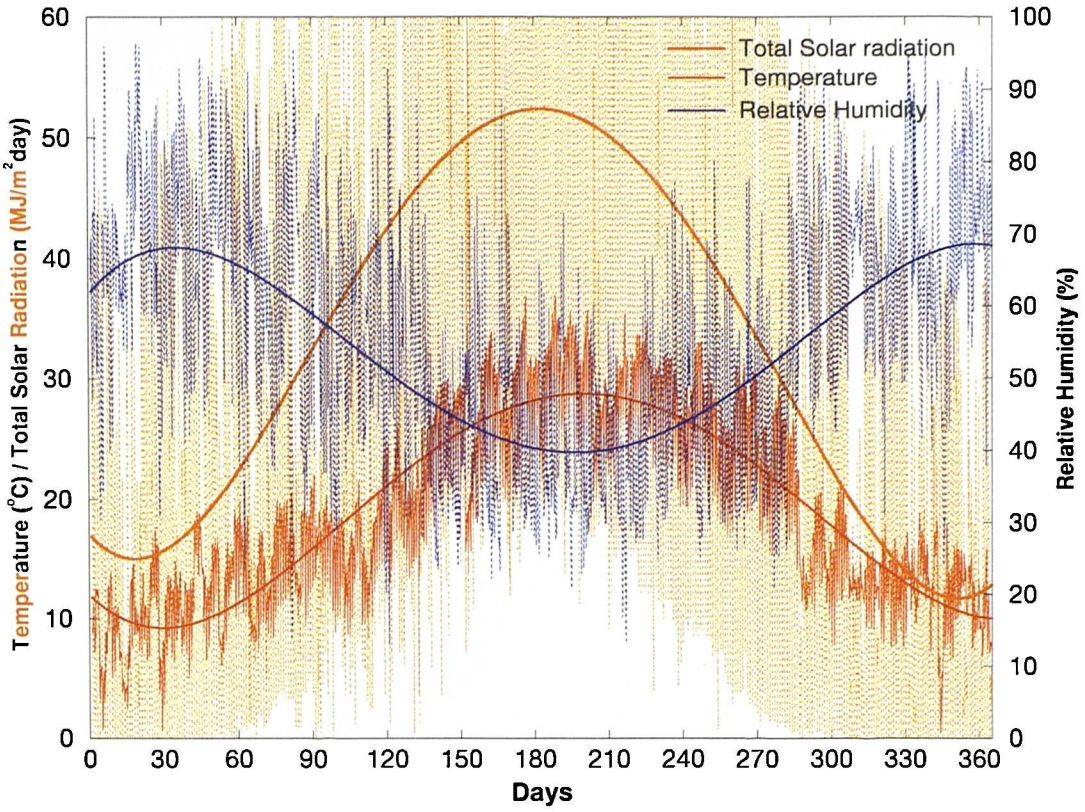

Figure 3-3. Athens whole year hourly data (7am-7pm) and 4th degree regressions

3.4.2 Data for simple calculations

This is a further step in climate data analysis is. There is a minimum amount of data required to perform these calculations. These calculations are performed by short programs or spread sheets with a database. Starting with the latitude, necessary for solar calculations, the following nine parameters can be provided for each month:

TMax	mean maximum temperature (°C)
sdMAX	standard deviation of daily maxima (K)
TMin	mean minimum temperature (°C)
sdMin	standard deviation of daily minima (K)
Tsd	standard deviation of the daily mean (K)
RHam	relative humidity (%) morning (6:00 or 9:00)
RHpm	relative humidity (%) afternoon (14:00 or 15:00)

Rain	rainfall total of the month (mm)
Irad	mean daily radiation (MJ/m^2 or Wh/m^2)

These data can be used as entry for simple calculation programs or to calculate mean temperature and standard deviation. These are useful to give an indication of the distribution and variability of temperatures and are used in the base degree-hour methods.

3.4.3 Data for computer simulations

There are many computer programs for the energy analysis of buildings. These programs use climate data to calculate, on an hourly or sub-hourly basis, a number of building performance parameters, such as energy use and air temperatures.

Since most sites can provide records of meteorological observations from previous years, one can always use the this data to create a "blended" year which can be used to represent those years. In the USA, this "blend" is referred as a TMY (Typical Meteorological Year), in Denmark as a DRY (Data Reference Year), in the UK as an "example weather year", in Germany as a "synthetic reference climate" and in the EU as a TRY (Test Reference Year), the term also adopted in Australia.

3.4.3.1 The Test Reference Year

Note that from now on, the European nomenclature (TRY) to describe the "blended" year will be used. A TRY should include the following properties:

- The sequence of meteorological data generated for a TRY should in some sense resemble the sequences registered at a given location.
- Relationships and correlation among the different series of a TRY should reflect the relationships and correlations observed in nature of the same series of measurements[3].

3. Although one can individually fit a set of data for meteorological measure with a stochastic model, the model still would not be realistic in a sense that the fitting would not account for the relationship among the variables.

- The series of meteorological data in a TRY should have a frequency distribution closely related to the long term distribution.

The procedure to generate a Test Reference Year is performed by comparing the Cumulative Distribution Function (CDF)[4] for each year with the CDF for the longer term comprising of all years used for the construction of TRY. The most common method of generation used is based on the technique of dividing the year into calendar months and the selection of the typical months by statistical methods from a period of several years. The comparison of the two CDFs gives an estimate of the proportion of values in the TRY less than or equal to a specified value and the closeness of each year's meteorological year to the long-term composite. For the comparison of the CDFs there are a number of statistical tools. One of them is the Finkelstein-Schafer (F-S) statistic comparing the closeness of each year's Typical Meteorological Summer (TMS) to the long-term composite.

A. Argiriou, (1999) carried out a study to compare the performance of different methods to generate TRYs. The study analysed the Sandia National Laboratories method (Bahadori and Chamberlain,1986; Marion and Urban, 1995; Petrakis et al., 1996) the Danish method (Lund, 1995) and the Festa and Ratto method (Festa and Ratto, 1993), in their original form and with some variations in the selection procedure. For comparison methods a TRY was also generated using simple averaging over the available period. The study used 20 years (1977-1996) producing 17 different TRY. The TRYs obtained were evaluated according to their impact on performance simulations for solar systems and the annual heating and cooling loads of a typical building. The results showed that the TRY giving the closest performance to the average performance of the systems as predicted using the 20-year weather data is the modified Festa-Ratto method.

4. The Cumulative Distribution Function (CFD) or more simply the distribution Function F of the random variable X, is defined for all real numbers $b, -\infty < b < \infty$, by $F(b) = P\{X \leq b\}$. In words $F(b)$ denotes the probability that the random variable X, takes a value less than or equal to b.

Any of the seventeen produced TRY could have been used for simulation purposes, producing seventeen different sets of results. These results could have led to the adoption of an oversized cooling system, if the hotter TRY is taken, or to an unrealistic natural cooling technique if using the cooler TRY. This study reflects the lack of standardization in this matter.

3.5 Climate study

3.5.1 Analytical study

By the previous sections can be deduced that further climatic studies must be carried out based on an hourly basis data. One of the methods of analysis is by analytical study. The most commonly used of these studies is by performing cumulative studies. In an attempt to compare results for the different climates available in hourly format, cumulative frequency and frequency distribution values were calculated for the whole year and summer time using data from the PASCOOL project for some Southern European cities.

Cumulative frequency is represented by a decreasing line, with the total number of hours as origin (y-axis) and the analysed parameter value exceeded in that time until reach 0. Frequency distribution shows the total number of hours between selected bins for the analysed parameters. The graphs were produced for relative humidity, solar radiation and dry bulb temperature. The periods (whole year and summer) were re-divided in 24 hours and occupancy time. Figure 3-4 shows an example for Seville for the period of the whole year.

These graphs, although very interesting, do not provide relationships between different conditions such as relative humidity, dry bulb temperature or solar radiation. Another method to analyse climate must therefore be used.

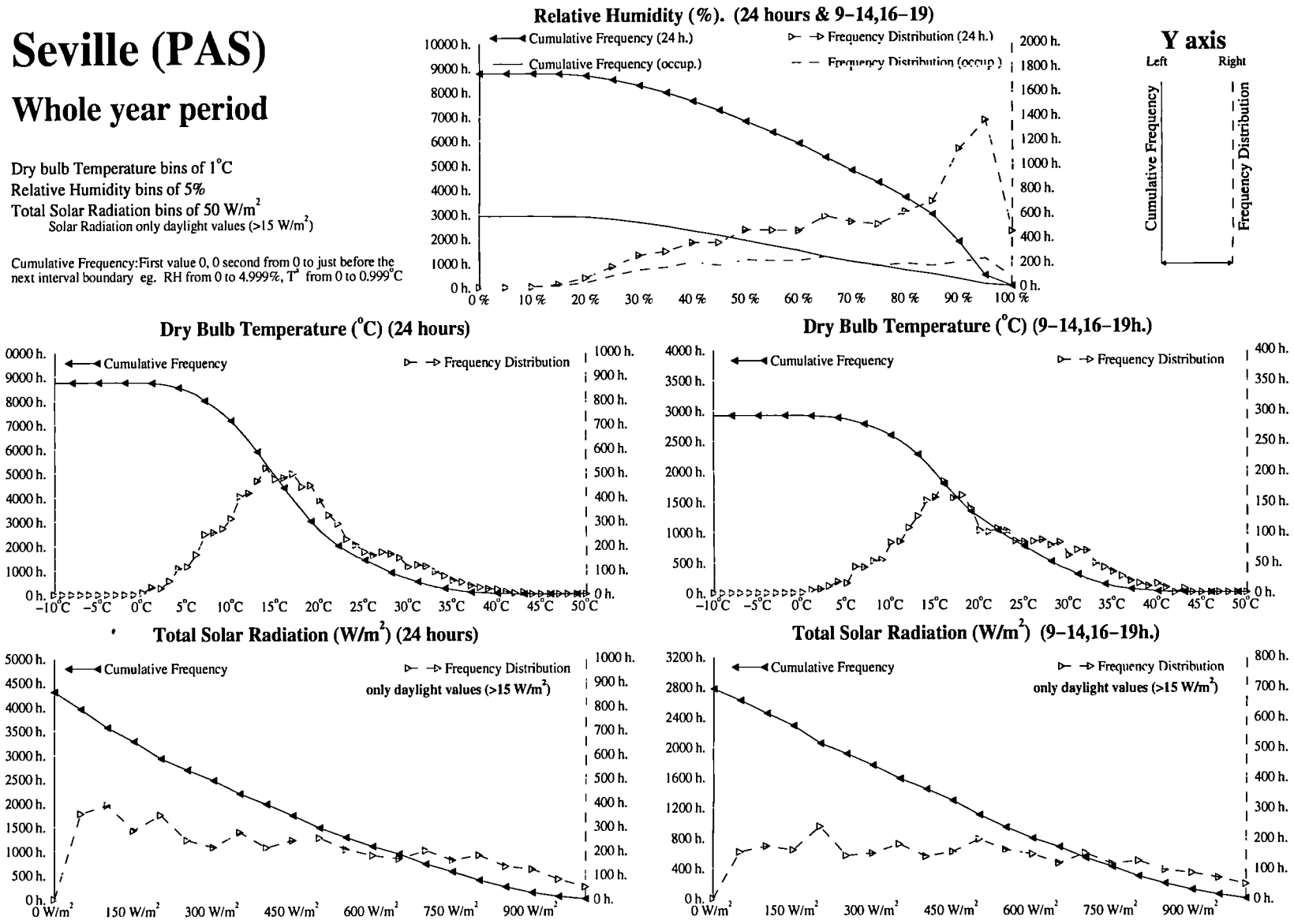

Figure 3-4. Frequency distribution and cumulative frequency for Seville (PAS)

3.5.2 Graphical study

In order to include a new dimension into the graphical study of climate, a psychrometric chart is going to be used. This is the only possible representation where different parameters can be displayed (and analysed) at the same time (See section 2.3).

By using the equations and the process explained in section 2.6, the climatic hourly data from the PASCOOL project was converted (for the cities presenting different format) to dry bulb temperature and moisture content and plotted into the simplified psychrometric chart. The data was plotted for four different situations: (i) whole year and 24 hours, (ii) whole year and occupancy time (9-14,16-19 hours), (iii) Summer (June-September) and 24 hours, and (iv) Summer (June-September) and occupancy time (9-14,16-19 hours). An example of one of these graphs is shown in Figure 3-5.

These graphs also include, plotted in red, the boundaries for cooling techniques, and the number of hours encountered in each envelope. This new concept is explained in section 3.5.2.1.

3.5.2.1 Boundaries for cooling techniques

The psychrometric chart has been divided by a series of lines, acting as boundaries for different zones or envelopes. These zones describe the ventilation or cooling technique that may be used to maintain the thermal comfort ambient conditions in that zone. First line is based on the dbt comfort limit of 25°C (See section 6.4.2) and corresponds to natural ventilation (NV). This limit can be extended up to 28°C dbt (Givoni, 1992) if combining natural ventilation with night cooling (NC). The third boundary 23°C *wbt*, has been estimated by experience accumulated during this study, and represent the zone were PDEC system might satisfy thermal comfort. Above 23°C wbt is considered that mechanical cooling is needed (MC). The other two zones (NV+l) and (MC+l) are not relevant, and represent the need of latent energy, required to dry the high content of water in the air.

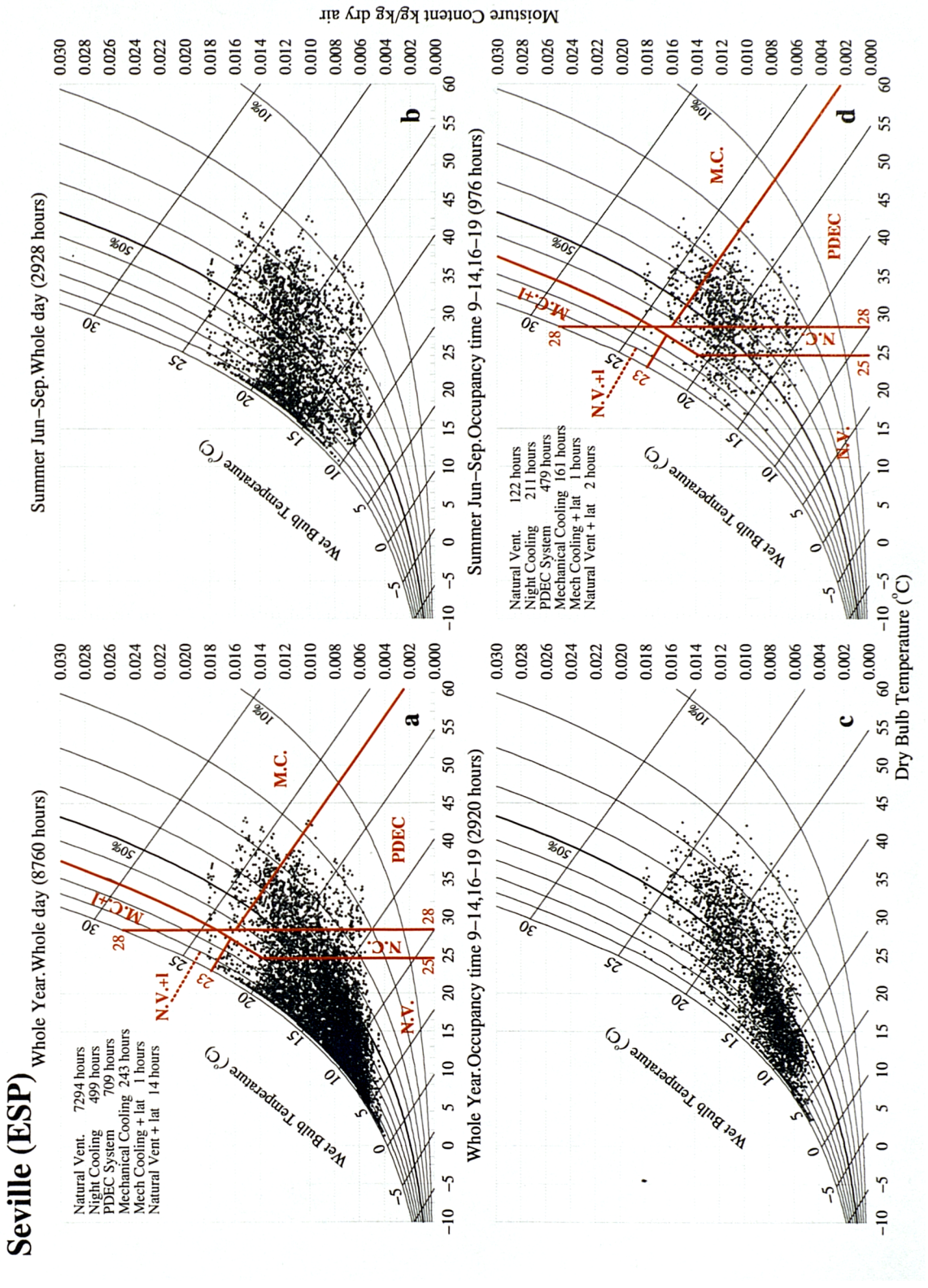

Figure 3-5. Climate graphical representation with cooling techniques boundaries

The number of hours encountered in the different envelopes will determine the cooling-ventilation technique (or combinations of techniques) recommended to maintain indoor comfort conditions. The location of these boundaries will be corroborated with thermal simulations as part of the future work, (See chapter 6 and 7).

3.5.2.2 Southern Europe map for cooling techniques

The work developed with the climatic data from the PASCOOL project was summarised in a map. The number of hours for envelope for each site was grouped in a 3D cylinder and plotted at its location (see Figure 3-6)

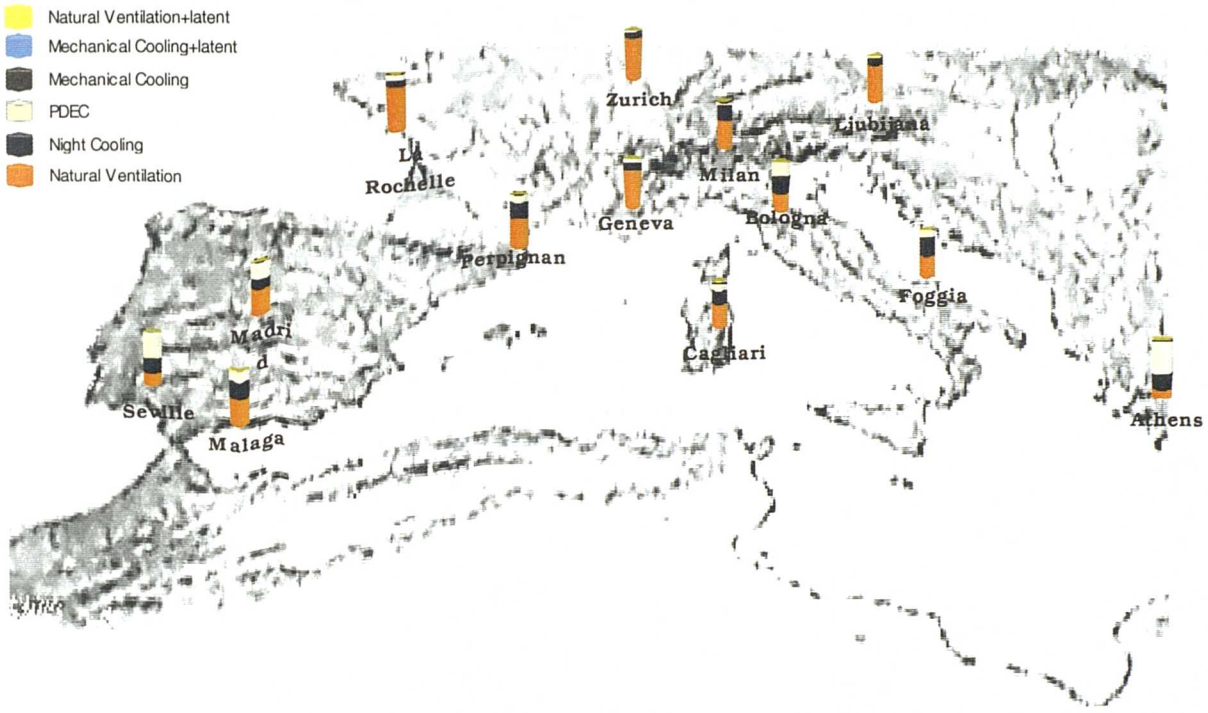

Figure 3-6. Southern Europe Cooling potential map. (Summer-occupancy hours)

No significant similarities or patterns were found among the sites. One conclusion is the need for the climatic analysis to include effects other than temperature or relative humidity such as wind speed or solar radiation. This will be achieved when the building performance take part in the process.

3.6 Climate case study

The aim of this case study was to compare the performance of two climate files (suitable for simulation) for the same location: Seville. One of the climate files comes from the PASCOOL project. The other climate file was obtained from J.F. Coronel from the Universidad de Sevilla. The latter is the file used in ESP to perform the simulations carried out within the PDEC project.

The comparison method used is based on the boundaries for cooling techniques described in 3.5.2.1. Even when these boundaries are not been corroborated by thermal simulation, the fact that they are the same for both files will establish a reasonable comparison approach. On a first visual analysis by plotting both climates onto the psychrometric chart, large differences were observed. The climate sent by the Universidad de Sevilla, from now referred to as Seville (ESP), seemed to be much warmer than the one obtained from PASCOOL, referred to as Seville (PAS).

Once the data is plotted, several FORTRAN programs count the number of hours in each cooling envelope. By looking at the number of hours in each envelope, it could be decided which cooling technique or combination of techniques to use. The number of hours encountered for both climates file is summarised in Table 3-2 and Table 3-3:

Table 3-2. Hours measured for Seville (PAS)

	Cooling technique						
Period	**NV**	**NC**	**PDEC**	**MC**	**MC+ I**	**NV+ I**	**total**
Whole year	7363	637	743	16	1	0	8760
Summer 24h	1703	498	710	16	1	0	2928
Summer 9-19h.	258	318	627	16	1	0	1220
Summer 9-14, 16-19h	234	276	455	10	1	0	976

Table 3-3. Hours measured for Seville (ESP)

	Cooling technique						
Period	**NV**	**NC**	**PDEC**	**MC**	**MC+ I**	**NV+ I**	**total**
Whole year	7294	499	709	243	1	14	8760
Summer 24h	1695	315	660	243	1	14	2928
Summer 9-19h.	122	221	638	236	1	2	1220
Summer 9-14, 16-19h	122	211	479	161	1	2	976

In order to compare the data for both climates, four bar graphs were generated. They are shown in Figure 3-7, (a) for the whole year, (b) for

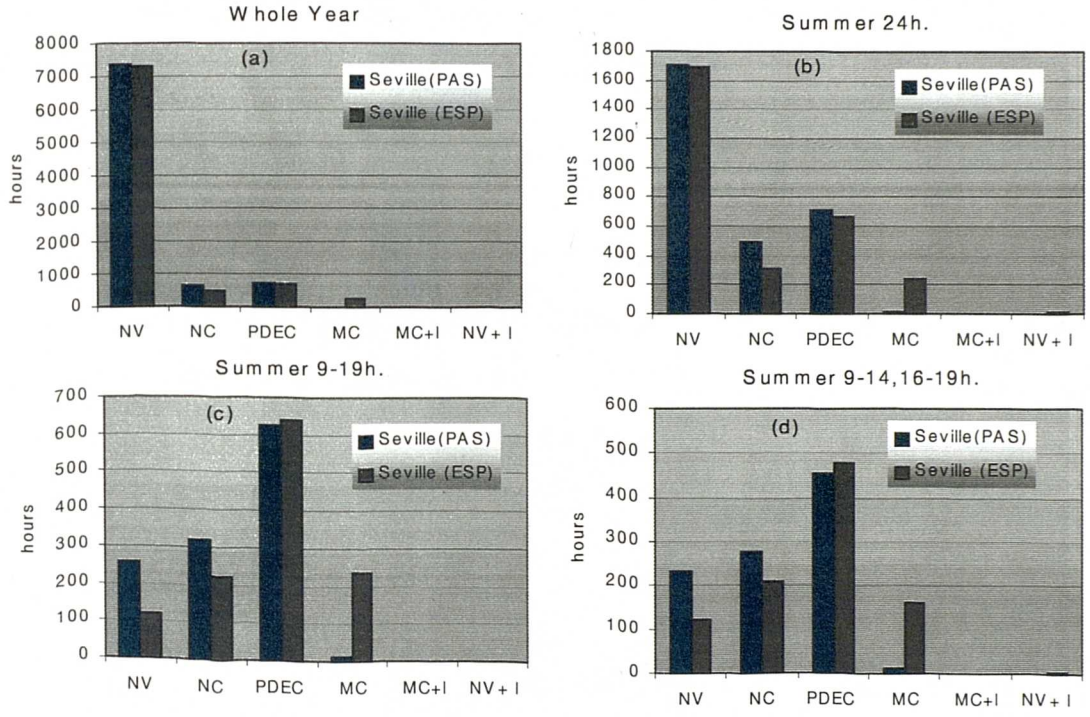

Figure 3-7. Comparison for Seville (PAS) and Seville (ESP)

summer and 24 hours, (c) for summer and the period between 9 and 19 hours and (d) for summer and the period between 9 until 14 hours and 16 until 19 hours.

By looking at the Figure 3-7a, little difference is observed. When the analysis concentrates in the other graphs (b, c and d), were the total number of hours is decreasing, the bar corresponding to mechanical cooling (MC) starts getting significantly bigger if comparing with the Seville PAS with the ESP file.

A notable difference of 227 hours for the MC envelope was found for the whole year period (Figure 3-7a), this value drops to 151 for summer period occupancy time with a lunch break (Figure 3-7d), which is still significant. By analysing the number of hours per envelope, a selection of the most suitable cooling technique can be made. It is here when the concept of overheating design criteria must be presented.

Overheating design criteria.

This recently created criterion helps free running buildings, by allowing a certain number of hours each year to fall outside comfort limits. These few hours of discomfort are justified by the energy saving and other benefits of using natural ventilation rather than mechanical cooling. There is no universally accepted criterion for predicting summertime overheating in passively ventilated buildings, although there is a general consensus throughout Europe that 27-28^{o}C is a realistic threshold. In Figure 3-8, the different values for some of the more relevant European institutions are shown.

According to this criterion, when using the PASCOOL climate for Seville, a PDEC strategy could be used for most of the year without the risk of discomfort. However when using the ESP climate file for Seville the criterion will not avoid the need of mechanical cooling to maintain comfort due to the larger number of hours exceeding the maximum allowed. Therefore a consequent more expensive installation will be required, a higher demand of energy and the following increment of CO_2 emissions.

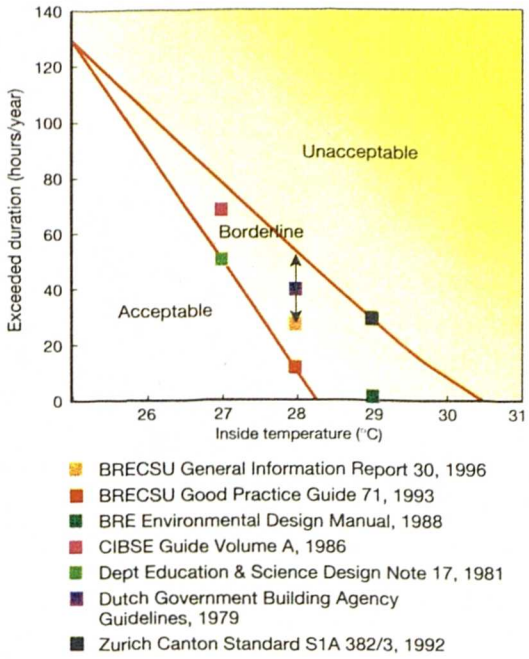

Figure 3-8. Overheating design criteria.

3.7 Summary

It is not easy to classify climate. Almost every location has its own particular climate. Attempts to find similarities among sites using XY plots failed. They are not accurate enough and they do not show the relationships between the different parameters. A process, by using the psychrometric chart, plotting hourly data was developed. This facilitates a study of the interaction between different elements such as dry bulb temperature and relative humidity. Some provisional boundaries to define areas that correspond with cooling techniques were established. Two different climates file for Seville were studied using these boundaries, finding notable differences. This could lead to the adoption of an inadequate cooling strategy depending on the file chosen. Since this is not subject to regulation, it can only generate a margin of fluctuation when analysing the results.

Climate must be analysed along with the building behaviour. This requires some validation via thermal simulation. This will be carried out in chapters 6 and 7.

Chapter

4 Thermal Comfort

"Our greatest weakness lies in giving up. The most certain way to succeed is always to try just one more time"

THOMAS ALVA EDISON

4.1 Preamble

This chapter deals with thermal comfort issues. It précis the psychological basis of comfort, the heat balance equation and regulatory mechanisms for warm and cold conditions. It also outlines the factors that influence thermal comfort, the common empirical and analytical indices to measure it and comfort requirements. It briefly describes the two well established thermal comfort models before moving onto the description of the Fiala model used in this thesis. The comfort envelopes, and their evolution are described. It also presents the adaptive behaviour theory and its relationship with comfort in free running buildings. Finally, it shows the newly developed comfort envelopes, assumptions, creation process and resulting equations.

4.2 Evolution of comfort

Socrates, around 400 BC, had some thoughts on the climatic suitability of houses, on how to build to ensure thermal comfort. Vitruvius (1st century BC) also wrote about the need to consider climate in building design, for reasons of health and comfort.

Up to the industrial revolution, thermal comfort was not a practical issue, as there were very few tools at our disposal to influence it. When it was cold a fire was lit, and when it was hot, the use of hand-held fans gave some relief. The heat storage capacity of caves was sometimes used for cooling, or, in some cultures, man-made tunnels and ventilation towers were used for similar purposes.

Heating technology improved from the late 18th century onwards and mechanical cooling became available during the early 20th century. Although Heberden (early 19th century) recognised that air temperature is not the only cause of thermal sensation and that humidity is a contributing factor, the first serious study on comfort was carried out by Haldane in England (1905). In the early 1920s Houghten and Yagloglou (1923) at the ASHVE (American Society of Heating and Ventilating Engineers) laboratories attempted to define the "comfort zone" for the first time. Analytical work started in the US in the middle 1930s where Winslow, Herrington and Gagge (1937) made a significant contribution.

Several disciplines became involved in the research activity of comfort, not just engineering, but physiology, medicine, geography and climatology. In architecture, Victor Olgyay (1963) was the first to bring together findings on the various disciplines and interpret these for practical purposes.

In order to analyse thermal conditions, the limits of thermal comfort must first be established.

4.3 Psysiological basis of comfort

The Human body continuously produces heat. This metabolic heat production comprises (i) basal metabolism, due to biological processes which are continuous and sub-conscious and (ii) muscular metabolism, emitted whilst carrying out work, which is consciously controllable (except for shivering).

The metabolic rate can be expressed as power density per unit body surface area [W/m^2], as the power itself for an average person [W] or in a unit devised for thermal comfort studies called the met. 1 met = 58.2 W/m^2. For an average sized man this corresponds to approximately 100 W. DuBois (1916) proposed an estimate of the body surface area, on the basis of body mass (*m*, in Kg) and height (*h*, in m), which is referred to as the "DuBois area" (A_D in m^2):

$$A_D = 0.202\, M^{0.425} \cdot h^{0.725} \tag{4-1}$$

The metabolic rate *M*, is compounded by four elements (ISO 8996), (i) base metabolism, *BM*, (ii) body posture, *BP* (iii) activity level, AL and (iv) body displacement, *BD*. The value is given in W/m^2.

$$M = BM + BP + AL + BD \tag{4-2}$$

The first element *BM*, depends on sex, age and weight/height ratio. Values are given for standard weight/height combination ratios, however, for age other than 35, these values need to be corrected. The formulae are listed below, for men and women respectively:

$$BM_{age} = BM_{35} + (35 - age)0.19 \tag{4-3}$$

$$BM_{age} = BM_{35} + (35 - age)0.15 \tag{4-4}$$

Body posture, *BP*, depends on whether the body is lying, sitting or standing. Activity level, *AL*, measures the motion of one or both hands, arms and trunk (nil, low, medium or high level). Body displacement, *BD*, takes into account whether the body is stopped, walking, running, etc.

The heat produced must be dissipated to the environment, otherwise a rise in body temperature will occur. The core body temperature is about 37ºC whilst the skin temperature can vary between 31ºC and 34ºC under comfort conditions (Fiala, 1999). Variations occur over time but also in different parts of the body, depending on clothing cover and blood circulation rate. There is a continuous transport of heat from deep tissues to the skin surface, from where it is dissipated by radiation, convection or (possibly) conduction and evaporation. The *traditional* heat balance equation for the body can be expressed as

$$M \pm R \pm Cv \pm Cd - E = \Delta S \qquad \textbf{(4-5)}$$

where

M = metabolic rate
C_v = convection heat loss
C_d = conduction heat loss
E = evaporation heat loss
ΔS = change in heat stored

If ΔS is positive, the body temperature increases, if negative it decreases. The heat dissipation rate depends on environmental factors, but the body is not purely passive, it is homoeothermic; it has several physiological regulatory mechanisms.

To warm conditions (or increased metabolic rate level) the body responds by vasodilation: subcutaneous blood vessels expand and increase the skin blood supply, thus the skin temperature, which in turn increases heat dissipation. If this cannot restore thermal equilibrium, the sweat glands are activated and the evaporative cooling mechanism will operate. Sweat can be produced for short periods at a rate of 4 l/h, but the mechanism is fatiguing. The sustainable rate is about 1 l/h evaporation is an endothermic process, it absorbs heat at the rate of some 2.4 MJ/l.

When these mechanisms cannot restore balance conditions, inevitable body heating (hyperthermia) will occur. When the core body temperature reaches about 40 ºC, heat stroke may develop. At about 42ºC death will probably occur.

To cold conditions the response is firstly vasoconstriction: reduced circulation to the skin, lowering of skin temperature, thus reduction of heat dissipation rate. Associated with this, "goose pimples" may appear, an atavistic phenomenon: the erection of hair, which would make fur a better thermal insulator. If this is insufficient, thermogenesis will take place: muscular tension or shivering, thus increased metabolic heat production. The deep-body tissues remain at the normal 37ºC. Body extremities, fingers, toes, ear lobes may be starved of blood and may reach temperatures below 20°C, or in severe exposure may even freeze, before the core body temperature would be affected.

When these physiological adjustments fail to restore thermal equilibrium, inevitable body cooling will occur (hypothermia). The deep body temperature may drop to below 35ºC. Death usually occurs between 25 and 30ºC (except under medically controlled conditions). Even if hypothermia is not reached, continued exposures to cold conditions, which require full operation of vasomotor and thermogenetic controls, can cause mental disturbances, hallucitanions, drowsiness and stupor (Lee, 1980; Grubich, 1961)

4.4 Factors influencing thermal comfort.

4.4.1 Simple variables

The variables that affect heat dissipation from the body and thus thermal comfort range from simple measurements i.e. dry bulb temperature (*dbt*), wet bulb temperature (*wbt*), globe temperature (*gt*), air speed (*v*), etc. to more complex factors. Some of them are outlined:

Mean Radiant Temperature (*MRT*), is the solid angle weighted average temperature of surrounding surfaces. It cannot be measured directly, but it can be estimated from *gt* readings. In still air *MRT=gt* but a correction for air movement of υ (velocity) is possible:

$$MRT = gt(1 + 2.35\sqrt{v}) - 2.35dbt\sqrt{v} \quad \textbf{(4-6)}$$

Dry Resultant Temperature (DRT), this is the average of *MRT* and *dbt*.

$$DRT = \frac{1}{2}MRT + \frac{1}{2}dbt \quad \textbf{(4-7)}$$

Environmental Temperature (*EnvT*), is also a composite of MRT and DBT, used in describing the heat exchange between the "environmental point" in a room and the internal surfaces:

$$EnvT = \frac{2}{3}MRT + \frac{1}{3}dbt \quad \textbf{(4-8)}$$

4.4.2 Thermal comfort indices

Two main types of these can be distinguished: Empirical measures, those that were produced by questionnaire studies, under defined environmental conditions and those produced by analytical methods, tracing the flow paths from metabolic heat production to the environment and considering resistances to such flows. The following are the most applicable indices:

Wind Chill Index (WCI), designed for outdoor use, it is used in cold climates to ascertain the cooling effects of wind.

Temperature Humidity Index (THI), also design for outdoor use, this is intended for use in warm humid climates.

Effective Temperature (ET), developed by Houghten and Yagloglou, at the ASHVE in 1923, is represented by a set of equal comfort lines drawn on the psychrometric chart. It is defined as the temperature of a still, saturated atmosphere, which would, in the absence of radiation, produce the same effect as the atmosphere in question. It thus combines the effect of dry air temperature and humidity. Used for more than 50 years, it is now been

superseded. ET over-estimates the effect of humidity, especially at lower temperatures (Gagge, 1971).

Wet Bulb Globe Temperature (WBGT), was developed by Yaglou for a simple field measurement of the old ET, for the control of heat casualties in US military training centres. It indicates the combined effect of air temperature, low temperature, radiant heat, solar radiation and air movement.

Operative Temperature (OT), is defined as the temperature of a uniform, isothermal black enclosure in which man would exchange heat by radiation and convection at the same rate as in the given non-uniform environment, or as the average of *MRT* and *dbt* weighted by their respective transfer coefficients:

$$\mathrm{OT} = \frac{h_r MRT + h_c dbt}{h_r + h_c} \qquad \textbf{(4-9)}$$

Resultant Temperature (RT), is based on measurements and votes in a test room after 0.5 hours of adjustment. It is a slight improvement of the ET scale, but only for rest or low activity conditions.

4.5 Thermal comfort models

The generalised thermal balance model (Eq 4-5) was first proposed by Gagge (1936). As conduction is normally negligible, this can be re-written as

$$M \pm R \pm C - E = \Delta S \qquad \textbf{(4-10)}$$

Since 1936 it has had several refinements and modifications. Before describing the new model used in this thesis, two former models must be outlined in order to justify the use of this new one.

4.5.1 The two node-node model

This model treats first the heat transfer from the body core to the skin, then from the skin to the environment.

The body's metabolic rate is M (W). Part of it is converted to work (mechanical power).

The mechanical efficiency is η = work/M

The remainder is the body heat production $M(1-\eta)$ expressed for unit body surface area is $M(1-\eta)/A_D$ in [W/m^2], where A_D is the Dubois area (see Eq 4-1).

The evaporation heat loss (E) has three components:

E_{diff} = due to vapour diffusion through the skin
E_{rsw} = due to evaporation of regulatory sweating from the skin
E_{resp} = respiration latent heat loss

These components are estimated as follows:

$$E_{resp} = 0.0173M(5.87 - \rho_a) \quad \textbf{(4-11)}$$

where

5.87 = Saturation vapour pressureat lung temperature, $35°C[kPa]$
ρ_a = vapour pressure of ambient air

The sensible heat loss is

$$C_{resp} = 0.0014M(34 - t_a) \quad \textbf{(4-12)}$$

where

34 = exhaled air temperature [$°C$]
t_a = Ambient temperature [$°C$]

none of them reach the skin surface, the heat that reaches the skin is

$$M_{sk} = M(1-\eta) - 0.0173M(5.87 - \rho_a) - 0.0014M(34 - t_a) \quad \textbf{(4-13)}$$

following are the heat transfer coefficients (conductances) used:

h_r = radiation conductance (from surface to MRT)(W/m^2K)

h_c = convection conductance (from surface to air)(W/m^2K)

$h = h_r + h_c (W/m^2K)$

h_{cl} = clothing conductance (W/m^2K)

h_e = evaporation heat loss conductance (W/m^2kPa)

The maximum possible evaporative heat loss from the body surface is

$$E_{max} = 16.7\, h_c(\rho_{sk} - \rho_a)F_{pcl} \quad \textbf{(4-14)}$$

where

ρ_{sk} = saturation vapout pressure at mean skin temperature(kPa)

ρ_a = vapour pressure of ambient air (kPa)

16.7 = Lewis relation. Ratio of evaporative and convective heat transfer coefficients (h_e/h_c) at sea level

F_{pcl} = vapour permeation efficiency from skin through clothing

then

$$E_{rsw} = W_{rsw}E_{max} \quad \textbf{(4-15)}$$

where $W_{rsw} = A_{sw}/A_D$ the "skin wettedness", the area of body surface exposed covered by a film of sweat (A_{sw}) as a fraction of the Dubois area.

From the area covered by clothing the sweat will evaporate by diffusion:

$$E_{diff} = (1 - W_{rsw})0.06E_{max} \quad \textbf{(4-16)}$$

but in absence of regulatory sweating, $E_{rsw} = 0$ then

$$E_{diff} = 0.06E_{max}$$

The total skin evaporation, adding the above (Eq 4-15) and (Eq 4-16) two terms is:

$$E_{sk} = E_{diff} + E_{rsw} = (0.06 + 0.094W_{rsw})E_{max}$$

or substituting the E_{max} expression (Eq 4-14)

$$E_{sk} = 16.7(0.06 + 0.094W_{rsw})h_c(\rho_{sk} - \rho_a)F_{pcl} \quad \text{(4-17)}$$

The sensible heat loss from the body surface is

$$R + C = f_{cl}h(t_{sk} - t_a)F_{cl} \quad \text{(4-18)}$$

where

f_{cl} = the fraction of body clothed

F_{cl} = insulation value of clothing= $1/(1 + 0.155hI_{cl})$

Now, substituting equations (Eq 4-13), (Eq 4-18) and (Eq 4-18) into (Eq 4-10) the complete thermal balance equation can be written as:

$$\begin{aligned}\Delta S = {} & M[(1-\eta) - 0.0173(5.87 - \rho_a) - 0.0014M(34 - t_a)] \\ & -16.7(0.06 + 0.094W_{rsw})h_c(\rho_{sk} - \rho_a)F_{pcl} - f_{cl}h(t_{sk} - t_a)F_{cl}\end{aligned} \quad \text{(4-19)}$$

4.5.2 Fanger's heat balance equation

Although the author (Fanger 1970-1982) refers to this as "comfort equation", it is actually a heat balance equation (Eq 4-10), arranged to give a zero storage component, which will be related to comfort through the PMV method.

Term H is used for $M(1-\eta)$ i.e. the body's net heat production, and as is considered thermal comfort, a condition of which that storage component, ΔS , is zero (apart for short term transient effects, reason to use other model) and as conduction loss, C_d is normally insignificant, the equilibrium condition can be written as:

$$H - E - C - R = 0 \quad \text{(4-20)}$$

from here the "double equation" might be written as:

$$H - E_{diff} - E_{rsw} - E_{resp} - L = K = R + C \quad \text{(4-21)}$$

where

L = dry respiration loss

K = heat transfer from skin to clothing surface

R = radiation loss

C = convection loss

The components of this are calculated as follows:

$$E_{diff} = \lambda m A_D(\rho_s - \rho_a) \tag{4-22}$$

where

λ = latent heat of evaporatoin of water (575 kcal/kg)

m = permeance of skin (6.1×10^{-4}kg/h m^2mmHg)

ρ_s = saturation vapour pressure at skin temperature (mmHg)

ρ_a = vapour pressure of ambient air (mmHg)

Substituting the appropriate numerical values and as $\rho_s = 1.92t_s - 25.3$ gives $E_{diff} = 0.35A_D(1.92t_s - 25.3 - \rho_a)$. It has been shown that the skin temperature for comfort conditions is $t_s = 35.7 - 0.032\, H/A_D$ substituting this in (Eq 4-22)

$$E_{diff} = 0.35A_D[43 - 0.061(M/A_D)(1-\eta) - \rho_a] \tag{4-23}$$

for comfort conditions E_{rsw} must be within very narrow limits and it has been shown that for average situations

$$E_{rsw} = 0.42A_D[(H/A_D) - 50] \tag{4-24}$$

The respiration latent heat loss is calculated as

$$E_{resp} = V(HR_{ex} - HR_{in})\lambda \tag{4-25}$$

where

V = pulmonary ventilation rate, found as 0.006 M

RH_{ex} = humidity ratio of air as exhaled

RH_{in} = humidity ratio of air as inhaled

λ = latent heat of evaporation of water

Substituting humidity ratios and vapour pressures yields

$$E_{resp} = 0.0023M(44 - \rho_a) \tag{4-26}$$

the dry respiration loss is calculated as

$$L = 0.0014M(34 - t_a) \quad \text{(4-27)}$$

When these three terms are subtracted from H, the remainder must be dissipated by conduction through the clothing (K) and subsequently by radiation and convection (R+C) from the surface of clothing.

$$K = A_D(t_s - t_{cl})/0.18I_{cl} \quad \text{(4-28)}$$

where

I_{cl} = insulation of clothing [clo]
t_s = skin temperature
t_{cl} = clothing surface temperature

and substituting the above expression for t_s:

$$K = A_D[(35.7 - 0.032H/A_D) - t_{cl}]/0.18I_{cl} \quad \text{(4-29)}$$

The radiation component is

$$R = A_{eff}\varepsilon\sigma[(t_{cl} + 273)^4 - (t_r + 273)^4] \quad \text{(4-30)}$$

where

ε = emmitance of outer surface of clothing
σ = theh Stefan-Bolzmann constant
t_{cl} = temperature of outer surface of clothing
t_r = mean radiant temperature

After substituting of the appropriate numerical values we get

$$R = 3.4 \cdot 10^{-8} f_{cl} A_D[(t_{cl} + 273)^4 - (t_r + 273)^4] \quad \text{(4-31)}$$

where f_{cl} is the ratio of clothed to exposed body surface.

The convection component is

$$C = A_D f_{cl} h_c (t_{cl} - t_a) \quad \text{(4-32)}$$

The magnitude of h_c (kcal/m^{2}hK) depends on air velocity (m/s):

The criterion (crit) is $2.05(t_{cl} - t_a)^{0.25}$ if

$$\text{crit} > 10.4\sqrt{v} \qquad \text{then } h_c = \text{crit}$$

$$\text{crit} < 10.4\sqrt{v} \qquad \text{then } h_c = 10.4\sqrt{v}$$

Substituting the above equations (Eq 4-13) (Eq 4-22), (Eq 4-27) and (Eq 4-31) into the double equation, yields the thermal balance equation for Fanger:

$$\frac{M}{A_D}(1-\eta) - 0.35\left[43 - 0.061\frac{M}{A_D}(1-\eta) - \rho_a\right] - 0.42\left[\frac{M}{A_D}(1-\eta) - 50\right]$$

$$- 0.0023\frac{M}{A_D}(44-\rho_a) - 0.0014\frac{M}{A_D}(34-t_a) = \frac{35.7 - 0.0032\cdot\frac{M}{A_D}(1-\eta) - t_{cl}}{0.18\cdot I_{cl}} \qquad \textbf{(4-33)}$$

$$= 3.4\cdot 10^{-8} f_{cl}[(t_{cl}+273)^4 - (t_r+273)^4] + f_{cl}h_c(t_{cl}-t_a)$$

4.5.3 The Fiala model

This mathematical model (Fiala, 1999) predicts human thermal responses and the associated thermal feelings in steady state and in transient conditions. The dynamic model predicts body temperatures, thermoregulatory responses, components of the environmental heat exchange and the overall, Dynamic Thermal Sensation (DTS) in cold stress, cool, neutral, warm and hot stress conditions. Thermal influences on human beings can be analysed for a range of activity of up to 10 met, as well as for various asymmetric environmental conditions and non-uniform clothing ensembles. The model comprises a passive and an active system.

4.5.3.1 Passive system model

A multi-segmental model of the human body incorporating thermally important body elements was used. Each element was made up of different body tissue materials by utilizing anatomical, thermophysical and geometrical data of the human body obtained from literature. The humanoid represents an average (white adult) person with respect to body weight, body fat content, body surface-area, basal values of body metabolism, skin evaporation, and cardiac output. Body compartments were subdivided further into spatial sectors to permit direction-dependent

simulation of environmental heat exchange in asymmetric conditions. Heat dissipation within the body was modelled by accounting for the combined effect of metabolic heat generation, blood circulation, and conductive heat transport. The calculation of body metabolism includes the impact of the human work efficiency as a function of the activity level.

The environmental heat exchange was modelled in detail to reflect the importance and complexity of these phenomena in practice. Convective heat losses were simulated by accounting for free and forced convection and their variation over the human body using local convection coefficients obtained from measurements reported in the literature. The simulation of the radiant heat exchange is body posture dependent and considers spatial asymmetric radiant fields, and the effect of solar direct and diffuse irradiation. The skin evaporation model is based on local mass and heat balances incorporating the effect of moisture diffusion through the skin, evaporation of regulatory sweat, accumulation of the sweat liquid on the skin, and the evaporative resistance of garments. A clothing model was developed which provides non-uniform thermal and evaporative insulation properties for use with the multi-segmental model. Respiration was modelled by considering both the convective and latent heat losses.

For solving the complex mathematical problem of heat transfer in the human body, advanced hybrid techniques were applied which provide fast and accurate numerical solutions associated with stable numerical behaviour. A finite-difference formulation of the bioheat equation has been developed which applies -with slight modifications- to a steady state and to transient heat transport in body tissue cylinders or spheres. The formulation of the boundary conditions at tissue interfaces and on the skin surface considers the effect of geometry on the dissipation of heat.

The numerical formulation of the passive system was tested using different analytical solutions for heat dissipation in cylinders and spheres. The validation was performed for diverse steady-state and transient analytical

solutions and showed both good agreement with the analytical solutions and a numerically stable behaviour. Even for large time-steps of one hour, the model provided reasonable results. In the case of (disproportionate) large time-steps and sudden changes of boundary conditions, the model was stable and rapidly converged to the final temperature values.

4.5.3.2 Active system model

The active system model of human thermoregulation was developed by means of statistical regression methods. The analysis of thermal and thermoregulatory responses obtained from different experimental studies covering a range of environmental temperatures between 5 and 50°C, and exercise intensities between 0.8 and 10 met, led to a temperature-based, non-linear active system model. Skin temperature was found to play a major role in human thermoregulation for the entire spectrum of environmental conditions, whereas elevated internal temperature was an important afferent signal for regulatory reactions against warmth and during exercise. Negative rates of change of the mean skin temperature were found to govern the dynamics of regulatory responses in the cold. The afferent signal analysis indicated that calorimetric variables, such as the skin heat flux, were inappropriate input signals into the regulatory centre. The non-linearity of the active system model was a result of considering the human thermoregulatory behaviour over a wide range of environmental and internal conditions.

The sweating response, Sw, was found to be a function of both positive and negative skin temperature error signals, $\Delta T_{sk,m}$, and positive and negative error signals from the head core, ΔT_{hy}. There were appreciable differences between the intensity with which 'cold' and 'warm' cutaneous receptors affect sweating. In cold environments the Sw-regulator seemed to be increasingly oriented toward maintaining body core temperature (during exercise) while warnings of 'cold' from the periphery were discriminated. Little effect resulted for negative error signals from the hypothalamus, whereas a pronounced effect on Sw resulted for ΔT_{hy} >0.5K.

The shivering action, Sh, was revealed to be responsive to punitive signals from 'cold' cutaneous receptors, i.e. $\Delta T_{sk,m} < 0$. Negative rates of change in the mean skin temperature, $dT_{sk,m}/dt$ appeared to govern the dynamic behaviour of Sh after a sudden fall in ambient temperature. The effect of ΔT_{hy} signals on Sh was weak. The model's shivering response was unaffected by positive $\Delta T_{sk,m}$ signals as well as positive $dT_{sk,m}/dt$ signals.

The vasoconstriction response, Cs, was found to be a primary function of 'cold' cutaneous receptors, i.e. negative signals $\Delta T_{sk,m}$ and $dT_{sk,m}/dt$. The effect of core temperature on the model's vasoconstriction appeared to be practically negligible. Cs was independent of the drive from 'warm' cutaneous receptors. The involvement of 'warm' cutaneous receptors (positive $\Delta T_{sk,m}$ signals) in the regulation of skin blood flow was found to be associated exclusively with the vasodilatation response, Dl, which depended also on positive ΔT_{hy} signals. However, Dl appeared to be independent of negative temperature error signals from either body site. It can be seen, therefore, that the functional relationships between Cs and afferent signals was similar to the relationship between Sh and these signals. Likewise, Dl responded to afferent signals similar to Sw. These results were interpreted as a sort of coupling principle between related responses that provide increased efficiency of regulatory defence mechanisms against thermal disturbances of the body.

The complete model was tested for a spectrum of ambient temperatures between 5 and about 50°C. The transient behaviour of the model was tested using transient changes in activity and in climatic conditions, e.g. step changes from neutral to cool, cold, warm and hot and vice versa, and from cold to hot, and vice versa. Good general agreement with measured data was obtained for the predicted thermoregulatory responses and the resultant body temperatures for the whole range of climatic conditions and types of exposure. The mean and local skin temperatures were reproduced to within the bounds of the measurement error observed in different experiments, typically ±1K. Larger differences, however, resulted for skin temperature

when sweating in the cold. The predicted body core temperature(s) deviated from corresponding measurements by less than ±0.5K as the typical uncertainty of experimental data. This elevated accuracy in the prediction of body core temperature arose from appropriate modelling of vasomotor responses.

The predicted increase in metabolism due to shivering in cold and severe cold environments differed from experimental observations generally by less than the assumed error band of the experimental data, i.e. about 50W. Greater discrepancies between measurement and prediction might, however, be expected for atypically lean or obese subjects especially for the shivering response. The passive system reflects an average person in terms of body size and fat content. The model also reproduced the dynamic thermal behaviour of subjects exposed to sudden downward changes in ambient temperatures, i.e. a transient peak of the metabolic activity (due to a rapid cooling of the skin), and an increase with time of the body core temperature (due to cutaneous vasomotor adjustments).

In moderate and thermally neutral environments, where body temperatures were regulated by vasomotor responses and where neither shivering nor sweating occurred, the predicted body core temperatures and skin temperatures deviated from measured data typically by less than 0.2K and 1K, respectively. Similar accuracies were also obtained for moderately exercising subjects, as well as for diverse combinations of environmental parameters, and for different clothing ensembles.

The sweating model reproduced the pseudo-motor regulatory behaviour of non-exercising subjects for the whole range of warm and hot ambient conditions. Differences between prediction and experimental observation were less than 50W. Both the transient behaviour, and the stationary plateau of skin evaporation, were predicted accurately. The reliability of the sweating model led to confident predictions of skin and core temperature in warm and hot conditions. Seemingly paradoxical dynamic effects such as

the fall in core temperature observed in experiments after moving from a cold to a hot climate were predicted.

The predictions of sweat rates during alternating periods of heavy work and recovery were in poorer agreement with experimental results than predictions for environmentally induced sweating. More independent experimental investigations seem to be required before more reliable algorithms for sweating during abrupt, large changes in exercise can be included in an active system model.

Systematic discrepancies (in some instances up to 5K) were observed between predicted and measured skin temperatures during sharp transient changes in exercise intensity in the cold where subjects were sweating. Based on an pilot experimental and a numerical study it was concluded that this was due to the manner in which experimentalists had attached thermocouples to the skin of subjects (i.e. sticky tape). Care over the attachment of temperature sensors, which might prevent skin evaporation, needs to be exercised when undertaking physiological studies.

The model showed good agreement with measured body core temperatures for steady as well as instantaneous exercise activity, and for different combinations of work load, ambient temperature, relative humidity, and clothing insulation.

4.5.3.3 Comfort model

The statistically founded thermal comfort model developed by Fiala, was used. It predicts the Dynamic Thermal Sensation, (DTS), for a wide range of environmental conditions and activity levels. Regression analyses revealed the temperature error signals from the skin, $\Delta T_{sk,m}$, from the head core, ΔT_{hy}, and the rate of the change in the mean skin temperature, $dT_{sk,m}/dt$, to be the responsible thermophysiological variables which govern the overall human warmth sense.

Both negative and positive signals from the skin, i.e. punitive signals from cutaneous 'cold' and 'warm' receptors, were involved in the sensation of temperature. Analysis of sensation votes during environmental transients and in warm and hot environments revealed, on the other hand, that the skin heat flux, as a calorimetric quantity was inadequate for modelling thermal sensation.

The influence of core temperature, which affects the comfort perception e.g. during exercise, was found to be a multiple process in which any elevation in core temperature appeared to be weighted by the level of thermal strain at the body's periphery, i.e. $\Delta T_{sk,m}$. This mechanism emphasizes the partial contribution of core temperature with rising cold stress at the skin surface. However, the model predicts a vanishing effect of negative ΔT_{hy} signals to DTS.

A strong dynamic component in thermal sensation was discovered which gives man anticipatory drive toward conscious behavioural action. Rates of change in the mean skin temperature were found to be the physiological origin of dynamic sensation events during skin cooling. However, the initial impulse of the maximum rate of change in the mean skin temperature was found to be the governing drive which dominates the dynamic thermal sensation during skin warming.

The transient comfort model was validated for gradual, sinusoidal, and sudden changes in environmental conditions, for transient exercise, and for steady climatic conditions. The predicted levels of (dis)comfort agreed well with experimental observations. The deviations were typically less than the expected standard error of inter-individual differences which is about 0.8 - 1.0 categories of warmth on the ASHRAE scale.

The Fiala model was chosen to carry out the comfort calculation because:

(i) It is a multi segmental model, allowing the body's behaviour to be simulated more accurately than the other models,

(ii) it is a dynamic model,

(iii) it includes as outputs, the regulatory responses, thus allowing a wider range of conditions than Fanger's model, and

(iv) the clothing level calculations are recalculated for each simulation, as part of the interactive model.

4.6 Comfort envelopes

Olgyay was the first to outline a comfort zone in architectural terms, i.e. the range of environmental conditions within which the average person would be comfortable. This early approach was represented into a cartesian graph, with dry bulb temperature and relative humidity as axis respectively (Figure 4-1). An aerofoil-shaped zone in the centre of the graph was the comfort zone. New lines were added to the graph to represent how different air velocities could extend the upper limit of this zone. Below the comfort zone, a family of lines indicated various levels of radiation that would compensate for the lower than comfortable temperatures.

Arens and his co-workers (1980) published a new version of this chart, applicable for persons wearing 0.8 clo, with a metabolic rate of 1.3 met (75 W/m^2). The comfort zone boundaries were adopted from ASHRAE Standards 55-74R (1985), an innovation was the use of EFR (see Section 4.4) evaluating the effect of directional radiation (see Figure 4-2a). Yagloglou (1923) was the first to use the psychrometric chart as a base for his "equal comfort lines" (see Section 4.4). Arens et al. (1980) also presented their bioclimatic chart in this format. ASHRAE used the psychrometric chart for the description of comfort since 1966, but their definition of the boundaries went thought a number of alterations as research progressed and opinions changed. The 1966 version gave the temperature limits by *dbt* (vertical) lines and the humidity limits by two *RH* curves. In 1974 (Figure 4-2b) the side boundaries changed to *ET* (see Section 4.4) lines, and the humidity boundaries were defined in terms of vapour pressure (horizontal lines).

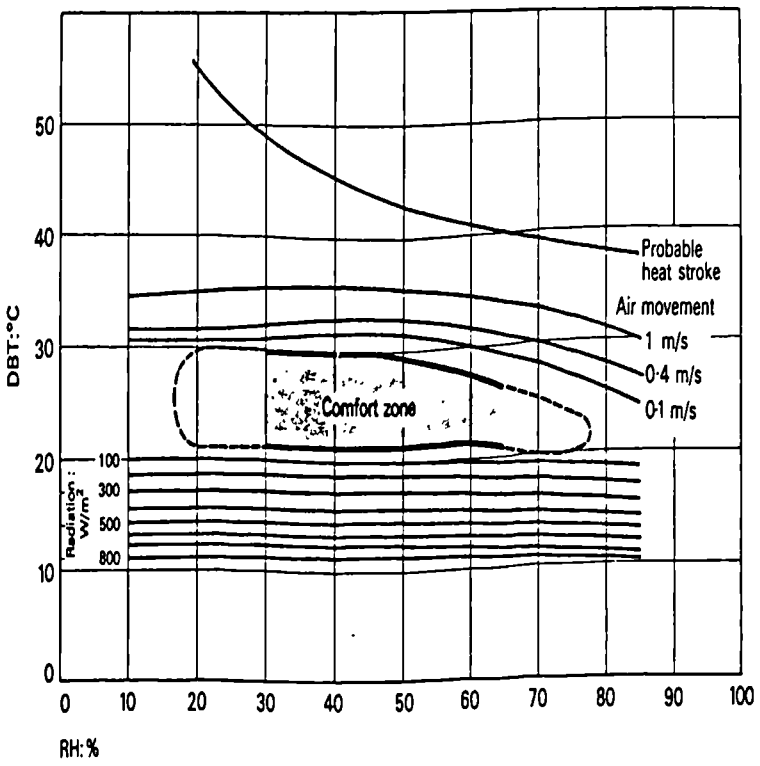

Figure 4-1. Olgyay's bioclimatic chart.

The argument for this was that the vapour pressure at the skin hardly changes (within comfort limits) thus the main determinant of evaporation (thus the cooling effect) is the ambient vapour pressure. 1981 was the first instance when summer and winter comfort were distinguished (Figure 4-2c). Humidity limits remained the same. In the 1992 revision, the temperature boundaries and the lower humidity limit remained the same but for the upper humidity limit, the chart reverted to the 60% RH curve. The rationale behind this was that higher humidities even at lower temperatures may have non-thermal ill-effects. In 1995 (Figure 4-2c') the side limits and lower boundaries again remained the same, but the upper humidity limits were changed to two *wbt* lines. The argument here was that this is a thermal standard, therefore other, non-thermal effects should not be included.

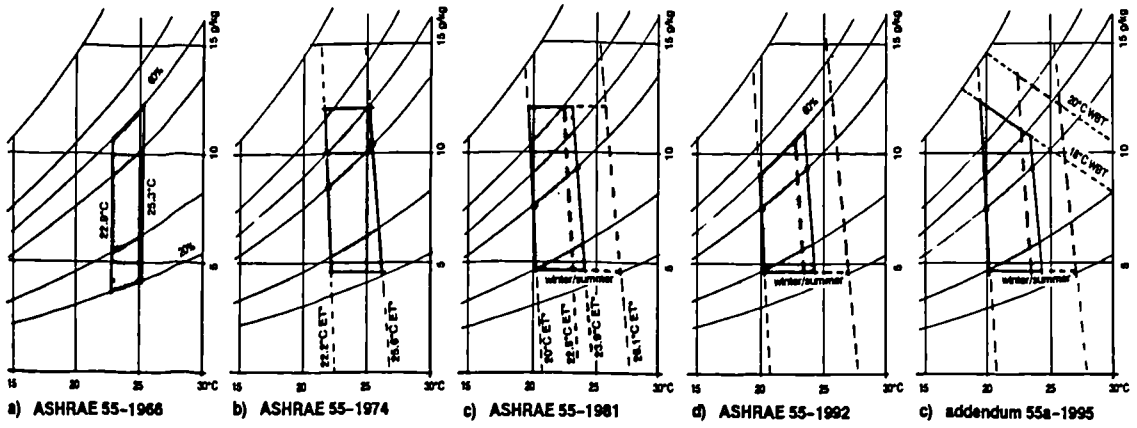

Figure 4-2. Historical development of the ASHRAE comfort zone.

By analysing the evolution of these comfort envelopes it can be seen that the size of the comfort area is growing. It is also found that the upper limit for the relative humidity is higher.

4.7 New comfort envelopes.

4.7.1 First approach

Using the Fiala model, clothing calculations and assumptions of adaptive behaviour, new comfort envelopes for summer periods in office buildings were developed. In a first study, (Figure 4-3) the effect of PDEC-environments on predicted thermal, regulatory and perceptual responses of occupants was studied for summer conditions in office buildings.

The subjects were assumed to be wearing typical summer clothing (0.55 clo) and be engaged in typical office activities (1.2 met). Based on that analysis, zones of comfort were defined for PDEC office buildings, considering two levels of air velocity (0.3 m/s and 0.8m/s). Also included was the impact of varying solar radiation on subjects' responses (0 W/m^2 and 25 W/m^2).

The analysis showed that even relative humidities of 80% were predicted to be acceptable for the PDEC-building occupants. Thus the comfort envelopes established a new upper limit for relative humidity, which allows PDEC

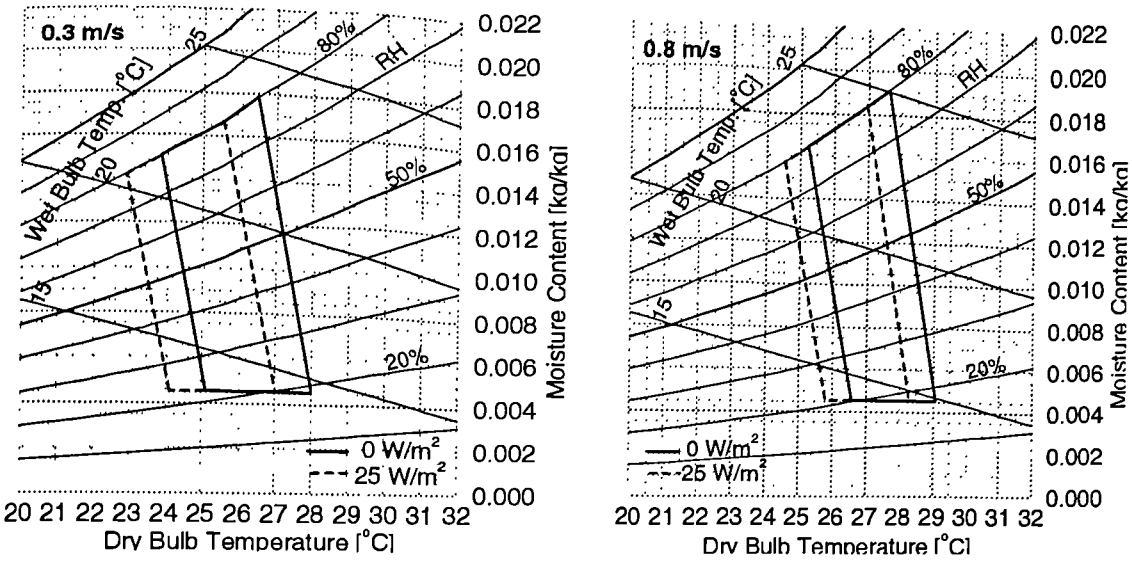

Figure 4-3. Comfort envelopes obtained from the first approach.

systems to operate above the traditional 60% limit, ASHRAE 55 (1992). However, the envelopes did not indicate the tolerance to higher temperatures which adaptive behaviour might enable.

4.7.2 Second approach

In order to quantify the impact of thermal adaptation in the existing comfort envelopes, the three most influential adaptive reactions were investigated: (i) changes in clothing insulation (ii) variation in local air speed (using fans) and (iii) the manipulation the amount of diffuse solar radiation (using blinds). In principle, these adaptive actions should enable occupants to feel comfortable in a wider range of environmental conditions.

Different summer clothing ensembles for men and women, and for different ranges of operative temperatures, (light ensemble for 20°C $<T_o<$25°C and a very-light ensemble for 25°C $<T_o<$32°C) have been considered. These differences considered both the use of lighter garment fabrics and the selection of different garment items i.e. long/short sleeve, lighter shoes, dress instead of a skirt and blouse, etc. An occidental office dress-code, however, has been respected in all cases.

The clothing was modelled in detail by applying individual items of an ensemble to the corresponding body elements of the multi-segmental model. The Fiala model was fed with the measured overall values of clothing insulation I_{cl} (clo), clothing area factor f_{cl} (-), and the evaporative resistance of the fabric $R_{E,f}$ (m^2kPa/W), obtained from literature, McCullough et al. (1985) and (1989).

Women-light outfit: bra, pantyhose, panties, skirt knee length, blouse long sleeve, open lady shoes and chair, I_{cl}=0.63clo, i_{cl} =0.34[1].

Women-very-light outfit: bra, panties, long thin dress with short sleeves, open ladies shoes and chair, I_{cl}=0.42clo, i_{cl} =0.28.

Men-light outfit: briefs, socks, light long trousers, long sleeve shirt, street shoes and chair, I_{cl}=0.69clo, i_{cl} =0.30.

Men-very-light outfit: briefs, socks, light long trousers, short sleeve shirt, sandals and chair, I_{cl}=0.43clo, i_{cl} =0.29.

Air speed may be just 0.2 m/s which ensures the required ventilation levels. If permitted by the management regime may move to work in more shaded areas (away from windows). Direct solar radiation should be eliminated by the building's own external shading devices. The investigated values were zero and 50 W/m^2 (the latter ensures high natural lighting level).

4.7.2.1 Process of development

The upper and lower limits of the new extended comfort envelopes were obtained from the former study, Fiala (1999) i.e. relative humidity of 80% and a moisture content of 0.0045 kg/kg, respectively. The right and left boundaries of the new comfort zones, were defined by the operative temperature (T_o) and relative humidity at which 10% of the people will be thermally uncomfortable, ASHRAE 55,(1992).

1. The overall values of I_{cl} and i_{cl}, were calculated by the Fiala model from the individual clothing items.

A file matrix with combinations of operative temperatures and relative humidities was created, along with the different clothing ensembles, air speeds and solar radiation values. These were used as the input data to the simulation program. Indoor operative temperatures were investigated for a range between 20°C<T_o<32°C in successive steps of DT_o = 0.5K. The relative humidities investigated ranged between 10%<RH<90% in steps of 2%. The diffuse solar intensifies subjected to analysis were 0 W/m^2 and 50 W/m^2. The considered air velocities were 0.2 m/s (for the range 20°C<T_o<25°C) and 0.3, 0.6, 0.9, 1.2 and 1.5 m/s (for the range 25°C<T_o<32°C). Clothing levels were studied separately for men and women, resulting in values of I_{cl}=0.69clo/0.43clo (for men light/very light ensembles) and I_{cl}=0.63clo/ 0.42clo (for women light/very light ensembles). A metabolic rate of 1.2 met, was used as the office activity level, ISO 7730 (1994). So, a total of nearly 26,000 different combinations of boundary conditions emerged.

The simulation series were conducted as individual two-hour-exposures to the steady environmental and personal conditions. Simulation results for which 8%<PPD<12% applies were filtered out for further data processing. This data is plotted onto a psychrometric chart. The required comfort limits of PPD=10% were obtained by linear regression through the filtered data for both the right-hand side boundary, i.e. DTS>0, and the left-hand side boundary, i.e. DTS<0. A good general correlation (0.85<|r|<0.93) for the linear regressions was achieved.

The analysis of the comfort boundaries indicated that there were no significance differences between men (0.69-0.43 clo) and women (0.63-0.42 clo) (Figure 4-4). For this reason only the results obtained for one sex (men) were considered in the further analysis, (0.69 and 0.43 clo).

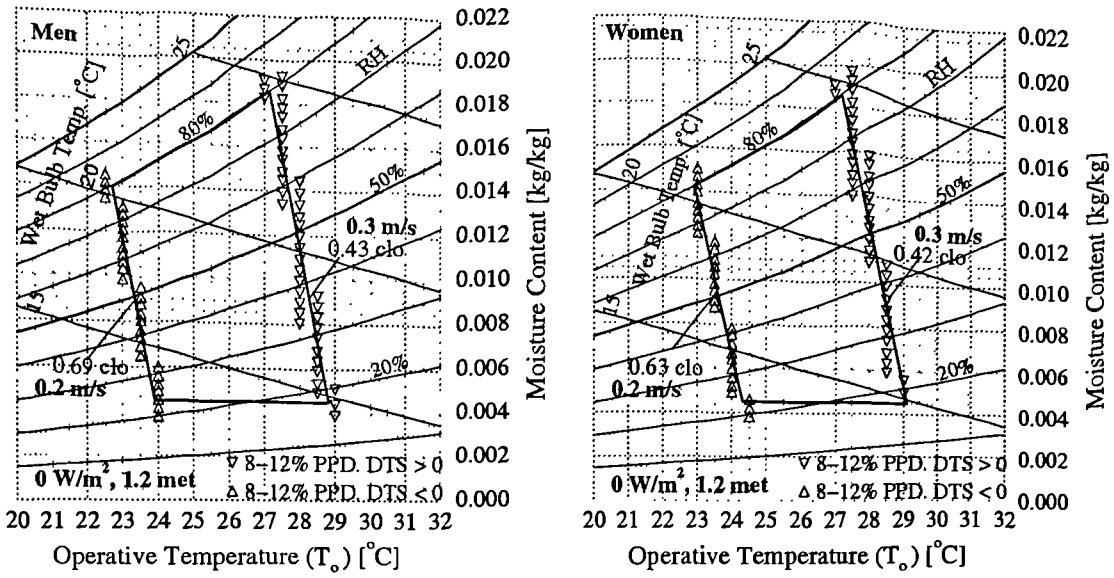

Figure 4-4. Men and women data comparison.

4.7.2.2 Analysis of the new comfort envelopes

In the absence of solar radiation (Figure 4-5), the new comfort envelope ranges between 22.7°C (80% RH) and 28.8°C (~17%RH) for minimum air speeds. This represents an enlargement of the tolerated temperature range of about 2 K when compared with the former comfort envelope (dashed lines in Figure 4-3) which was developed using a constant clothing level. A further extension of about 0.7 K towards warmer temperatures was achieved by increasing the air speed from 0.3 m/s to 0.6 m/s. However, further increases in the air speed produced successively less increase in tolerance to high temperatures. This is because at increased air velocities, the air temperature perceived as comfortable, approaches the temperature of the body surface.

To counter the thermal effect of diffuse solar radiation of intensity 50W/m^2, the operative temperature must be reduced. This is indicated by the shift of the comfort envelope by about 2 K, indicating a strong effect of solar radiation on thermal comfort. It can be seen in Figure 4-6 that the effect of air speed on comfort is more pronounced when solar radiation enters the

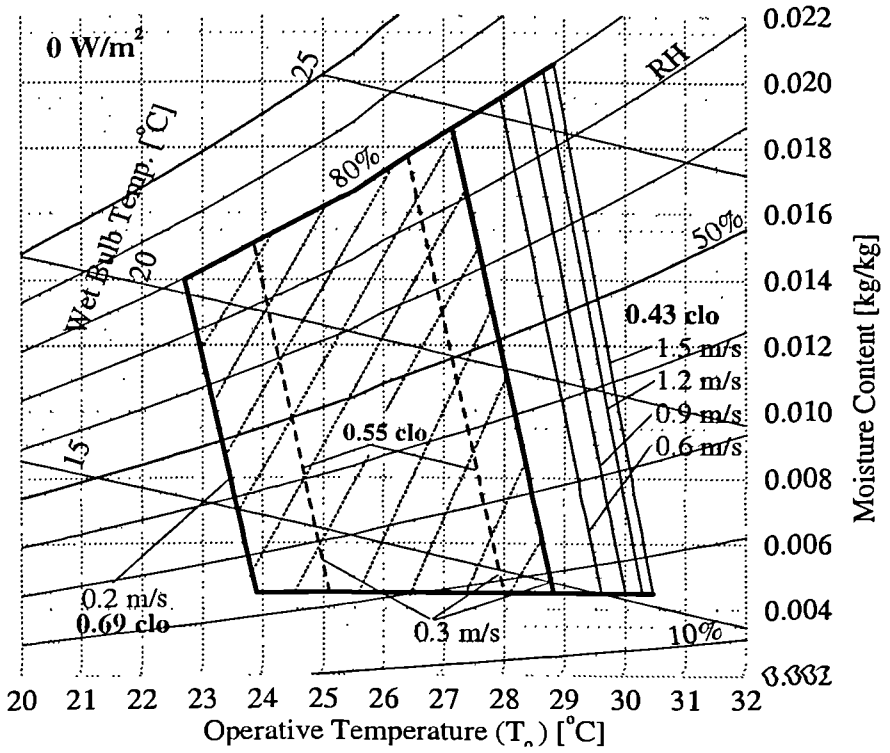

Figure 4-5. Comfort envelopes for 0 W/m² of solar radiation and different air speeds.

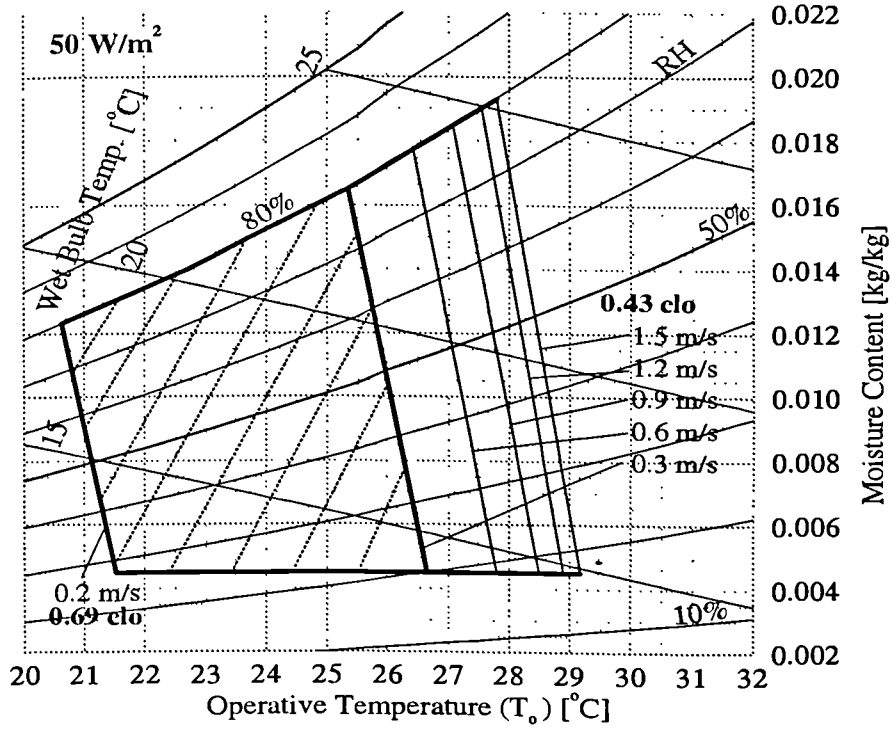

Figure 4-6. Comfort envelopes for 50 W/m² of solar radiation and different air speeds.

space than when it is excluded. This is because elevated air speeds are capable of removing more heat from the irradiated body surface.

So, an increase of air speed from 0.3 m/s to 1.5 m/s extends the acceptable comfort conditions in the presence of solar radiation by 2.4 K, but only by 1.7 K in the absence of solar radiation. In both cases the variation of *RH* with temperature was found to be linear at a rate of about 2.5×10^{-2} K/*RH*% which agrees well with published data obtained from comprehensive experiments, (Rohles & Nevins, 1971).

4.8 Summary

The comfort study carried out in this chapter ends with the presentation of the extended comfort envelopes that have been derived for hot summer conditions in office buildings. The adaptive behaviour of occupants has been investigated by considering changes in the clothing level, air speed and solar radiation. As a result, the new comfort envelopes extend from 22.7°C (80% *RH*) to 28.8°C (~17% *RH*) in absence of solar radiation. This is about 2 K wider than that obtained in the first approach, (Fiala et al. 1999). In the presence of diffuse solar radiation of 50 W/m^2 the comfort envelopes shift towards cooler air temperatures by about 2 K.

Increasing the air speed leads to an acceptance of warmer conditions but this effect becomes less efficient as the air speed continues to rise. It was also found that increasing air speed is more effective in the presence of solar radiation.

These extended comfort envelopes were developed for PDEC buildings. However, they may also be used to examine summer comfort conditions in other types of office buildings in which thermal adaptation is possible.

Chapter

5 *Passive Downdraught Evaporative Cooling*

"I do not seek. I find"

PABLO PICASSO

5.1 Preamble

This chapter describes Passive Downdraught Evaporative Cooling (PDEC). It outlines its background and physical principles i.e. evaporative cooling and heat and mass transfer processes. The advantages of using the system are outlined in Section 5.2. It also shows the building structure and the different operational modes. A literature review based on the use of PDEC in Section 5.8, and another dedicated to legionella issues at the end of the chapter.

5.2 Background

Passive Downdraught Evaporative Cooling (PDEC) is an energy efficient system based on natural ventilation which includes the cooling effect by evaporating microscopic drops of water. These drops of water, are injected into a hot dry air stream using micronisers. As the droplets evaporate the

relative humidity increases and the dry bulb temperature decreases achieving the desired cooling effect.

Natural ventilation is based on the existing air forces and density difference to move air through the building; and can contribute to a sustainable environment by reducing the electrical energy used in buildings. It not only reduces (or eliminates) the need for electrical energy to operate chillers, but even more significantly, it reduces the need for electricity to drive fans and pumps. Most naturally ventilated buildings imply narrower plans allowing the utilisation of daylight, thereby also reducing electrical demand for electrical lighting.

Ventilation is used to provide acceptable indoor air quality. Natural ventilation it is one of the oldest forms of ventilation strategy: used in the Middle East with wind towers. Recently, various projects have been carried out based on the PDEC strategy (Bahadori, 1985), such as experimental buildings in Arizona in USA (Cunningham & Thompsom, 1986) or the 'Avenue of Europe' cool towers at the Seville Expo'92 (Rodriguez et al. 1991].

More recently Ford & Associates have incorporated PDEC towers within a new 12000 m^2 Pharmaceutical research and Development Laboratory in Ahmedabad in Northern India. It has been shown by simulation linked to physical testing, that PDEC can maintain thermally comfortable conditions in general purpose office spaces.

5.3 Why PDEC?

The UK, along with most other countries, has recognised the need for sustainable development. This means that building designers must satisfy the needs of today's users without leaving problems to be solved by future generations.

By using the PDEC strategy in buildings, several benefits are obtained such as reducing the dependency on non renewable energy sources, and thereby

reducing atmospheric pollution arising from the gaseous emissions associated with the combustion of fossil fuels.

Carbon dioxide (CO_2) emissions will be reduced due to the energy saving provided using PDEC, thereby helping to reduce the greenhouse effect. Emissions of ozone depleting substances (mainly CFCs and HCFCs) which result in damage of earth's protective ozone layer, will also be reduced. Important proportions of these emissions are from the refrigeration system used in the cooling of building (as the high CFCS contents refrigerant R-22). This reduction will help within the accepted plans of the United Nations (Agenda 21), the European Union (the Fifth Environment Action Plan: Towards Sustainability) and the EC's White Paper on Economic Growth, Employment and Competitiveness.

There are substantial economic benefits by the substitution of air conditioning with PDEC technology. Based on the 12000 m^2 laboratory building mentioned above, in Ahmedabad, Northern India (PDEC, !999) the capital cost of this PDEC building is 10% less than the same building with conventional air conditioning. Furthermore the annual running costs are predicted to be 75% less than the equivalent air-conditioned building.

A survey of over 1000 public and commercial buildings in Greece (Santamouris, 1992) has shown that the typical annual energy consumption for non-air-conditioned buildings is 140 kWh/m^2, while that for air-conditioned buildings is in the range 226-250 kWh/m^2. Such energy statistics, while not necessarily being exactly translatable to other Southern European members states, will represent a trend which is likely to be representative for Italy, Spain and Portugal. Since electricity is the predominant energy source for air-conditioning systems, there is great potential for energy savings and reduction in CO_2 emissions, through the introduction of PDEC systems in non-domestic buildings.

The experimental demonstration of the technical feasibility of PDEC (Cunningham & Thompson, 1986) in Arizona, and subsequent verification

of consistent results (Givoni, 1991) has revealed both technical benefits (avoidance of fans, chillers, duct work, etc.) and some of the limitations (large supply and exit shafts, open interior of building) of PDEC.

The further investigations (Alvarez, 1992) for Expo'92 has led to development of simulation tools to model aspects of PDEC and gain a greater understanding of some of the control problems associated with the use of microniser assemblies.

PDEC systems offer the following advantages:

- PDEC has the major advantage of avoiding the need for refrigerants. In existing buildings the potential of replacing conventional air conditioning with PDEC removes the problem of refrigerant use.
- Delivered energy use in conventional air conditioning is a small proportion of total energy use in a typical office building. However, because a large proportion of that is electrical energy, it is much more significant in primary energy terms.
- In terms of technical benefits, the simplicity of the principle of the system facilitates the growth of the system in emerging economies with hot dry climates.
- In terms of consumer protection, PDEC is likely to provide an improvement over conventional air conditioning which is associated with certain aspects of 'sick building syndrome'.

5.4 The principles of PDEC

5.4.1 Particle evaporation

PDEC systems are based on evaporative cooling-effect. This is an important application of mass transfer theory. This occurs whenever a gas flows over a liquid (see Figure 5-1). Evaporation occur from the liquid surface, and the energy associated with the phase-change is the latent heat of vaporisation of the liquid. Evaporation occurs when liquid molecules near the surface

experience collisions that increase their energy above that needed to overcome the surface binding energy.

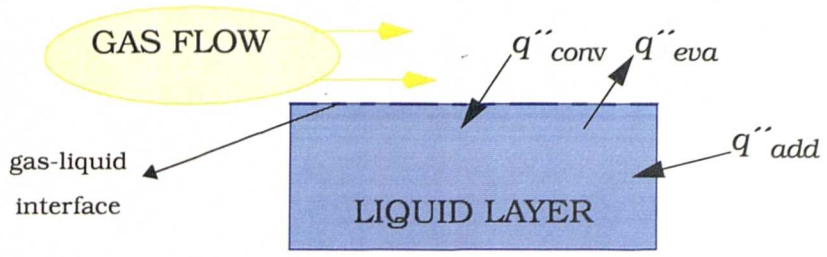

Figure 5-1. Gas flowing over a liquid showing heat exchanges.

The energy required to sustain the evaporation must come from the internal energy of the liquid, which then must experience a reduction in temperature (the cooling effect). However if steady-state conditions are to be maintained, the latent energy lost by the liquid due to evaporation (q''_{evap}), must be replenished by energy transfer to the liquid from its surroundings. Neglecting radiation effects, this transfer may be due to the convection (q''_{conv})of sensible energy from the gas or to heat addition (q''_{add}) by other means, as, for example, by an electrical heater submerged in the liquid. Applying conservation of energy to a control surface about the liquid it follows that for a unit surface area,

$$q''_{conv} + q''_{add} = q''_{evap} \tag{5-1}$$

where

q''_{evap} = latent energy lost by evaporation
q''_{conv} = sensible energy from the gas by convection
q''_{add} = energy added by other means

and where the latent energy lost by evaporation may be approximated as

$$q''_{evap} = n''_A h_{fg} \tag{5-2}$$

where

n''_A = evaporative mass flux

h_{fg} = latent heat evaporation of the gas

If there is not heat addition by other means, Eq 5-1 is reduced to a balance between convection heat transfer from the gas, and the evaporative heat loss from the liquid.

The principle of evaporative cooling is based on the relative large amount of energy required to convert water from its liquid form into its gaseous form, vapour. While the heat energy required to raise the temperature of water by 1 °C is 4.18 kJ/kg, the specific latent heat of vaporisation is 2257 kJ/kg. In the case of the evaporative cooling system this energy is supplied primarily by the intake air, whose heat content and capacity to hold vapour are indicated by its dry-bulb temperature and relative humidity.

A single water drop in a non-saturated environment experiences heat, mass and momentum transfer processes as follows

- If the air is warmer than the drop, the temperature gradient at the drop-air interface provokes a net heat transfer from the air to the drop surface.
- The concentration of water vapour near the water surface gives way to water diffusion from the drop surface to the non-saturated air. This water diffusion follows evaporation of water from the drop; due to the latent energy of this phase change. This mass transfer is strongly coupled to the heat transfer.
- If there is a relative movement between the drop of water and the surrounding air, a transfer of momentum between them will occur. This transfer of momentum tends to increase the rate of both the heat and the mass transfer. Thus the physical action of water drops falling through the interior air of the building may accelerate the cooling process

The first two phenomena have opposite effects on the thermal state of the droplet. The heat transfer tends to increase the drop temperature (t), whereas the mass transfer causes the drop to cool down.

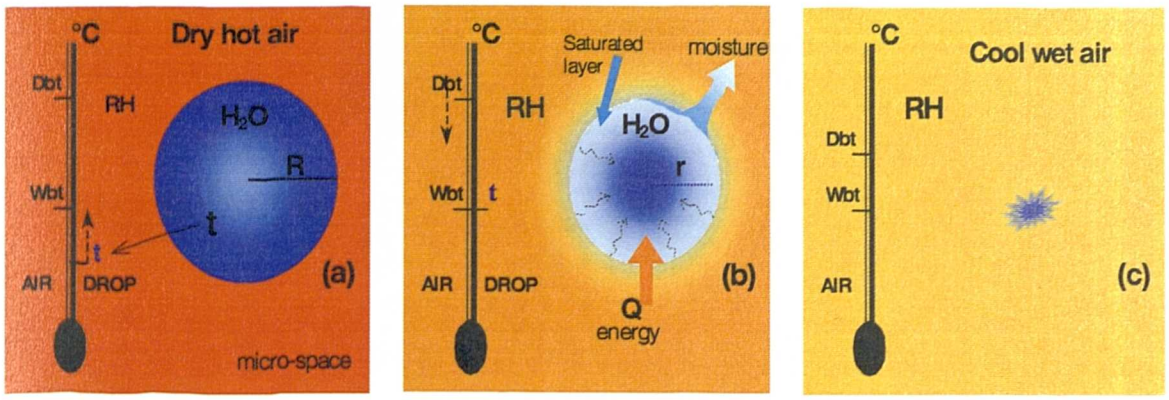

Figure 5-2. Evaporation process of a drop in a non-saturated environment.

As a result of these two opposite tendencies, an equilibrium drop temperature is reached (the wet bulb temperature of the air). Once the drop has reached the wet bulb temperature, the latent energy needed to evaporate more water is supplied only by the surrounding air and so the latter is cooled.

From the former considerations, two different periods in the evaporation of a single water drop in air can be distinguished (Lefebvre, 1.989):

- The drop temperature is changing from its initial temperature to its equilibrium temperature (air wet bulb temperature), Figure 5-2a-b.
- The drop is at its equilibrium temperature and the radius decreases with the evaporation, Figure 5-2b-c.

5.4.2 Evaporative cooling processes

There are four different types of evaporative cooling processes. These are more easily identified if using the simplified psychrometric chart (see Section 2.6). The processes are show in Figure 5-3.

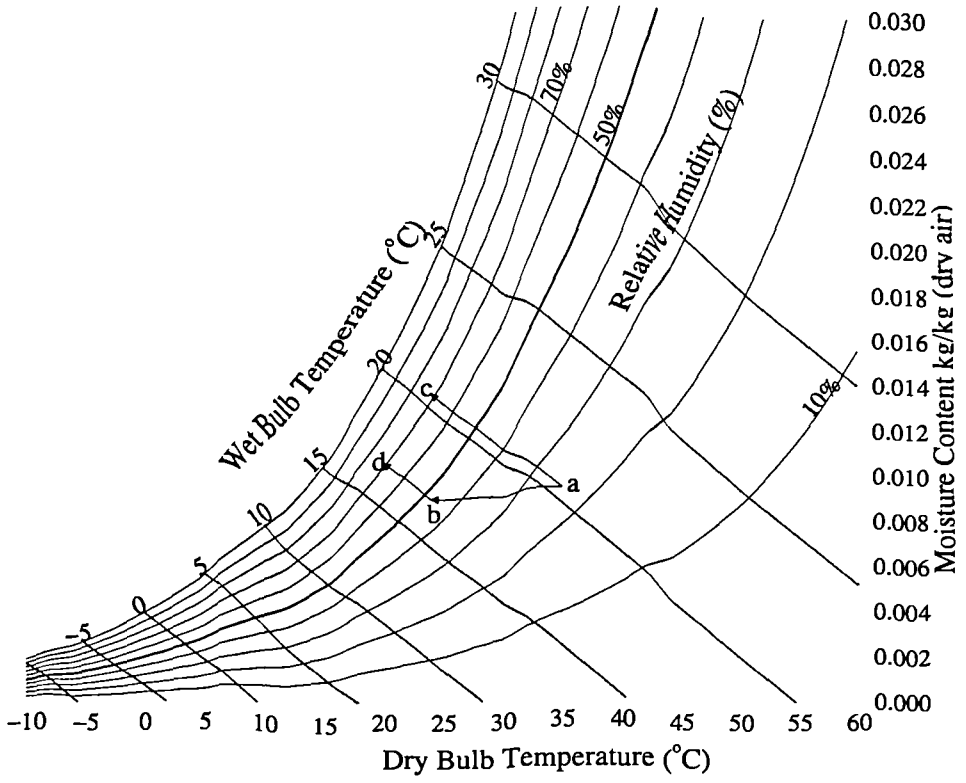

Figure 5-3. Evaporative cooling processes

Passive indirect evaporative cooling. Results from conductive heat transfer between a solid and a liquid. When the ceiling, or walls, are in contact with water, they can be cooled down acting then like radiant/ convective cooling panels. The process, represented in Figure 5-3 by the segment a-b, does not increase the relative humidity of the cooled spaces.

Active indirect evaporative cooling. In the process, ambient air passes through a primary circuit, where it is cooled by contact with the wetted heat exchanger. The zone-delivered air passes through the secondary of the circuit by the heat exchanger surfaces. There is no relative humidity added in this process, and the graphical representation in Figure 5-3 corresponds to the segmet a-b.

Direct evaporative cooling. This approach involves the evaporation of water into the delivered air stream, with a consequent relative humidity increase. Other than the use of micronisers, or other mechanical devices to

inject water into the air, there are other direct evaporative cooling techniques such as trees or grass that emit water into the air. This process moves along a constant enthalpy or wet bulb temperature line as shown by segment a-c in Figure 5-3.

Active direct evaporative cooling. This approach is similar to the one for active indirect cooling with the difference that the cooled air is directly delivered to the target zone.

There is also a combination of active direct and active indirect evaporative cooling. This approach is named two stage evaporative cooling. It is used when the required temperature is lower than could be achieved by any of the other approaches. It involves a pre-cooling process by an indirect heat exchanger (segment a-b in Figure 5-3), followed by the direct evaporative cooler (segment b-d in Figure 5-3).

5.5 Elements of a PDEC building

Four of the main architectural elements that constitute a PDEC building are shown in Figure 5-4 (Supply tower, capture zone, occupied zones and exhaust air routes).

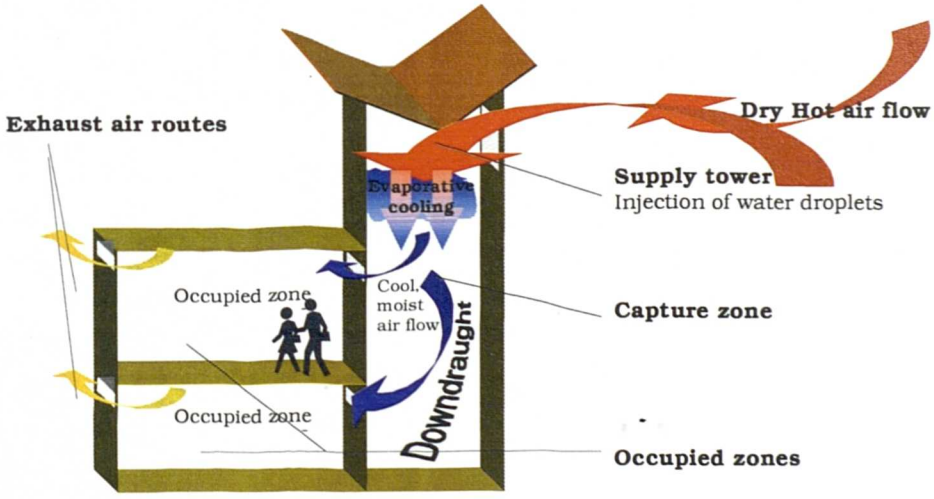

Figure 5-4. Main architectural elements of a PDEC building

The *supply tower*. Hot dry air enters the building via the supply tower, also called PDEC tower. The entrance of the tower is guarded by static or moveable elements that protect it against undesirable wind effects[1] or external agents such as rain, birds, etc. Inside the tower are micronisers what produce the evaporative cooling effect. The tower may also permit daylight to enter the building contributing the natural lighting of the building. The *capture zone* is a space where the cooled air accumulates. It is directly linked to the occupied spaces via openings, either in the floor or in the ceiling, from where the cool air is delivered. Depending on the building cooling demands, the capture zone can be a small sealed lightwell or shaft or if is bigger, it can be an atrium. The *occupied zones* are the spaces to be cooled. They must be link to the capture zone by manually or automatically controlled openings. The cool air passes through the occupied zones leaving via the exhaust zone. The *exhaust air route* is the zone from where the cooled air leaves the occupied zones. Figure 5-5 shows a picture of a real building which was used as an architectural exercise in implementing PDEC.

Figure 5-5. Pavilion of Americas in Seville EXPO´92

1. Positive pressures can drive undesirable hot dry air into the capture zone or negative pressures can draw cooled air out of the capture zone.

The real building has to be divided into PDEC zones. These are the areas influenced by the same tower. Figure 5-6a-b shows the whole building with the four corners, called courtyards. The section (Figure 5-6c) and the plan (Figure 5-6d) are also included.

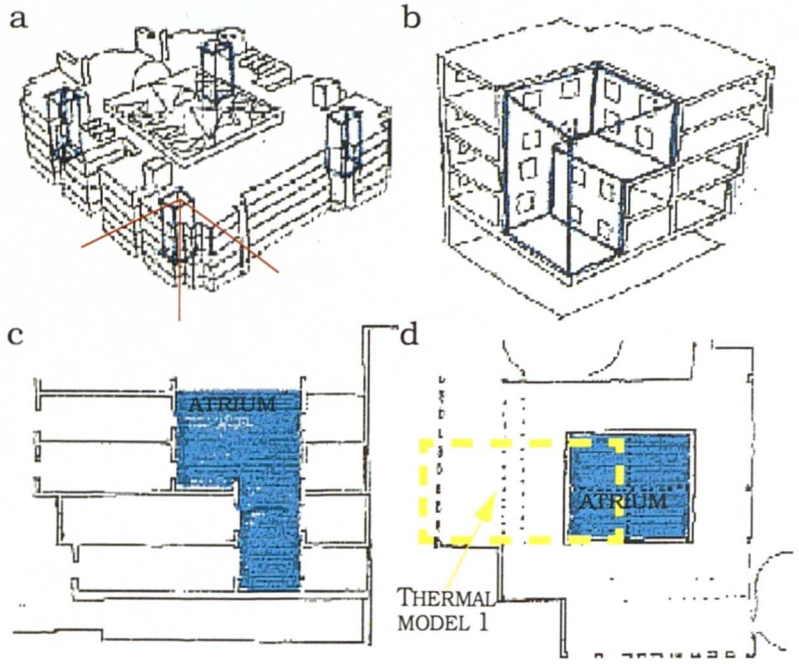

Figure 5-6. Diagram of the implementation of the PDEC system in the Pavilion of Americas.

The blue area represents the atrium, used as the capture zone. The dashed yellow rectangle in Figure 5-6d corresponds with the simplified model used in chapter 6 for the simulations, Figure 6.1.

5.6 Experimental building

The experimental building located in Catania was used during the PDEC project to compare measured data with the simulation results. Figure 5-7 shows the experimental building designed for Catania.

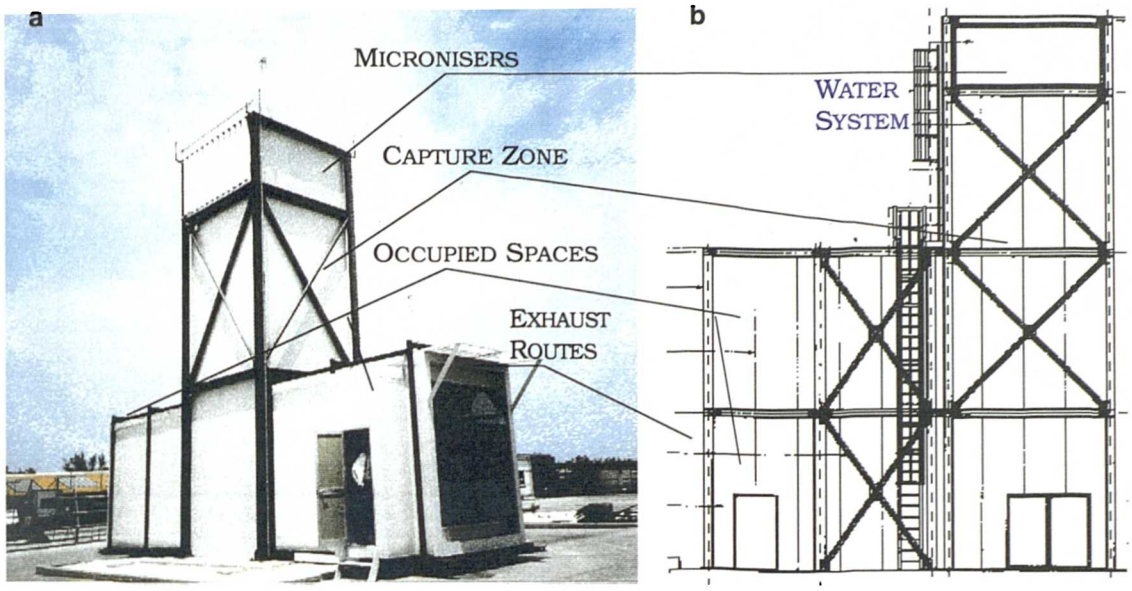

Figure 5-7. Catania building and architect drawings.

The water circuit is a small pump system with the filters and micronisers. The diagram for the Catania building is shown in Figure 5-8.

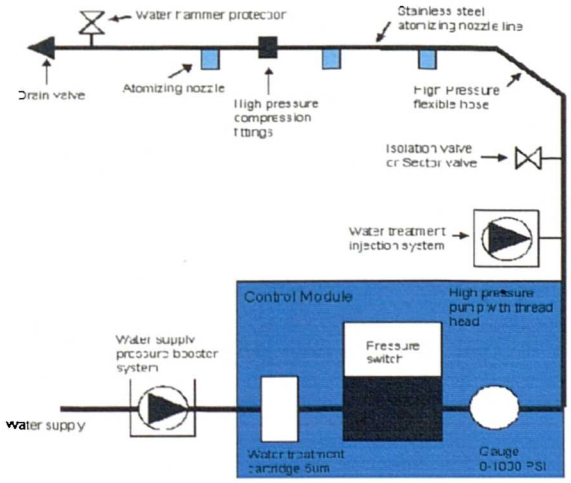

Figure 5-8. Micronisers water circuit in the Catania facilities.

5.7 Operating modes

PDEC combines the cooling effect of the evaporative cooling with natural ventilation, to deliver cooled air into the occupied spaces. This will reduce and in some cases replace the need for mechanical cooling. In striving to achieve this goal, the system is assisted by other low-energy cooling strategies as night cooling (or night venting) or natural ventilation. PDEC can be considered at the top of the passive systems to cool a building, before mechanical cooling is needed. The lower step of the systems use, can be natural ventilation. The sequence of systems usage before switching on (if needed) mechanical cooling to maintain indoor comfort could be:

- Natural ventilation
- Natural ventilation + night cooling
- Natural ventilation + night cooling + PDEC
- Natural ventilation + night cooling + PDEC + mechanical cooling

These systems are explained in more detail in the thermal simulation chapters 6 and 7.

5.8 Literature review

5.8.1 PDEC and passive systems

Givoni (1992) discusses issues of thermal comfort standards, including the ASRHAE comfort zone and techniques of graphical climate data analysis, as well as the use of building bio-climatic charts in the information of buildings design guidelines, especially for hot climates. Revised building bio-climatic charts are described for the first time in this paper. The boundaries of applicability of various building design strategies and passive cooling systems in different climates is discussed. These strategies are based on the expected indoor temperatures achievable with the different strategies and include daytime "comfort" ventilation, the utilisation of the structural mass for thermal storage in conjunction with nocturnal ventilation (night cooling) and direct and indirect of evaporative cooling.

The potential of different passive cooling strategies for popular residential buildings in Israel is evaluated by Hassid [1994], using the building energy simulation programs ESP-r and DOE2.1.E. The passive cooling strategies considered are: night cooling, ground cooling, evaporative cooling (direct and indirect) and radiative cooling. The basis of the study is a reference building characteristic of popular residential homes in Israel. Two climatic regions are considered, typical days are analysed, an average summer day and a particular hot day in the spring. The relative merits of each strategy as well as their savings potential are discussed.

Picard (1993) proposes to share theoretical and practical knowledge gained in the evaporative cooling field in a joint project between CSTB and Gazette de France. A performance assessment of evaporative systems is presented that was undertaken though numerical simulation for various building and locations. Implementation of indirect evaporative cooling is presented for two operations. Design issues and potential of the technique are discussed based on a two-year marketing study. Today, the trend in France for office buildings would be to view indirect evaporation as a complementary cooling technique due to its limited performance. Future research areas are outlined based on the proposals made at a 1991 IEA workshop.

The design of thermal and energy efficient buildings requires a combination of the investigation of the passive performance, natural ventilation, mechanical ventilation as well as structural and evaporative cooling of the building. Only when these fail to achieve the desired thermal comfort should mechanical cooling systems be considered. Few computer programs have the ability to investigate the comfort regulating methods at the design stage. The QUICK design program (Mathews et al., 1994) can simulate these options with the exception of mechanical cooling. In this paper, QUICK's applicability is extended to include the analysis of basic air-conditioning systems. This paper addresses validation in general and the purposes a procedure to establish the efficiency of a program's load predictions. This proposed procedure compares load predictions by the ASHRAE, CIBSE,

CARRIER, CHEETAH, BSIMAC and QUICK methods for 46 case studies involving 36 buildings in various climatic conditions. It is shown that system size and energy usage can be reduced by more than 60% by using a combination of passive and mechanical cooling systems as well as different control strategies.

The performance of an indirect evaporative cooler using TRNSYS code was studied by Klitsikas (1994), by simulating its operation in a typical building, using the weather data of Athens. They calculated comfort hours and the hours of cooler operation per day. The sensitivity of the performance upon night ventilation rate and the size of the south window glazing was also investigated. Simulation results showed that the cooler, increases the number of comfort hours per day inside the building, since the indoor temperature is significantly cooler when the system operates than under the free-floating conditions. It was found also that night ventilation increases the comfort hours of the building while reducing the hours of operation of the cooler.

Williamson (1985) describes an approach to assess thermal comfort based on the Predicted Mean Vote concept, as a suitable index of discomfort for housing with evaporative cooling. This index accounts for all-important environmental factors and in addition allows dynamic modelling of human responses to the thermal environment, such adjusting clothing levels and metabolic rate. The computer program TEMPAL is used to predict internal environmental conditions within a dwelling. TEMPAL is shown to be sufficiently accurate for this purpose by comparing predictions with monitored conditions. Using this technique the thermal conditions produced by evaporative and refrigerative cooling plant are compared.

One of the key-factors when designing PDEC buildings is the tower. A design was proposed (Bahadori, 1985) to improve the performance of wind towers for natural ventilation and passive cooling. Under similar climatic and design conditions, the new design is capable of delivering air to the building

at higher flow rates. It can also cool the air by evaporation to lower temperatures. Momentum, mass and energy analyses are carried out for the proposed design. The results are presented in graphical forms which may be used as guidelines for employing the design for specific applications in the hot, arid areas of the world. An example is given to show the use of the results.

5.8.2 Legionella issues

One of the more controversial issues that PDEC systems must face when observed as an alternative natural cooling technique, other than the obvious building and thermal limitations, is the legionella risk, addressed in meetings, conferences and wherever PDEC has been presented. An extensive research to solve this difficulty has been carried out, and is presented in this section.

Legionella bacteria, the causal agent of Legionnaire's Disease, is a water-based organism which causes infection when inhaled in an aerosol form. Many building water systems have been linked to outbreaks of Legionellosis, and the bacteria have been isolated from numerous different sources. One of the most frequently cited causes of endemic outbreaks of Legionellosis is the operation of evaporative cooling towers.

Legionnaires' Disease is a severe, progressive form of pneumonia which is fatal in up to 15 percent of cases. The estimated rate of infection is 6 cases per 100,000 head of population in the USA (CDC, 1993). The route of infection is through inhalation of an aerosol spray containing the viable bacteria. Some studies (BACS, 1989) have suggested that infection may also be caused by aspiration of water containing the bacteria

The bacterium is fastidious in its nutritional requirements, and initially proved difficult to culture, with an absolute requirement for both iron and the amino acid L-cysteine to grow. Temperature for optimal growth is in the region of 36°C though growth can occur between 20°C and 40°C. Below

20°C the bacteria is dormant though still viable, above 45°C the bacteria will start to die off over time (BSI, 1992). Studies have shown (NHMC, 1989) that the bacteria can survive in a dormant, viable condition for periods of up to two years even in waters with very low nutrient levels.

Several natural water systems and many man-made water systems have been shown to refuge the Legionella bacteria. Some man-made systems from which Legionella bacteria have been isolated are:

- Mains water supplies
- Cooling towers
- Potable hot and cold water systems
- Re-circulating water humidifiers

These systems can become amplifiers, providing ideal conditions for the growth of Legionella bacteria. In order for the Legionella bacteria to be infectious it must be inhaled deep into the lung. The quantity of bacteria required to initiate infection will vary between individuals.

Legislation requires that systems are operated in such a way that the risk of Legionellosis to employees, contractors and members of the general public is minimised. One of the major changes in the UK has been in the approach to water management programs after the advent of The Health and Safety Executive's guidance notes HS (G) 70 (HSC, 1994) and the Health and Safety Commissions' Approved Code of Practice for the Prevention or Control of Legionellosis, (HSE, 1993). Some of the key elements in this legislation are the requirements for a responsible person to be nominated to manage the water treatment program.

Also required is a defined route of communication between the responsible person and the other members of an organisation. As there can be no responsibility without authority under English law, one tends to find that the responsible person is a senior manager or director of the company. The aggressive approach of the Health and Safety Executive, supported by local

Environmental Health Officers, in prosecuting both companies and individuals for failure to take reasonable precautions to control risks from Legionellosis, focuses the attention of these individuals. With significant fines and the possibility of jail sentences most organisations find it beneficial to comply with the legislation.

The legislation (HSC, 1994) mentions many specific water systems but makes it clear that all water systems should be included. This is performed by following the steps set out below:

- Perform a risk assessment of all of the water systems on site
- Appoint a responsible person to manage the water treatment program and write down the route of delegated authority
- Produce a written plan of maintenance to minimise the risk, this includes both remedial works and ongoing maintenance, with written methods covering each task
- Train all of the personnel who will be involved in the route of delegated responsibility
- Implement and manage the written maintenance plan, this should include recording each task performed in a site log book
- Regularly review the program to ensure that control is being maintained

The legislation applies not only to plant operators but also to contractors, suppliers and consultants who may be involved in these works. Design of new and modified plant must take into account the requirements of HS(G) 70. Any organisation which does not feel that it has sufficient competency in house, may appoint consultants, to provide the risk assessment and written plan provided the organisation appointed could prove its competency.

HSE (1993) includes many design, operation and maintenance criteria to help minimise the risk of Legionellosis from building water systems included among these are:

- avoid temperatures in the range 20°C to 45°C for potable water systems
- avoid dead-legs in distribution systems
- install de-stratification pumps for water heaters
- routine cleaning and chlorinating every six months for evaporative cooling systems
- routine cleaning and chlorinating every month for shower heads
- maintain cooling systems in a clean condition with the application of routine water treatment programs
- install high efficiency drift eliminators
- avoid construction materials which may harbour Legionella or support its growth
- Design and construct systems to allow ease of access for cleaning and chlorinating works and to enable systems to be taken out of service for such cleaning as required.

Routine testing of cooling systems for the presence of viable Legionella bacteria should be considered as the only way to show that the water treatment program is providing effective control (Brundrett, 1992). It is possible to operate cooling systems such that viable Legionella bacteria are not detected in the bulk water. It is suggested that Legionella testing is not a substitute for good maintenance procedures, but should be an integral part of those procedures. These maintenance programs need not involve excessive cost, but do require some managerial input.

A survey was carried out by Hodgson (1998) from 5838 samples taken from different water systems: evaporative cooling towers, drinking water supplies, hot water heaters and potable water distribution systems. Results

shown that just 6% of the samples were Legionella positive for the cooling towers, against 12% for hot water heaters, and 7% for potable distribution water systems. These results demonstrate that there is not an extra risk of Legionella linked to cooling towers. Some specific requirements could be applied to buildings with PDEC system due to its particular design as follows. (i) the micronisers used to spread the water can be treated as a shower head regarding treatment procedure, (ii) the water supplied by the micronisers can be treated as drinking water (which will improve its storage conditions).

If, for any reason, the risk of Legionella is high, the water supplied by the micronisers can be pre-heated (possibly by solar panels) to 60°C for 2 hours or to 70°C for a rapid kill of 100% of the bacteria (NHMC, 1989).

Another method to eliminate the bacteria from the water is by using UV radiation. A powerful UV radiation of 254 nanometers wavelength damages the DNA's bacteria causing its death. This does not alter the chemical composition of the water nor its characteristics. Although this system is more expensive, results are guaranteed (Rex Iberica S.A.)

5.9 Summary

This chapter has shown the ongoing research related to natural ventilation techniques and especially with the PDEC system. The advantages of using passive cooling techniques have been pointed out. The PDEC system, elements and operational modes have been explained. The controversial legionella issue, always related with the PDEC systems, has been examined.

Chapter

6

Thermal Simulation Analysis. Model I

"The difference between 'involvement' and 'commitment' is like an eggs-and-ham breakfast: the chicken was 'involved', the pig was 'committed'."

UNKNOWN

6.1 Preamble

This chapter introduces the thermal simulations. It presents the background of the PDEC modelling techniques and the emulation process used. The chapter describes the first of two thermal models developed, and presents the results obtained. The analysis of the results is outlined at the end of the chapter. Some of these results will influence the second thermal model described in the next chapter.

6.2 Simulation processes

Simulation is defined as the examination of a problem often not subject to direct experimentation by means of a simulation device. Also as the imitative representation of the functioning of one system or process by means of the functioning of another "a computer simulation or an industrial

process". In the field of building design, these processes can represent from movement simulation to estimate the building population build-up at critical points such as evacuation at emergency conditions, to capital and running cost predictions to predict any variable, such as inflation rate, fuel inflation or building life. Energy analysis systems are used to provide insight into issues of comfort, energy savings, management strategies or the impact of various operational scenarios. These energy tools deal with the system discretisation to solve energy equations by finite difference (or other methods), including factors such as radiation, air flows, heat sources, climate, etc., combined with the plant simulation, i.e. single or multi zone systems. They are better know as DTS (Detail Simulation Program). One of these programs is ESP-r (ESRU, 1998) and is the one used for this research.

6.2.1 Simulation tool: ESP-r

The program ESP-r (Environmental Systems Performance) was developed by the Energy Simulation Research Unit (ESRU) at the University of Strathclyde in Glasgow. The version used in this work was ESP-r Version 9 Series, ESRU (1998).

ESP-r requires a simplified presentation of the building. This is done by grouping together areas of the building with similar thermal characteristics into one computational zone. For geometrically complex buildings, the geometry input is a tedious process, requiring manual input of all co-ordinates (although recently a translator has been developed which can interpret DXF files generated by AutoCAD). A type of construction, and boundary conditions, have to be assigned to each surface. Construction types are taken from a multi-layer construction database, which has to be assembled from in-built or user-defined materials. Internal heat gain and heating system profiles have also to be defined.

The heart of the program is the main calculation engine, bps. Input file generation, simulation and results analysis can be co-ordinated via the graphical menu-driven project manager, *prj*. A binary random access results

file is generated by *bps* and is accessed by the module *res* to obtain the results in either graphical or tabular form. Surface shading and the internal distribution of solar radiation are calculated by the module *ish*. The distribution of internal longwave radiation can be calculated using the module *mrt*. A binary climate file is used by *bps*. This is generated via *clm* from an ASCII file which can be created by the user. Measured values of casual gains and infiltration rates can be supplied for each simulation time-step via separate files. The following module versions were used: prjv2.1a, bpsv8.1a, clmv6.5a, ishv1.3b, mrtv2.4b, resv4.10b.

The main inputs that ESP-r used in this work are building location, zones geometry, orientation, contructions, materials. Occupancy level, periods, and internal gains. Operation modes, air flow rates, infiltration values and set point temperatures. Climatic conditions, temperature, humidity, radiation, wind speed and direction. The main outputs that have been used from ESP-r in this work are zone temperature and relative humidity and air flow rates in the zones.

ESP-r incorporates extensive checks to try and identify data errors. The program is mainly installed on SUN workstations, although it can be compiled on other UNIX platforms (no PC version is available). It is freely available to researchers and is used in 24 countries. The program is constantly being expanded to include new facilities such as: air flow analysis (simple zone-based, as well as linked to a CFD code; detailed plant modelling; calculation of 2D and 3D heat flows; and lighting energy use linked to daylighting and visualization of the building using RADIANCE.

6.2.2 Emulation technique

At the time of this research none of the existing building simulation codes were able to explicitly model PDEC systems based in fogging nozzles or micronisers. The American programs BLAST (Osbaugh and Moore, 1998) and DOE2 (Peterson and Hunn, 1983) incorporate models of active evaporative cooling systems and the Dutch program ACCURACY has an

evaporative cooling tower model (Niu and Van der Kooi, 1997). The South African model EASY can in principle model passive direct evaporative cooling (Mathews et al.,1994), but delivered cooling flux is predicted on the basis of scheduled air exchange rates. Giabaklou and Ballinger (1996) have incorporated a passive direct evaporative cooling model that does predict the induced air flow rates into the Austrian program CHEETAH. However, this is based upon a rather crude single zone mass flow algorithm. Furthermore, the model is limited to consideration of water flowing along vertically suspended filaments, for which convective heat transfer is modelled using a bundled tube correlation.

More recently, as part of the PDEC project (see Chapter 1.2), an attempt was made to incorporate a stand alone "PDEC tower model" (Rodriguez et al., 1991) into the simulation program PASSPORT+ (Alvarez et al., 1995). Because this software is still under development and not yet widely available and in order to maximise the user base of PDEC performance evaluation methods, this research concentrates on using the modelling capabilities of standard programs. Methods for emulating PDEC have therefore been sought.

To simulate the PDEC performance a specific application from ESP-r is used. ESP-r allows the user to change the heating/cooling set point of a certain zone at each simulation time-step by using a boundary file. If an ideal control is applied to that zone, providing the cooling or heating needed, the set temperature will be the zone temperature. The boundary file contains time and dry bulb temperature. The latter has been reduced by 70% of the wet bulb temperature depression of ambient air. This boundary file is used as the zone set temperature. Providing there is an "unlimited" cooling device, the temperature in the zone will be maintained at the set point temperature. This emulates the effect of the evaporative cooling process occuring inside the zone.

Note that the emulation process is crude because it is based on the assumption that the air entering the capture zone is 70 % of RH, whatever the external relative humidity is. This leaves some question marks that will addressed in the second model.

6.3 Thermal model 1

With this first approach of emulating the PDEC system, the aim is to evaluate whether a relationship between simulation results and climate data can be established. A simplified model, corresponding to a slice of a building has been considered. The simulation results will be plotted together with the climate data that has been used to generate them. This first approach studies the effect of building mass and internal heat gains on the thermal performance of the building for one scenario: night cooling plus PDEC.

6.3.1 Description of the model

The model was approached by modelling a typical "slice" of one intermediate floor of a typical PDEC building (see Figure 5.6). It consists of 3 thermal zones. These are Perimeter, Core and PDEC Capture zone as shown in Figure 6-1.

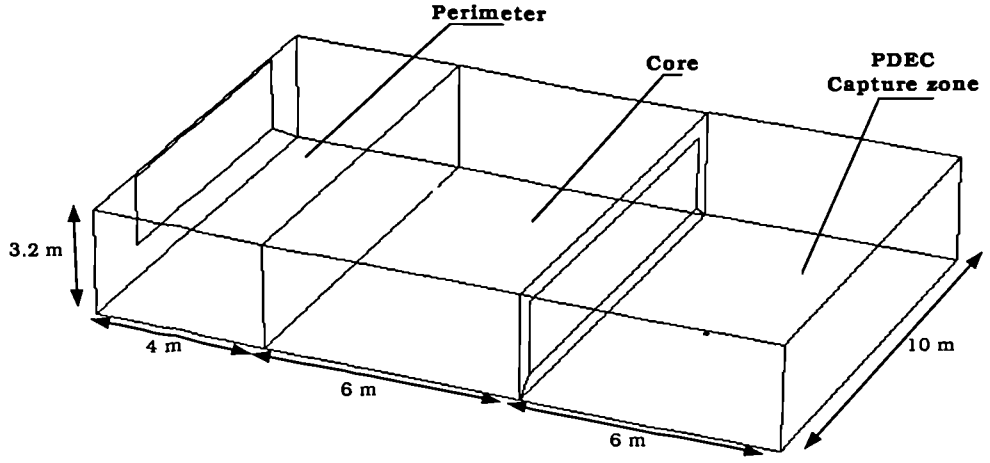

Figure 6-1. Geometry and zones distribution of the model

The proposed building is located in Seville, for its dry and hot climate. The building is used as an office. The space is divided by moveable screens and fixed partitions. The space dimensions have been considered by design experience, and related to the real depth plants applied in naturally conditioned and daylit buildings.

Geometry and constructions

The Perimeter zone is 4 m deep, giving a floor area of 40 m^2 and a volume of 128 m^3. Has a double glazed window (U-value = 2.75 W/m^2K) covering just under half of the external wall area. The external wall is breeze block, with 70mm insulation and 15mm plaster. The lateral walls are made of leaf brick with plaster both sides. The floor was assumed to be carpeted, thereby de-coupling any thermal mass from the zone air. A different construction file was generated to simulate the low-mass model: both side wall were substituted by double glazing screens and a suspended ceiling with 250mm air gap rather than original exposed ceiling.

The Core is 6 m in depth, resulting in a floor area of 60 m^2, and a volume of 192 m^3. The wall facing the supply zone is composed by a 40 mm. insulation layer in the middle and breeze block (70 and 110 mm) and 15 mm plaster in both sides. For the low-mass model the same changes to those for the perimeter zone were made.

The PDEC capture zone was modelled as an "open space"[1] (with fictitious walls, and connected to an adiabatic environment). This is the zone where the boundary file (see 6.2.1) is referred. It was assumed that the roof will be insulated and shaded, and that the heat loss and gain characteristics of a possible top floor will not differ from intermediate floors.

1. This is the terminology used to describe a different thermal zone, which is not separated from the next zone by real walls or windows.

Occupancy and internal gains.

The building was assumed to be occupied from 08:00 until 20:00 on weekdays and unoccupied at weekends. Occupancy density of 1 person per 14 m^2, resulting in a heat gain of about 7 W/m^2. (Katsikakis & Laing, 1993), and average internal gains from lights and equipment was 27 W/m^2. From this, three different values of 10, 30 and 50 W/m^2 for low, medium and high internal gains rates were adopted. These values have been widely adopted along the research study for other projects and simulations and based on CIBSE guide C, section 6 (1999).

Operation mode

Night venting at 4 ac/h was assumed to operate from 23:00 to 07:00, weekdays and weekends. A rate of 20 ac/h from the Capture zone to the Core zone was assumed for the occupied hours (08:00 – 20:00), which was assumed to operate uninterrupted for this period. The same rate of 20 ac/h from the Core zone to the Perimeter zone was imposed. This hypothetical value of 20 ac/h will ensure the PDEC system will satisfy worse case conditions. A background infiltration of 0.5 ac/h was set for the remaining hours. No airflow network has been implemented, instead the PDEC system is assumed to work in "free float"[2] mode.

2. Free float mode describes the system function where no control is been applied, leaving the zone "free" to behave.

6.3.2 Presentation of the results

The principal aim is to investigate the behaviour of the PDEC system together with hot climatic conditions. The period of analysis was summer, from June until September (September is still a warm month in Seville). Only the occupancy period (08:00 - 20:00) for weekdays, when PDEC is working, will be analysed.

Results are presented by plotting the data into the simplified psychrometric chart (ref. chap 2). These graphs include sets of data, for external (climatic) and results (zone) conditions. The four different series of data plotted are:

- Climatic conditions that terminate at a comfortable condition (inside the comfort envelope). Referred as *Climate, comfort* (green circles).
- Climatic conditions that terminate at an uncomfortable condition (outside comfort envelope). Cited as *Climate, no-comfort* (red circles).
- Zone temperatures that are inside the comfort envelope. Referred as *Zone, comfort* (cyan circles).
- Zone temperatures that are outside of the comfort envelope. Referred as *Zone, no-comfort* (orange circles).

The comfort envelope used as the "target" area has been selected from the extended comfort envelopes developed by the author (Martinez et. al., 1999) and corresponds to the $0W/m^2$ and air speed of 0.3 m/s. The reason for choosing the no radiation comfort envelope is because the core zone (where the simulation results are taken from) is considered to be affected by solar radiation. The graphs are grouped by internal gains, for both low and high mass buildings:

Note that the results of the simulations (zone temperatures) and the corresponding climatic conditions that generate them, which appear out of the comfort zone for the left side (DTS negative, or cold temperatures) will be ignored because the focus of this research is cooling not heating.

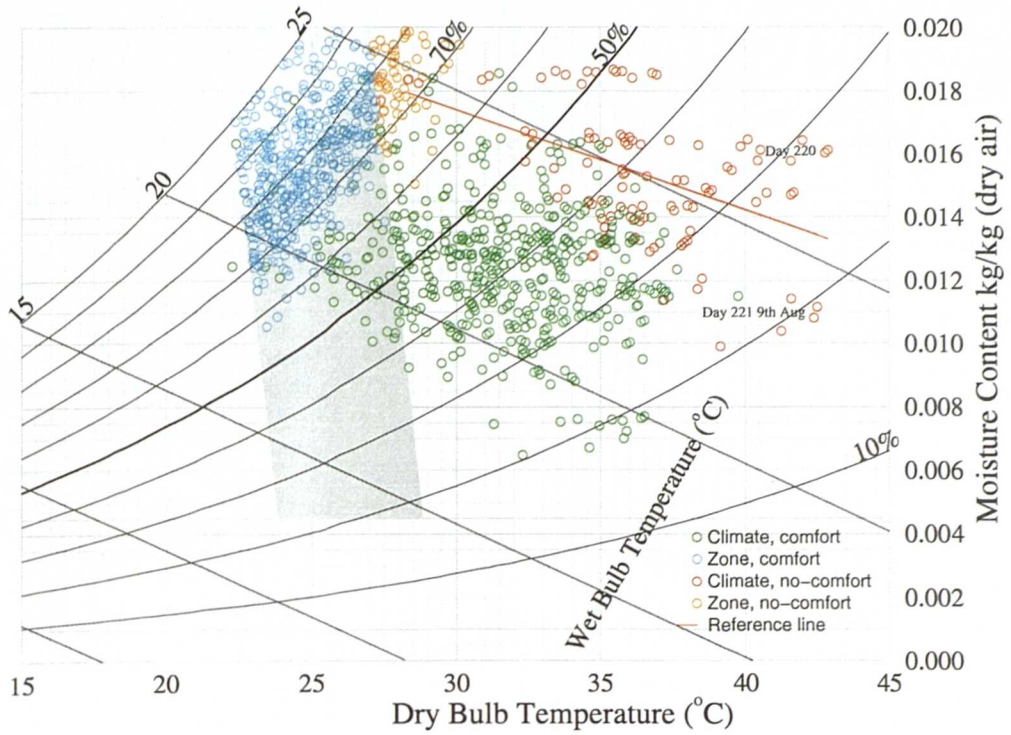

Figure 6-2. Low mass building, 10 W/m^2 internal gains.

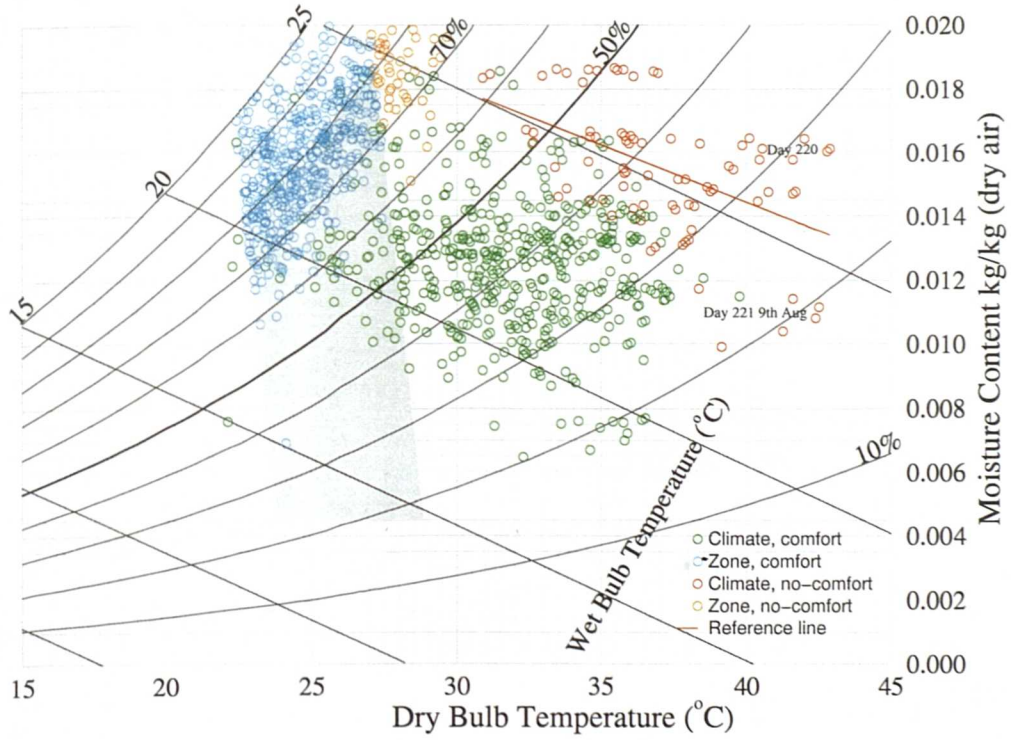

Figure 6-3. High mass building, 10 W/m^2 internal gains.

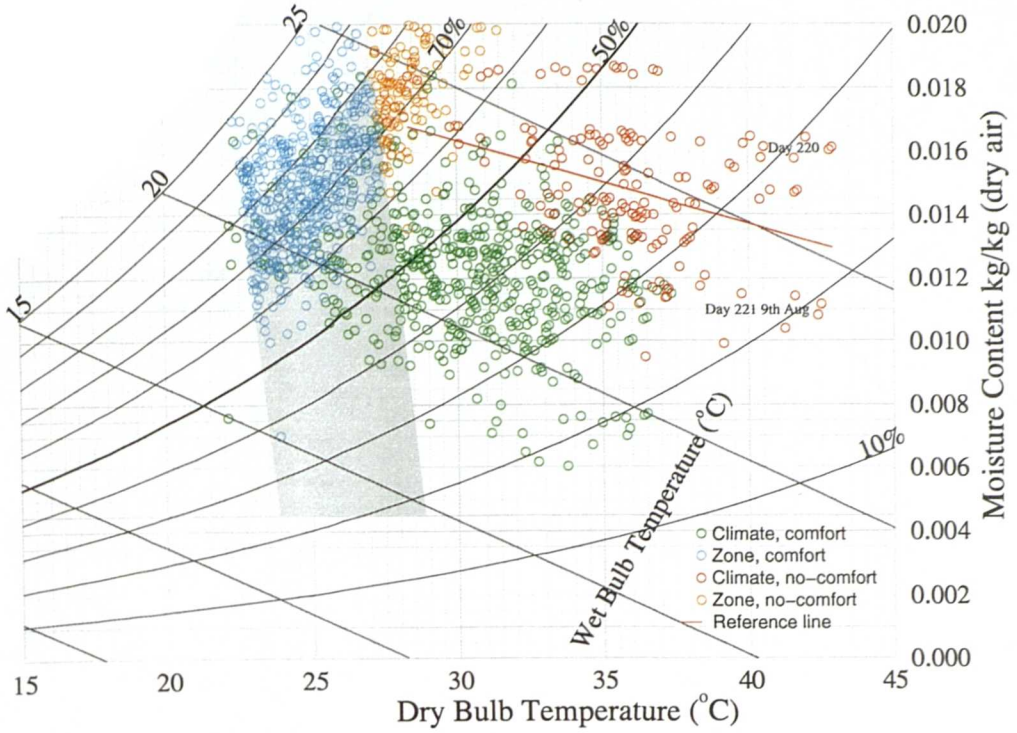

Figure 6-4. Low mass building, 30 W/m^2 internal gains.

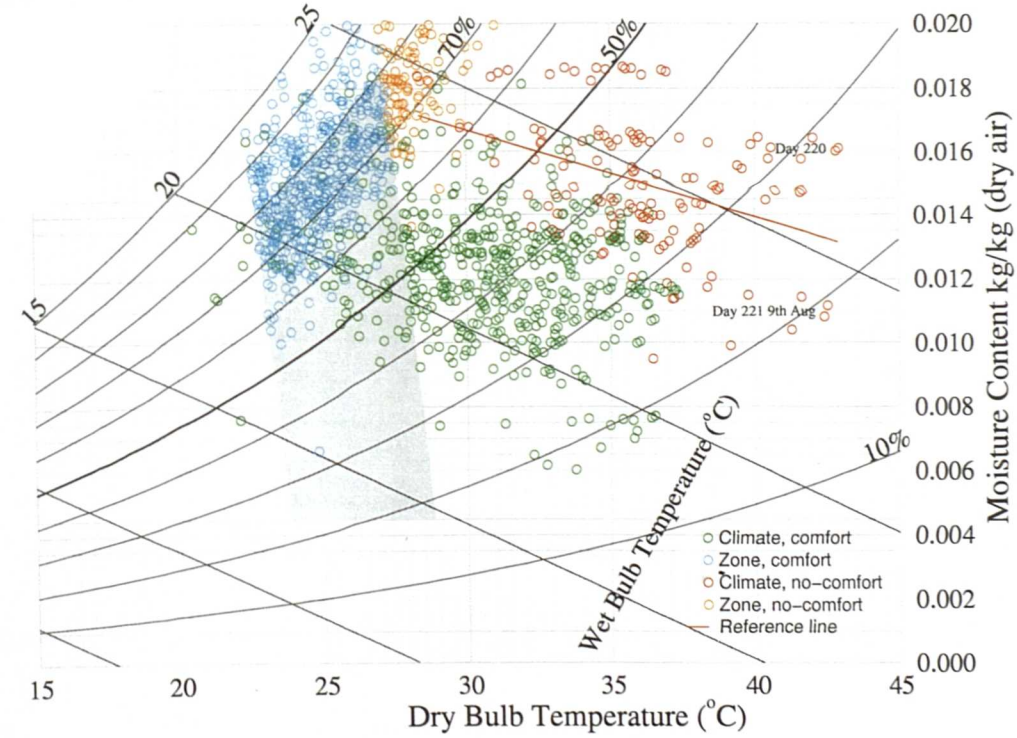

Figure 6-5. High mass building, 30 W/m^2 internal gains.

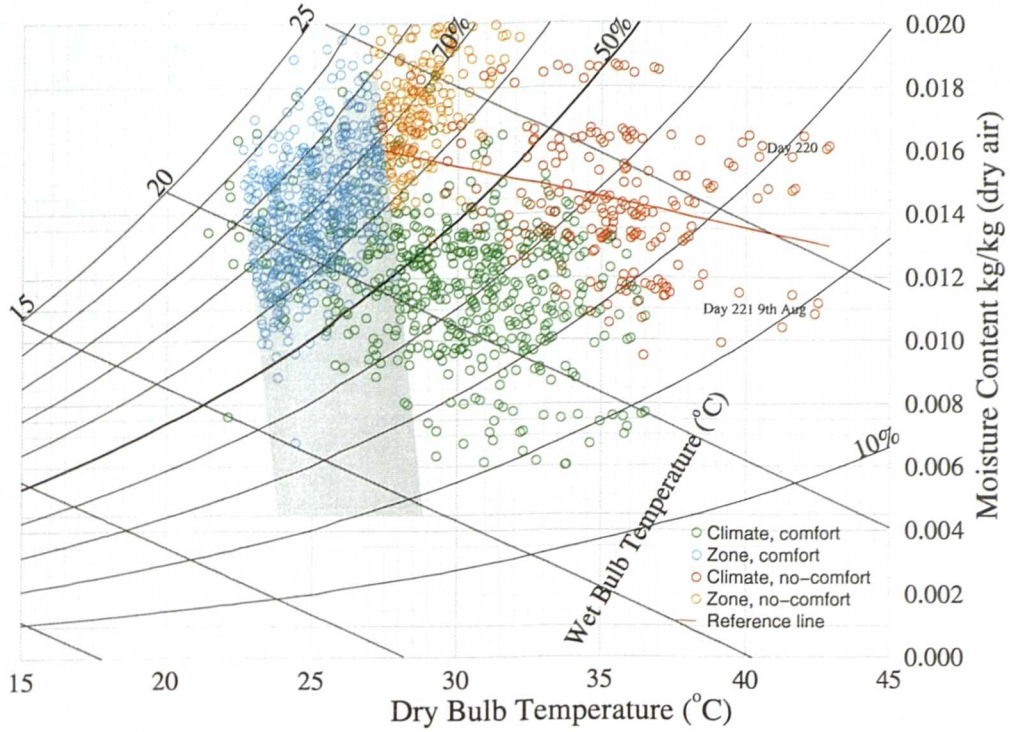

Figure 6-6. Low mass building, 50 W/m^2 internal gains.

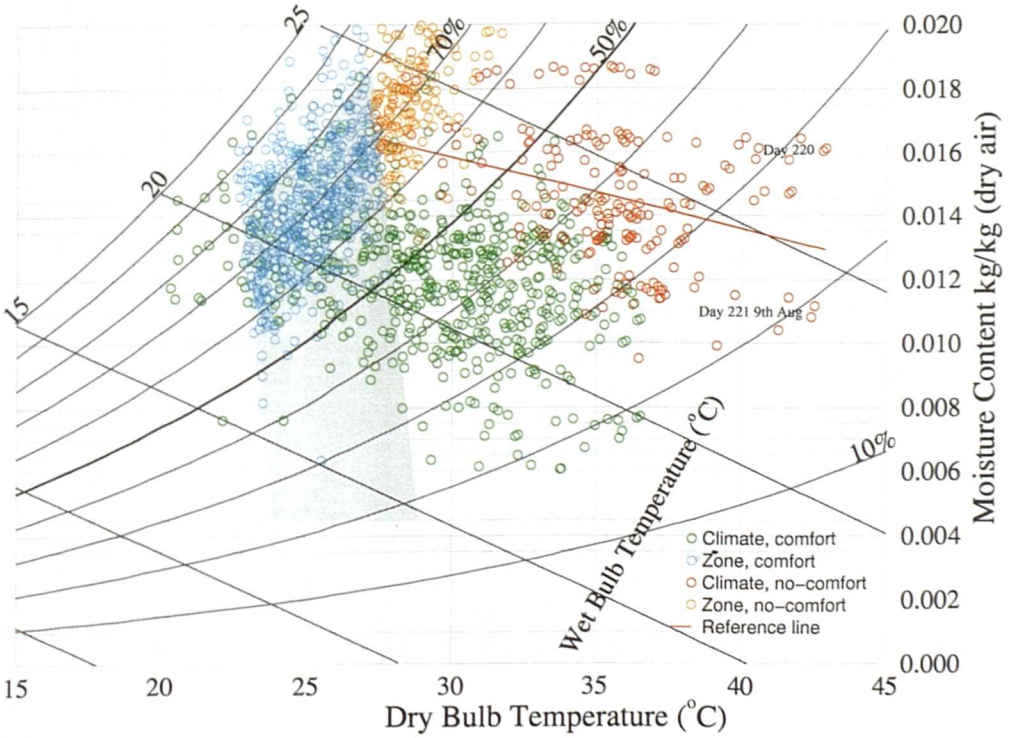

Figure 6-7. High mass building, 50W/m^2 internal gains.

6.3.3 Analysis of the results

There are several parameters that can be analysed from these results.One of the more interesting is to identify a line between the red (no comfort origin) and green (comfort origin) data. This will establish a boundary between ambient conditions which results in comfort in a PDEC building with certain internal gains and thermal mass and those which do not, for the same building.

The ***reference line*** used in the graphs represents a linear regression of the set of climatic data that produces uncomfortable results. Note that this is not the boundary for PDEC/non PDEC operation, but illustrates very well the behaviour of the six different models. Values around 0.65 of variance were obtained for this regressions.

By grouping the results by building mass and internal gains in all possible combinations can be outlined:

10,30 and 50 W/m^2 and low-mass (Figures 6-2,6-4 and 6-6)

- the first that can be noticed is the fact that the reference line is moving downwards, from an original position near to the wet bulb temperature of 25°C, for the 10 W/m^2, to a position nearer the 20°C wet bulb temperature line, for the 50 W/m^2.
- Several green points (comfort origin points) appear on the left side of the comfort envelope for the 30 and 50 W/m^2 cases, against only one point for 10 W/m^2.
- The number of non-comfort points above the 80% relative humidity line decrease when the internal gains rise from 10 to 50 W/m^2.
- The location 36.5°C – 24% RH is a comfort origin point for 10 and 30 W/m^2 but becomes a non-comfort one for 50 W/m^2.
- The first hour of the day 221 (hottest day of the year) is moved to the comfort envelope for 10 W/m^2, but not for 30 or 50 W/m^2.

- As expected, the final comfort points inside of the envelope are closer to its right hand boundary when the internal gains are higher.

10,30 and 50 W/m^2 and high-mass (Figures 6-3, 6-5 and 6-7)

- As before, the reference line is moving closer to a lower wet bulb temperature when the internal gains are increasing.
- Like in the previous case, the number of non-comfort points above the 80% relative humidity line decrease when the internal gains rise from 10 to 50 W/m^2. Several green points (comfort origin points) appear on the left side of the comfort envelope for the 30 and 50 W/m^2 cases
- Again, the first hour in the morning for day 221 (hottest day of the year) is moved to the comfort envelope for 10 W/m^2, but not for 30 or 50 W/m^2.
- Also the final comfort points inside of the envelope are closer to the right boundary when rising the internal gains.

Low-mass, High mass and 10 W/m^2 (Figures 6-2 and 6-3)

- The reference line is slightly closer to the 25°C for the high-mass one.
- One climate point, for 36.5°C dbt and 26% RH is a comfort point for the high-mass case but not for the low-mass case.
- Only the presence of 2 comfort points on the left side of the comfort envelope for the high-mass one seems to be the first sight perceptible difference.

Low-mass, High mass and 30 W/m^2 (Figures 6-4 and 6-5)

- The reference line is slightly closer to the 25°C for the high-mass one.
- One spot, for 36°C dbt and 24% RH is a comfort point for the high-mass case but not for the low-mass one.
- An increasing number of points on the left side of the comfort envelope for the high-mass case can be observed.

Low-mass, High mass and 50 W/m^2 (Figures 6-6 and 6-7)

- The reference line is still slightly closer to the 25°C *wbt* for the high-mass case.
- The "missing" spot is now at 36.5°C *dbt* and 18% *RH*, being a comfort point for the high-mass case but not for the low-mass one.
- As before, there is an increasing number of points on the left side of the comfort envelope for the high-mass case.

6.3.3.1 The hottest day of the year (8thAugust)

The hottest day of the year is Saturday 8th of August, with maximum dry bulb temperatures greater than 43°C at 15:00 and a minimum of 23°C at 05:00. This day was preceded by another very hot day with maximum *dbt* of 40°C and a night minimum of 21°C. The day after was also a very hot day with a maximum dbt of 42°C and a severe minimum at night of 24°C. The combination of these three extremely hot days and nights, starting with a Friday plus the fact that night venting operates all week and PDEC does not operate at weekends explain the reasons for the high temperature during the first hours of Day 222 (10th Aug.). PDEC in not capable of providing indoor comfort conditions even for temperatures of 33 °C and 25% RH.

6.3.3.2 Wet bulb reference line

Since the beginning of the PDEC project, the boundary between whether or not a PDEC system will be able to provide comfort conditions was required. At that time a "provisional" line, parallel to the wet bulb temperature line (about 23 °C) was adopted, but with no data to corroborate it. That was also the line adopted when analysing climate (Chapter 3.5.2.1) in this research.

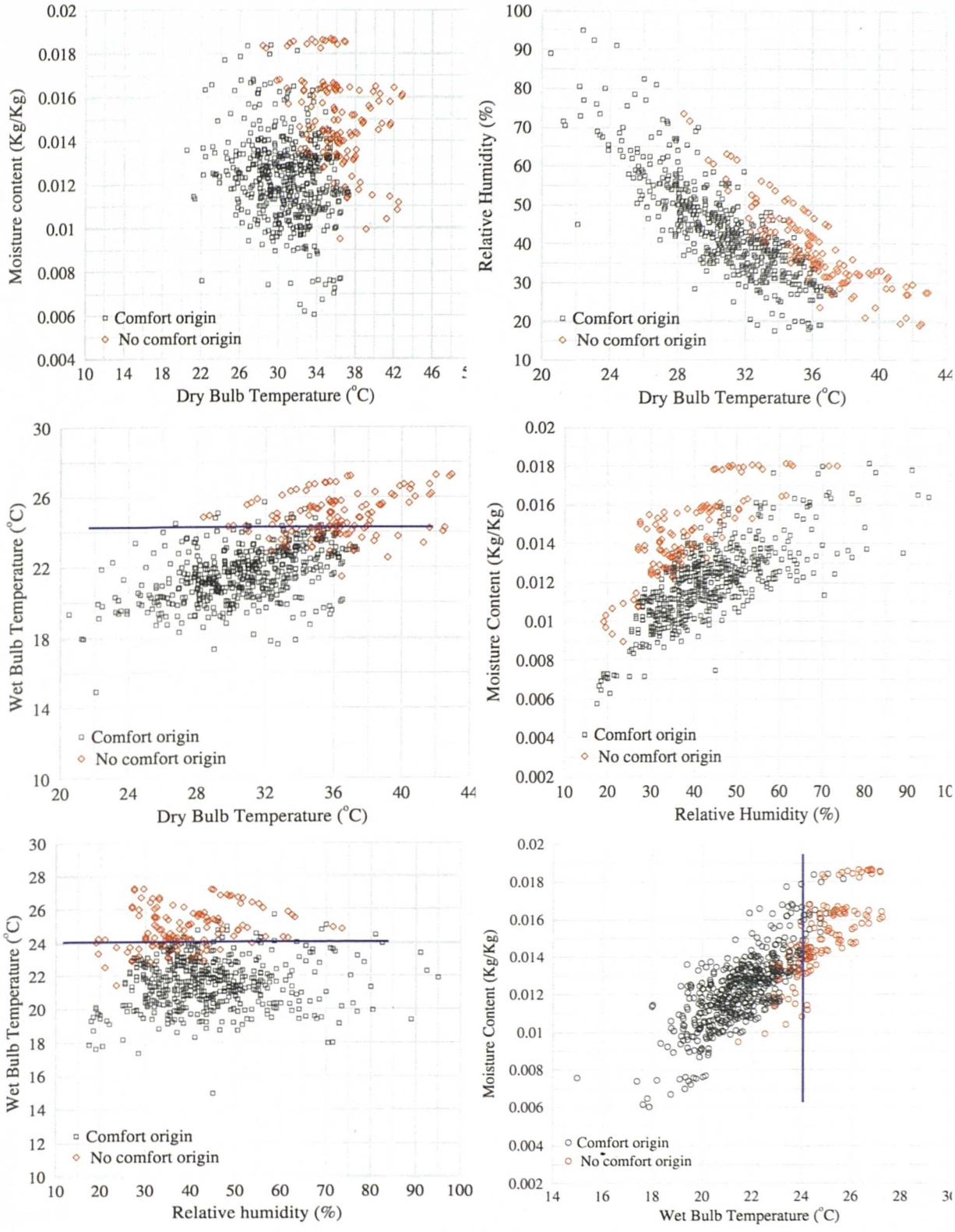

Figure 6-8. Climatic data plotted for a combination of psychrometric parameters and including a 24°C *wet bulb reference* line

By analysing the common area where, comfort and no-comfort, origin data coexist (Figures 6-2 to 6-7),or at the reference line (in red), a line parallel to the wet bulb temperature line can be noticed. As an additional study of this research, and for the fourth case, (30 W/m^2 internal heat gains and high mass building), all possible combinations of plotting the climatic data for the different psychrometric parameters have been carried out (See Fig 6.8).

The new line, referred to as the *wet bulb reference line,* could be moved along the 24°C wet bulb temperature line. If that supposition is compared with the other graphs where *wbt* is plotted it seems like this value could be accepted. For those graphs which do not involve *wbt*, no parallelism to any of the axes can be found. Some factors, like the hottest day of the year, must be borne in mind, as a discharge for those points that appear to break the "rule".

6.3.3.3 Building slope line

By plotting the number of hours of discomfort for the six different cases analysed, against the internal gains of the building and grouping the data by building mass, the graph in Figure 6-9 is obtained.

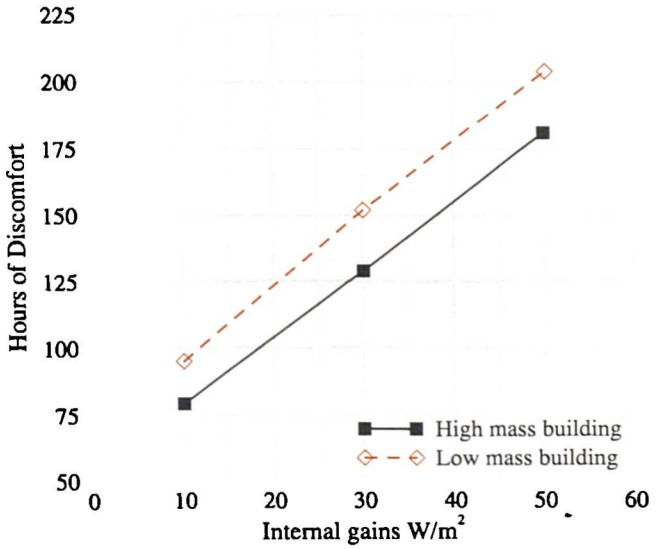

Figure 6-9. Building slope theory, model I

It is observed that a linear relationship exists for both building mass cases and a parallelism is maintained between them. This is what is being called the building slope. It is possible that if this is extended for the type of building and climates the comfort could be predicted by analysing the appropriate line.

6.4 Summary

The main conclusion is that the behaviour of the model is as expected. For higher internal gains, the PDEC capability to achieve comfort is lower. This capacity is slightly better for the high-mass cases than for the low-mass ones. It is interesting to point out that this condition may follow a line parallel to the wet bulb temperature between certain dry bulb temperatures (27-35°C), and for a relative humidity lower than 70%

PDEC is capable of maintaining comfort conditions up to an external dry bulb temperature of 37°C and relative humidity of 27% (high-mass 10 W/m^2). On the other hand, and as has been shown before, a "missing" point of non-comfort origin appears for lower temperatures in the different cases, (note that these values have been observed only for RH ≤ 30):

- 36.5°C dbt and 18% RH (50 W/m^2, low-mass)
- 36°C dbt and 24% RH (30 W/m^2, low-mass)
- 36.5°C dbt and 26% RH (10 W/m^2, low-mass)

PDEC potential, varies depending on the outdoor conditions, not just for the analysed day, but of the day or days before, and on the night preceding the analysed day. If it has been hot, this decreases its potential, as has been shown in "the hottest day" comments.

The boundary file is fixed, calculated based on the climatic data. It does not consider *RH*, in the sense that, even if this is too high, the boundary file is still applying a 70% reduction of the wet bulb temperature depression. This will affect to the high relative humidity encountered in the results. This is a simplified model, and will only establish the basis for a further more

complex analysis. Due to the latter, the conditions obtained in the core zone between the left and right temperature boundaries above the 80% relative humidity line are also considered as comfortable, bearing in mind that a humidity control in the model will avoid this happening.

Presenting data on the psychrometric chart, even when it is more difficult and demanding leads to a new perspective and allows the analysis of results in a graphical way and facilitates the identification of *wbt* line where PDEC is not working.

Chapter

7 *Thermal Simulation Analysis. Model II*

"Victory goes to the player who makes the next-to-last mistake."

CHESSMASTER SAVIELLY GRIGORIEVITCH TARTAKOWER

7.1 Preamble

This chapter introduces the thermal simulations carried out for the second model. It presents the differences of this model compared with the last approach. An analysis of the different scenarios has been graphically analysed. The psychrometric chart has also been used to identify the cooling boundaries. The conclusions and findings are at the end of the chapter.

7.2 Thermal model II

7.2.1 Description of the model

This model is based on some of the conclusions derived from the previous analysis. In this case, the building is going to be high mass since the last model showed that it is the more profitable case for passive buildings.

Geometry

As the previous thermal model (Chapter 6) a typical slice of the building has been used, which extends from the southern facade, through the perimeter and core (occupied areas) to half the width of an atrium. The first floor has been considered to develop a representative performance of the building. The second floor could also been used, but by using the first one, the pressure of cooled PDEC-air at the face of the openings between the core and the capture zone could be studied.

Contructions

It has been assumed that the building will be of well insulated heavyweight construction. The partition which separates the core and the perimeter zones is specified as a glazed wall with an internal blind. For surfaces which have no physical separation between adjacent spaces, a thin film has been specified, with no solar absortion, perfect thermal conduction and no thermal storage properties. Any surface which is not bounded by another zone within the building or ambient conditions is specified as adiabatic, otherwise the environment within this other zone is used as the boundary condition. The composition of the principal opaque contructional elements is as follows:

External Wall (1.42 W/m^2K)	
Rendering	0.0012 mm
Mineral fibre	0.100 mm
Inner leaf block	0.100 mm
Floor (0.35 W/m^2K)	
Dense plaster	0.0015 mm
Heavy mix concrete	0.210 mm
Cement screed	0.015 mm
Synthetic carpet	0.020 mm

Partition wall (0.55 W/m^{2}K)

Dense plaster	0.0015 mm
Breeze block	0.110 mm
Air	0.010 mm
Polyurethane foam board	0.030 mm
Breeze block	0.070 mm
Dense plaster	0.0015 mm

Internal heat gains and occupancy

To provide a basis of consistency between the two models, the same internal gains (10, 30 and 50 W/m^2) and occupancy profile (from 08:00 to 20:00 hours weekdays only) as those used previously have been adopted.

Air flow network and control

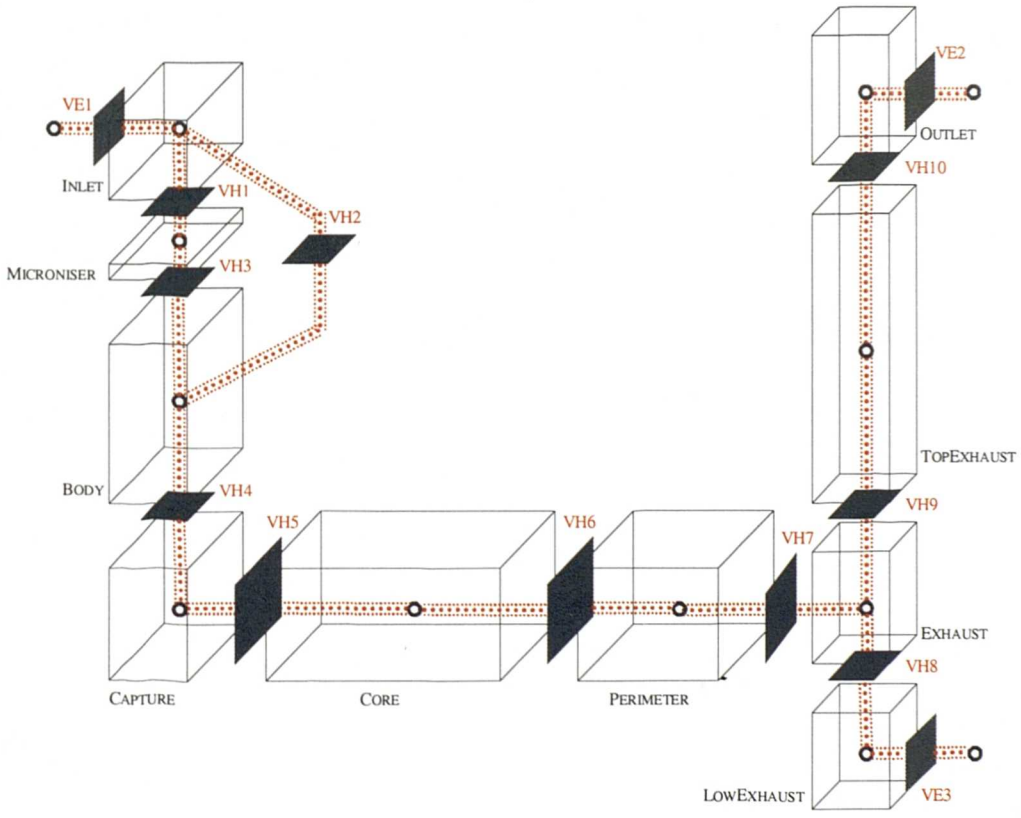

Figure 7-1. Geometry of the model and air mass flow network

The previous simulation approach was based upon idealised PDEC and ventilation air supply in response to time of day and internal conditions (see 6.3.1). The combined heat and air flow model was designed at the outset to be capable of predicting realistic mass flows in response to internal and ambient conditions, and to be able to predict the effects of control exercise at the points of air supply. The purpose of this model is to determine the air exchange rates which could be expected for different nodes of operation within the PDEC building. In Figure 7-1this air flow network is presented.

7.3 Results

7.3.1 Thermal comparison of scenarios

The first analysis will include the results from the three different scenarios and for the different internal gains. These are grouped by cooling technique i.e. (i) natural ventilation (Figs 7.2 - 7.4), (ii) natural ventilation plus night cooling (Figs 7.5 - 7.7) and (iii) natural ventilation with night cooling and PDEC (Figs 7.8 - 7.9)..

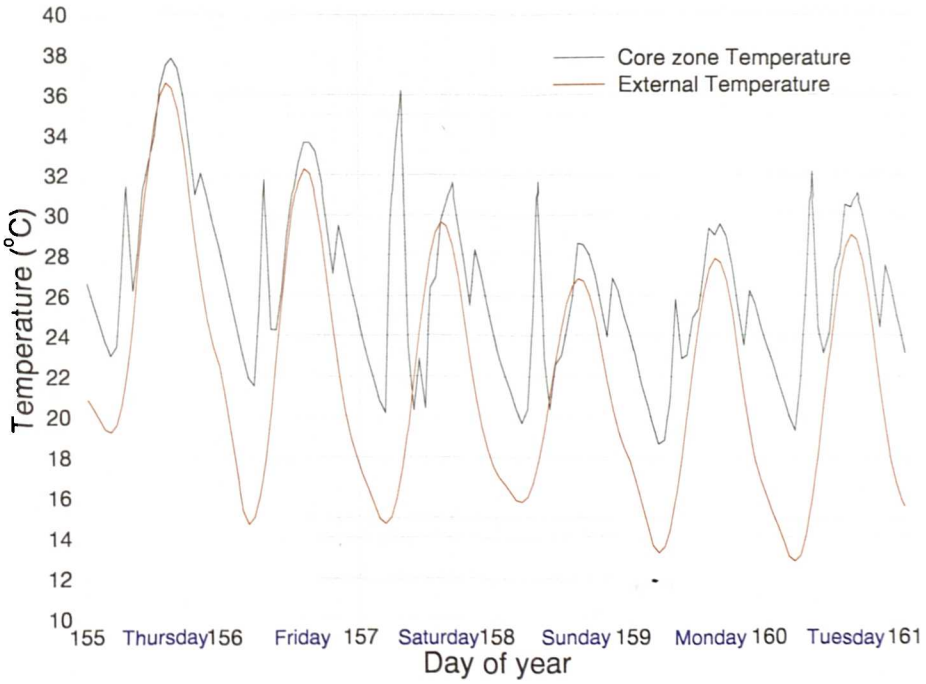

Figure 7-2. Natural ventilation, 10 W/m^2

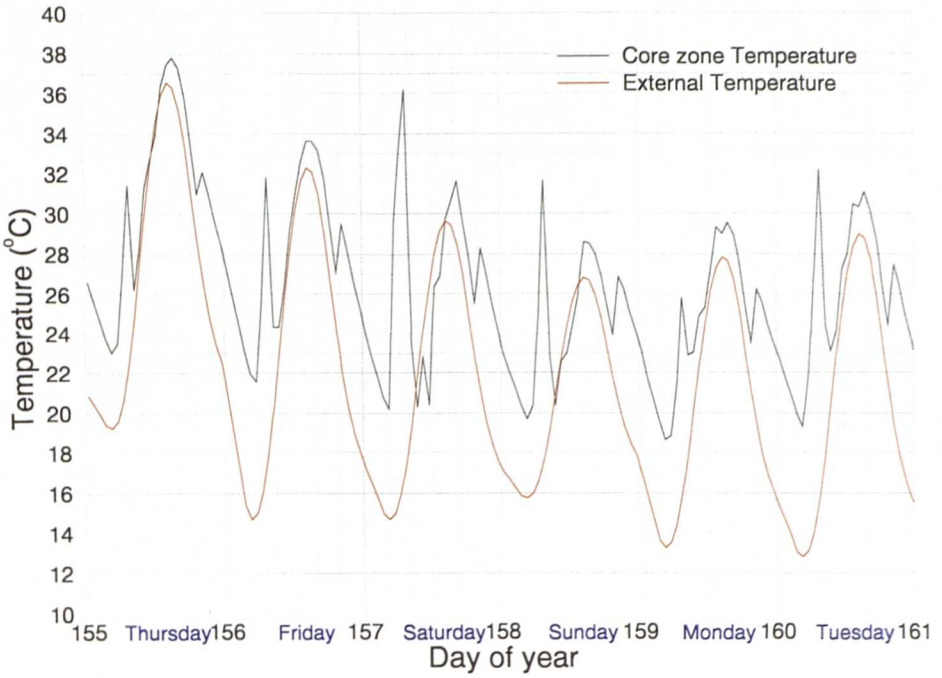

Figure 7-3. Natural ventilation, 30 W/m^2

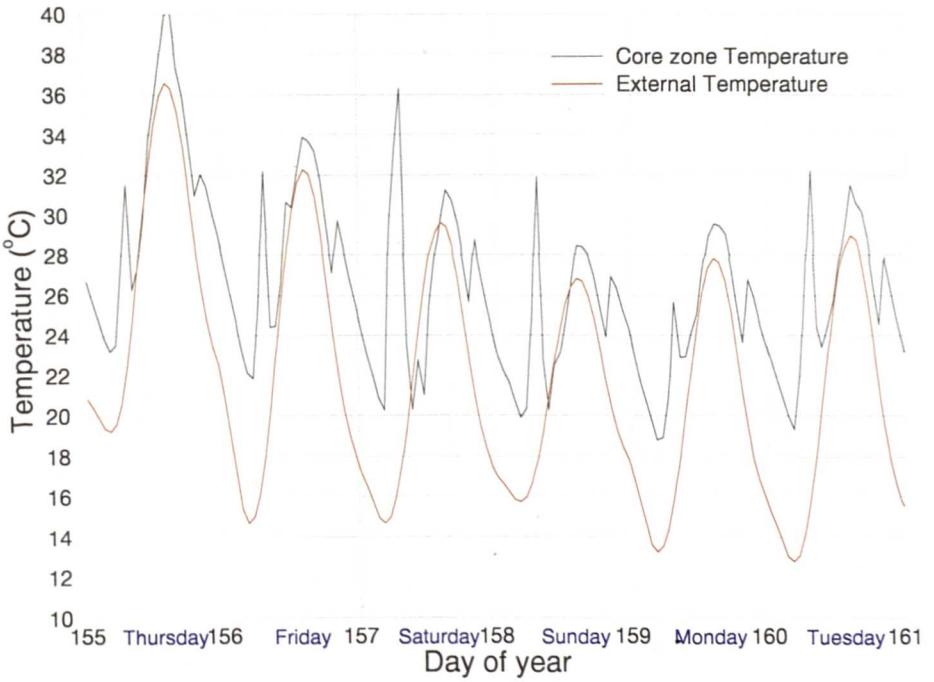

Figure 7-4. Natural ventilation, 50 W/m^2

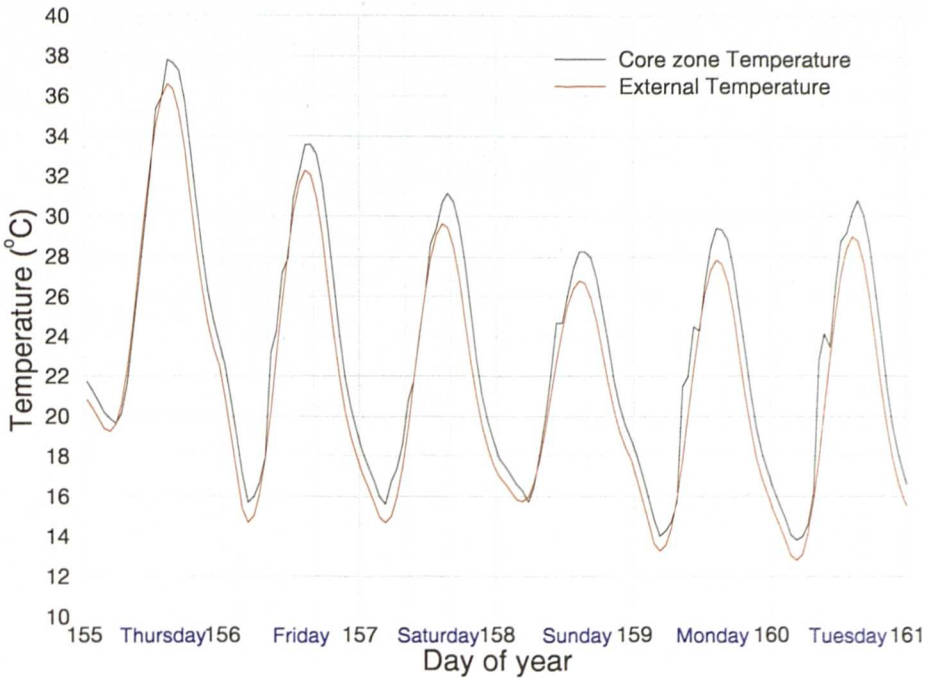

Figure 7-5. Night cooling plus natural ventilation, 10 W/m^2

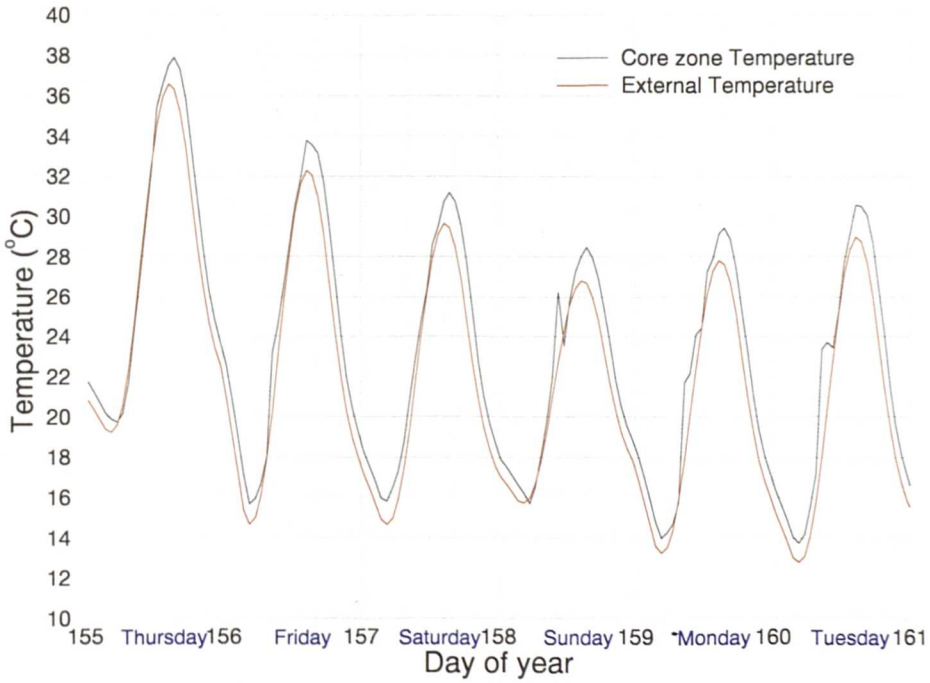

Figure 7-6. Night cooling plus natural ventilation, 30 W/m^2

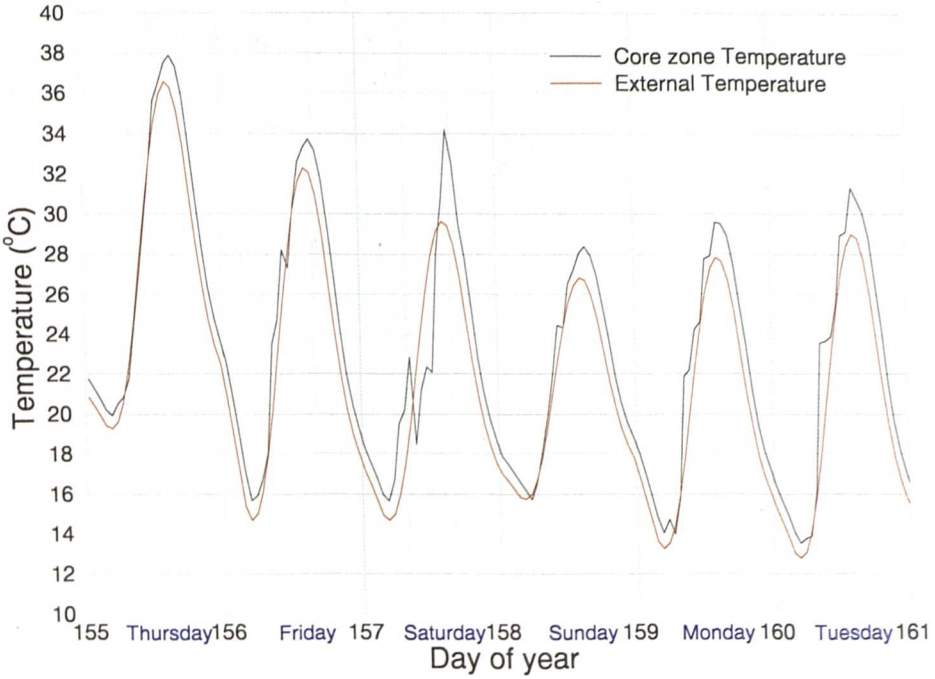

Figure 7-7. Night cooling plus natural ventilation, 50 W/m^2

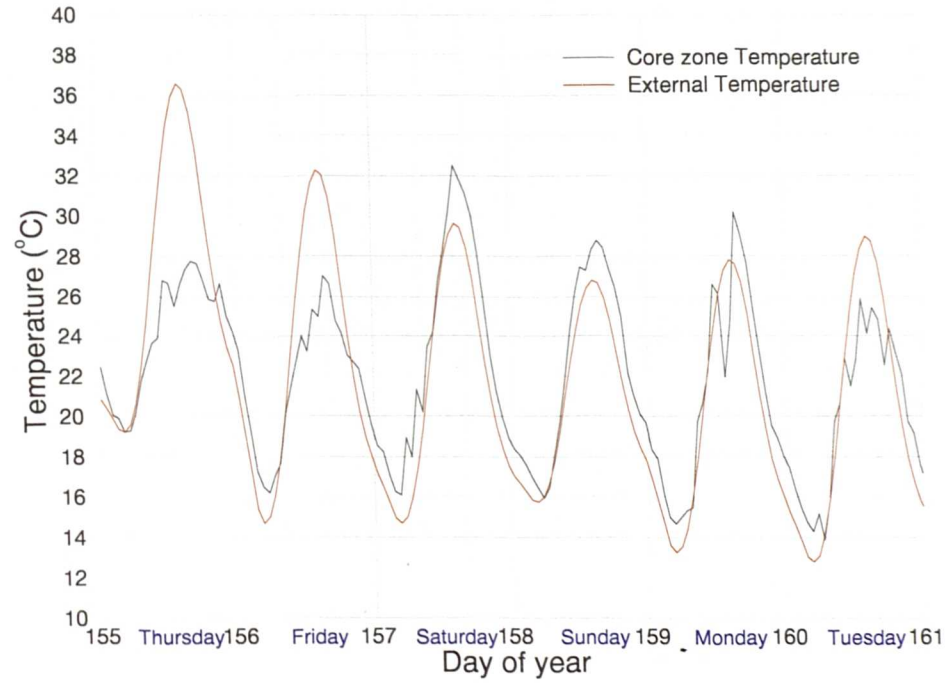

Figure 7-8. Night cooling, natural ventilation and PDEC, 10 W/m^2

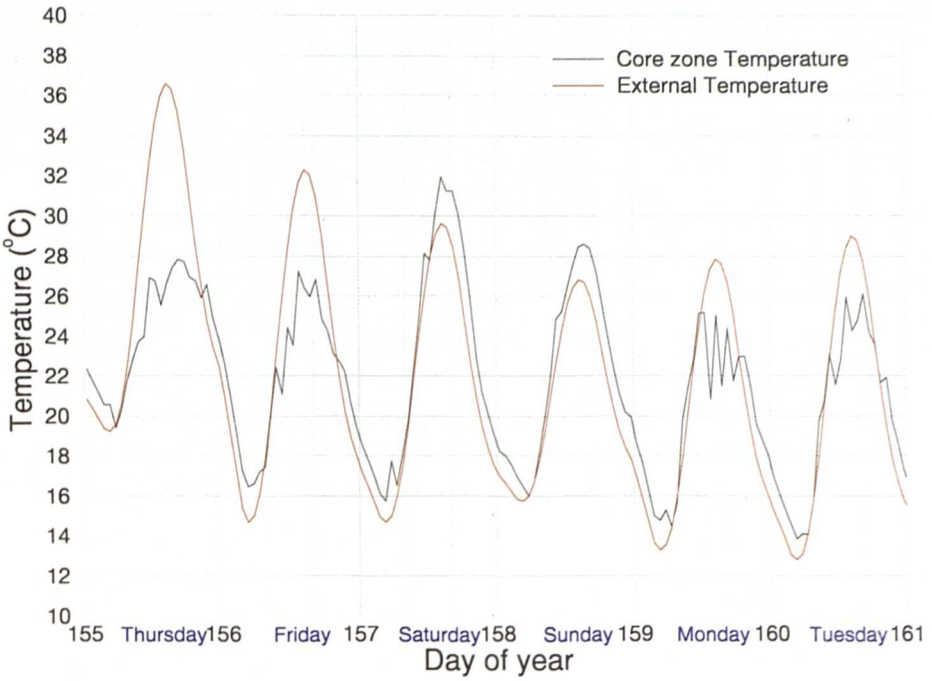

Figure 7-9. Night cooling, natural ventilation and PDEC, 30 W/m^2

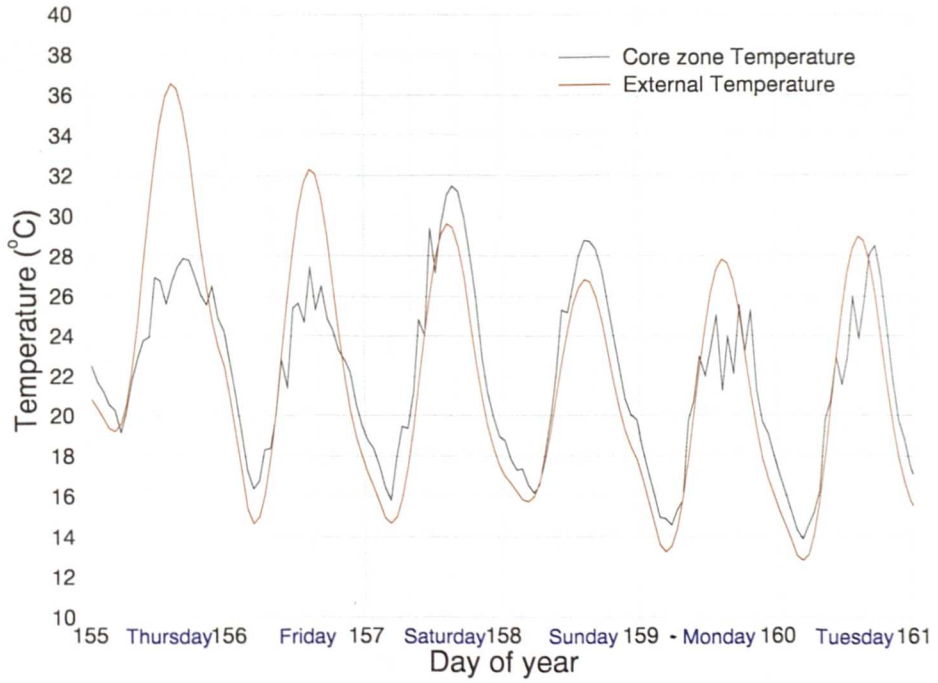

Figure 7-10. Night cooling, natural ventilation and PDEC, 50 W/m^2

In order to analyse these sets of results, some grouping must be arranged. Since they relate to three different cooling strategies, this will be the key for the groups:

Natural ventilation; 10, 30 and 50 W/m^2 internal gains. (figs 7-2, 7-3 and 7-4)

The patterns of the three graphs are as expected. Cross ventilation happens from 8:00 until 20:00, but not the rest of the day. This produces the sudden temperature peacks, early and late during the day. By looking at the temperature in the zone, there is almost no difference for the three different internal gain cases.

Night cooling plus natural ventilation; 10, 30 and 50 W/m^2 internal gains. (figs 7-5, 7-6 and 7-7)

The patterns of the three graphs are also as expected. Due to the night cooling acting together with day ventilation, the shape of the zone temperature follows the pattern of the ambient temperature. The value of the temperature in the zone is up to 2^{o}C higher than in the outside. No reason has been encountered for the sudden peack that appears on the day 157, Saturday, for the third case, 50 W/m^2. The climate file was revised, and the simulations were repeated several times. The rather complex simulation model, very low time-step (every five minutes) and high interactions (up to 1000) to find solutions to the combined thermal-flow system were concluded as the reason. There is no difference, or very little, between the three cases.

Natural ventilation plus night cooling and PDEC; 10, 30 and 50 W/m^2. (figs 7-2, 7-3 and 7-4)

The pattern, as in the other cases, as expected. Now the PDEC system is active. It can be observed how this keeps the temperature considerably lower than the outside temperature.

The difference that PDEC makes can be seen by comparing weekdays with weekends, when PDEC system is switched off. The oscillation that appears in the weekdays, is due to the use of a new hysteresis control of the VH5 opening. This new facility, controls the percentage of opening from a adjustable minimum to a maximum. It also requires the variable to control, zone temperature in this case, and the percentage to open or close per step. Several simulations were carried out in order to avoid the oscillation but with no success.

7.3.2 Air speed in the occupied zone. Comfort influence

Air speed is one of the factors that influences thermal comfort (see Chapter 4.4). The new extended comfort envelopes presented in Chapter 4 offer the different ranges of comfort depending on air speed, from the minimum, to a maximum of 1,5 m/s. By identifying the air speed that circulates through the zone at any time, and using the corresponding comfort envelope with that air speed, a considerable increase in hours of comfort is encountered. This relationship is the basis for suggesting a "dynamic" estimation of comfort. In order to estimate the average air speed in one zone, it must first be considered where the air is entering and leaving the zone. In this case the occupied zone is the CORE zone, (see Figure 7-1). Air is entering (or leaving, depending on the cooling strategy) through the wall next to the CAPTURE zone, and leaving (or entering) through the wall next to the PERIMETER zone. It is assumed that this flows unidirectionally. This means that for these assumptions the following formula can be applied:

$$v = \frac{\dot{V}}{A} \qquad \textbf{(7-1)}$$

where:

v = average air speed [m/s]

$\dot{V}$ = volume flow of air [m^3/s]

A = transversal area [m^2]

The (assumed constant) cross-sectional area for this zone is 18 (6x3) square metres. This gives an average air speed of 0,23 m/s for a volume of 15000 m^3/h. The comfort envelopes used for evaluating the simulation were used depending on the air speed in each case. This was developed by post-processing the data and comparing the results with the corresponding equations.

7.3.3 Graphical results

The aim of this section is to complete the boundaries for natural cooling techniques "map" started in Chapter 6. The same graphical method has been used (see Chapter 6.3.2). Obtained graphs are presented next.

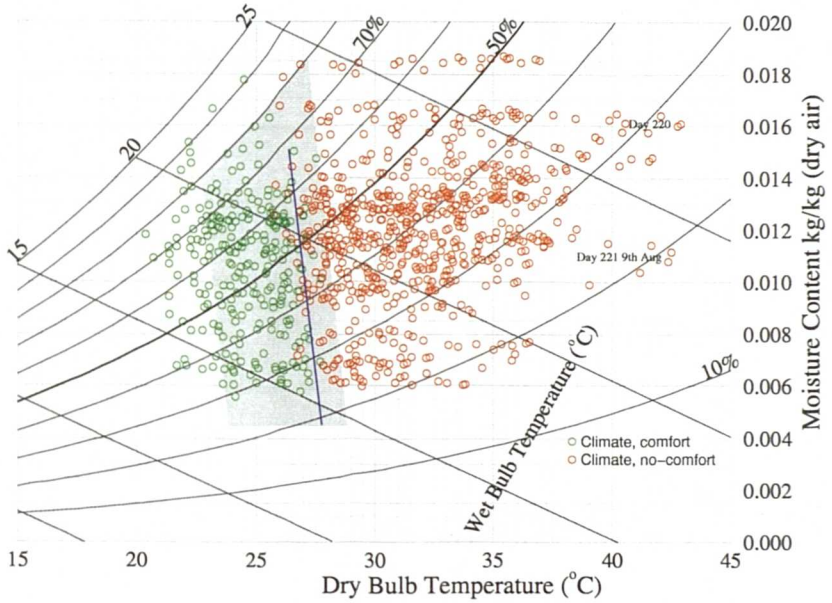

Figure 7-11. night cooling, 10 W/m^2

The aim is to find the boundary of where natural ventilation plus night cooling is enough to maintain indoor conditions. The blue line, represents the frontier between the red circles (hourly ambient conditions that do not generate comfort) and the green ones (these do generate comfort).

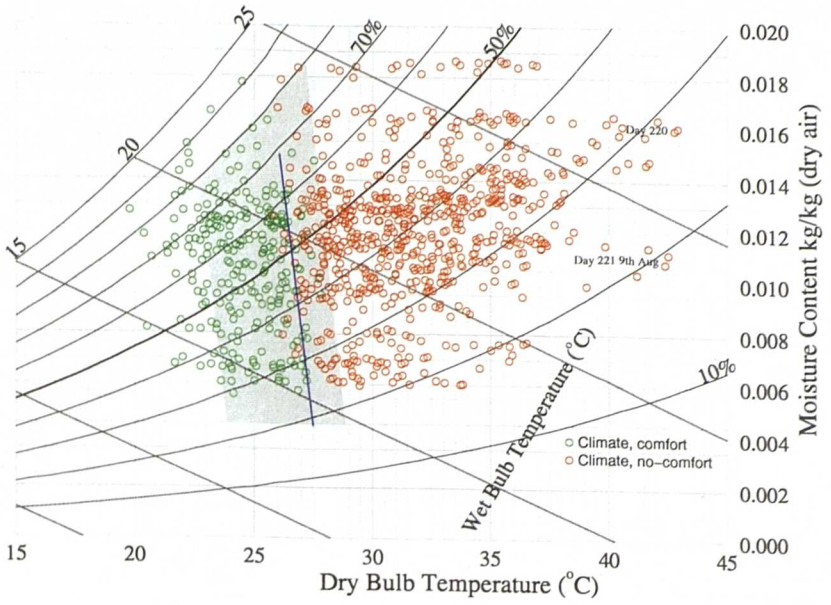

Figure 7-12. night cooling, 30 W/m^2

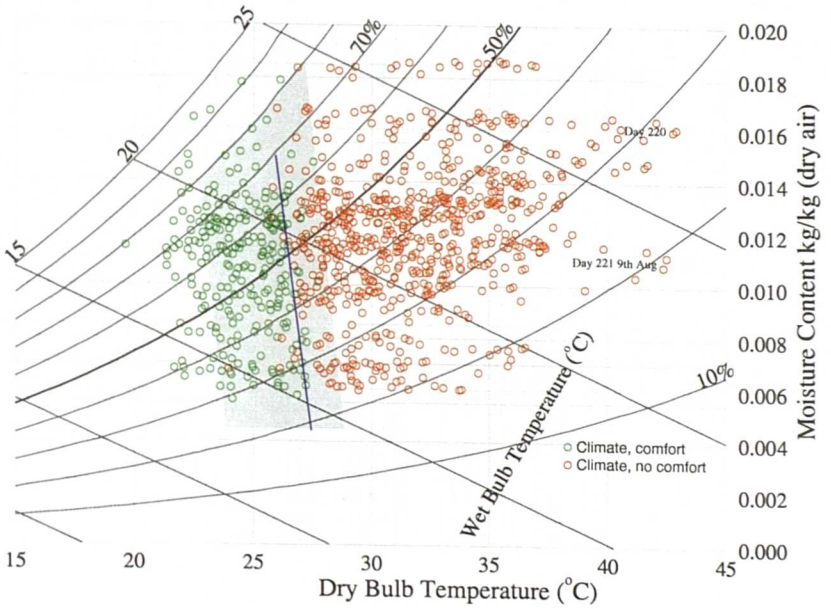

Figure 7-13. night cooling, 50 W/m^2

7.3.4 Boundary lines for natural cooling techniques

By plotting together the findings of 7.3.3 with ones of Chapter 6, a psychrometric chart with the boundaries for the different cooling techniques can be presented as shown in Figure 7-14.

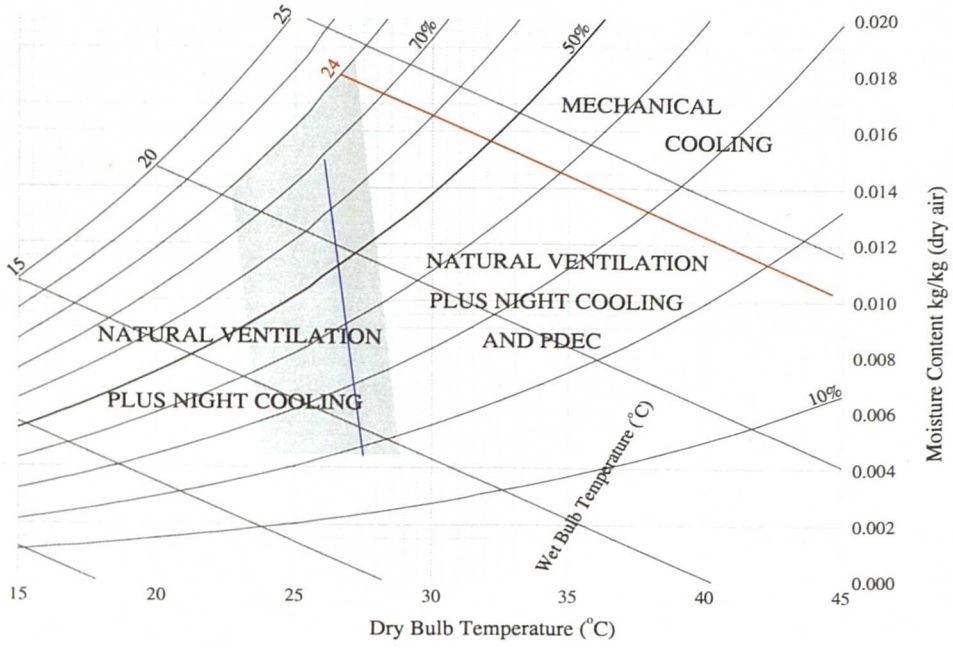

Figure 7-14. Boundaries for natural cooling techniques.

These boundaries represent the results of thermal simulations for an average high mass building, for a value of 30 W/m^2 internal gains. The conditions have been evaluated using the extended comfort envelopes (Martinez et al., 2000) described in Chapter 4, section 7. This means, that the boundaries have validity for summer conditions, and if the occupants have the adaptive behaviour allowance.

These boundaries have been demonstrated as acceptable, but can only be taken as a reference to orientate with the technique/s to use. Further thermal simulation are recommended with the particular specifications of the building.

7.3.5 Slope of the building

Following the graph generated in Chapter 6 (Fig 6.9), a similar graph has been generated for the results obtained in this Chapter, Figure 7-15.

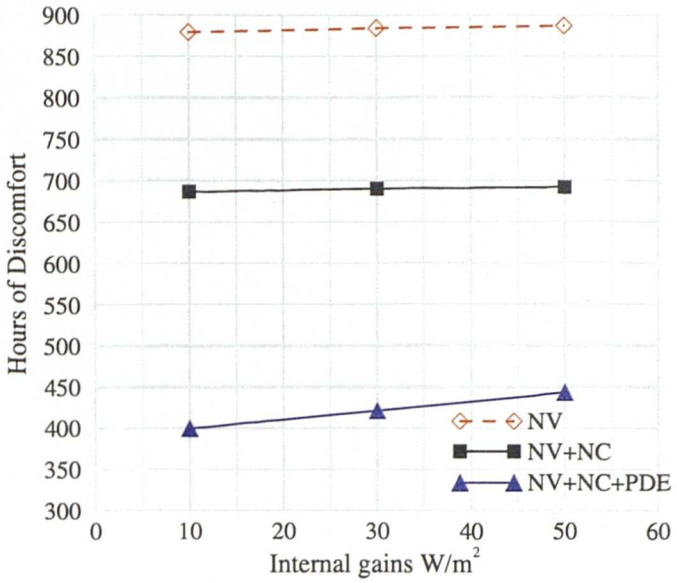

Figure 7-15. Building slope theory, model II

Two main conclusions can be derived. This model shows a lower influence of the internal gains when the building is well ventilated. It also shows that the slope of the building, due to this minimum difference, is maintained.

7.4 Balancing PDEC and natural ventilation

Passive cooling techniques are evaluated by the level of thermal comfort achieved in the building. This research has shown that it is not only air temperature, but also other factors such as air speed, which influence the level of thermal comfort. Achieving thermal comfort in a building depends on balancing all of these factors. This will differ from building to building.

If the occupants of a naturally ventilated building start to feel uncomfortable, some aspect of the building´s control system must change in an effort to re-establish thermal comfort. At this point, when local air speeds are at their maximum under a natural ventilation regime, the system

becomes insufficient. Switching on PDEC in the building could be the answer. However, PDEC requires a low air speed to function properly. If the air speed is reduced too much or too suddenly, the occupants could start to feel even less comfortable. Therefore, it is important to know at what point the introduction of PDEC into a naturally ventilated building can make comfort levels worse. If this is determined, some form of control system could be put into place to ensure that the cooling effect of PDEC is always beneficial to the performance of the building. There is no point using PDEC if the occupants are going to suffer.

Furthermore, when natural ventilation is operating at its maximum limit, the air speed will also be at its maximum. Occupant comfort will have reached the limit of the comfort envelope and PDEC will be required to be introduced to maintain occupant comfort. This is a critical moment because PDEC requires lower air speeds than natural ventilation. The effect of this mixing of PDEC air and naturally ventilated air on the comfort envelope needs to be examined for each building. The effect of reducing both air speed and air temperature must be virtually unnoticed by the occupants to ensure their comfort levels remain within the comfort envelope.

This issue is one which should always be considered when PDEC is an option for a building. It is not simply enough to say that PDEC will improve occupant comfort as it is a cooling technique. Its interaction with natural ventilation must be analysed.

The proposed control system to determine the operational status in a PDEC system needs to consider several issues. As mentioned before the system must be aware of the air speed, *dbt* and *RH* of the zone and outside conditions at all times. The level of indoor comfort should be calculated according to the measured parameters.

The control system is also based on assumptions such as the expected daytime thermal performance curve. This curve can be evaluated giving an expected pattern. Based on this pattern, the emerging conditions can be predicted (based on that day measurements) and react on time. PDEC systems do not react immediately to the control input, since the cool air has to be moved from the top of the tower to the delivered zones.

By combining the thermal comfort input with the expected daytime pattern and knowing the likely response of the building, the system will act as a servo mechanism capable of optimizing the resulting building performance.

7.5 Summary

The main result of this chapter is the fact that a new boundary in the psychrometric chart can be established (blue line in Fig 14), completing the natural cooling techniques "map".

Another conclusion derived from this study is that for a well ventilated high mass building, the internal gains do not affect too much of the performance of the building. Most of the results are included in the discussion, Chapter 8, and conclusions (Chapter 9).

Chapter

8

Discussions of results and suggestions for further work

"Only two things are infinite, the universe and human stupidity, and I'm not sure about the former."

ALBERT EINSTEIN

8.1 Preamble

The aim of this research has been to promote the use of Passive Natural Cooling Systems. There are currently not enough easy-to-use "tools" that promote the use of natural cooling techniques. This problem could be overcome by applying the fundamentals of this thesis in a user friendly application to analyse the cooling potential of a given building at any location. This would reduce the need to perform a complex simulation analysis. Therefore it will make the analysis of natural cooling systems available to more people.

Every building, due to factors such as its location (climate) and occupancy, has its own unique performance characteristics. The maximum

performance (and therefore maximum cooling potential) is reached by applying good design principles. A building with a good design and good performance characteristics in one situation may not prove as good in another. For example, it may have the wrong climate (too hot) or a more narrow (or demanding) comfort envelope.

The slope discovered in the behaviour of high versus low mass buildings (comfort hours/internal gains) in Thermal_1 could be applied to a group of buildings with similar characteristics. This would allow suitable applications for buildings of different thermal mass to be investigated.

Further studies could analyse the comfort requirement for a dynamic temperature response (parallel to the day-pattern). It would therefore be possible to observe the effect on building performance due to a less demanding comfort envelope. This may influence the design of a building as extending the comfort envelope by only a small amount may significantly improve the building performance.

A new analysis process could be to determine the climate and plot it on the psychrometric chart. The building would be described in terms of parameters such as its mass and internal gains. The boundaries for NV, NV+NC, and NV+NC+PDEC would be determined. This would allow the number of hours of discomfort for a summer occupancy period to be determined from the psychrometric chart. This figure could then be compared with the overheating criteria in the design brief and a decision made on whether there is a need for an air conditioning system.

The choice of climate to plot on the psychrometric chart is an important one. During the research, several climate files for Seville were obtained. Analysis showed that there were significant differences between the climate files in terms of the number of hours for which mechanical cooling was required. Therefore, the choice of climate file can affect the results and introduce significant errors. For example, a hotter climate may over-predict the need for mechanical cooling whereas a cooler climate may under-predict this

need. There are no regulations covering this issue of climate files and thus a climate file can be chosen which produces the desired results.

It has been shown that plotting only a month-line on the psychrometric chart is not enough. In such a case, a very hot night is not reflected and this could make a NC system unsuitable. Similarly, a very cold night (swing) will allow a warmer day to be chilled with natural techniques. Therefore, a shorter time period must be plotted on the psychrometric chart.

Dynamic calculation of data requirements such as the air speed, solar radiation and dry bulb temperature in conjunction with the comfort will allow more accurate solutions to be determined. This could be an interesting issue for further work.

8.2 Pre-evaluation of a site potential for natural cooling techniques

Close to the ending of this thesis, several practical applications to the work were used. A new paper was also been submitted related with this subject. The extended abstract is outlined next:

Natural cooling techniques could provide summer indoors thermal comfort conditions for a notable number of locations. Even for those, warmer sites, where mechanical cooling is required, these techniques could assist the mechanical system with the resulting saving of energy and resources.

Natural ventilation techniques range from, (i) an elemental day natural ventilation, whilst ambient temperature is within comfort limits, (ii) night cooling, where the mass of the building is cooled during the night, compensating some of the heat generated during the day and (iii) evaporative cooling systems, where generally water is involved in the process. The latter is depicted by the Passive Downdraught Evaporative Cooling (PDEC) system (Bowman et al. 2000). A technique where warm dry air is cooled by evaporating microscopic droplets of water into it (Alvarez, 1992).

To establish which technique or combination of them is suitable in each case, several factors such as climate conditions, indoor comfort requirements and the building performance itself must be considered.

An average floor of a standard high-mass building was modelled. Using the Seville climate data, extensive thermal simulations were run for the different cooling techniques, and their combinations. The conditions predicted inside, along with climate data used, were plotted in a simplified psychrometric chart and compared with the formerly comfort envelopes developed (Martinez et al. 2000) establishing whether the outdoor climate conditions will provide indoor comfort or not. By looking at where the climate conditions swing from "comfort generators" to "non comfort generators" for the different techniques, some boundaries can be established. These boundaries represent whether a cooling technique provides indoor comfort conditions or not. Although these boundaries might slightly vary depending on the building specifications this approach is valid to obtain a first impression of the potential or restrictions of a site.

The Seville climate hourly data has been plotted into 4 different psychrometric charts: 24 hours for the whole year, and, 24, occupied and non-occupied hours for summer. The cooling boundaries were overlaid, and the number of hours encountered in the different envelopes counted. It was found, that compared with former simulations carried out for the same site and the same cooling strategies (under the PDEC project), the number of hours where mechanical cooling was required was much smaller, almost acceptable if applying the overheating criteria rules. This is due to the fact that the comfort envelopes used consider the adaptive behaviour of occupants, along with the air speed and solar radiation values present at the simulation, instead of unchanging comfort envelopes.

This combination of elements, climate, comfort and the building itself not only provides an easy identification of the potential for using natural cooling techniques, but also plays an important role in favour of them.

An example of this analysis is presented in Fig 8.1.

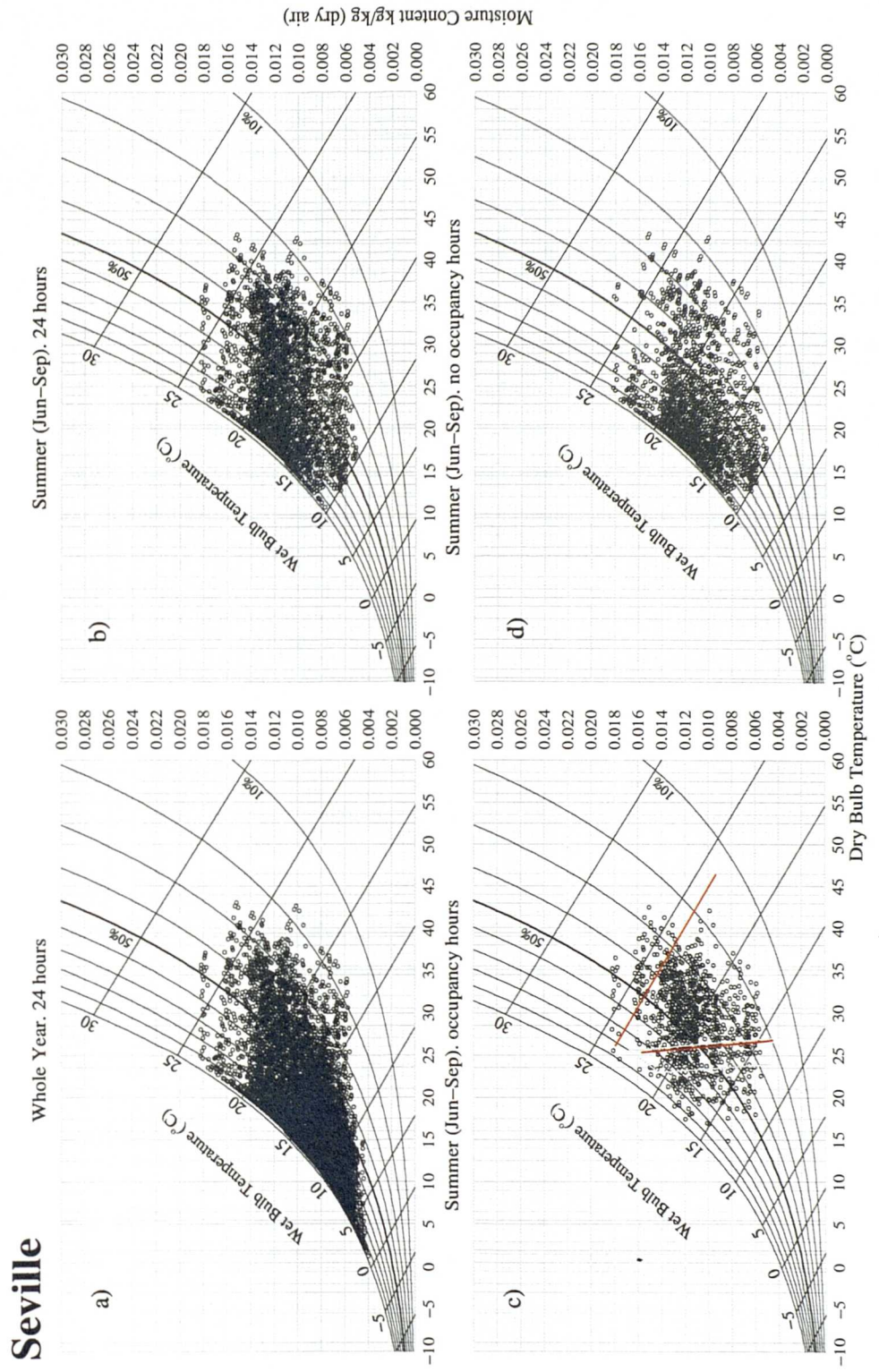

Figure 8-1. Study of Seville potential for natural cooling techniques

By looking at the graphs, some conclusions can be derived. The first thing that can be observed is the that the climate is severe hot, (Fig. 8.1a). No much difference when compared with the summer, Fig. 8.1b, this means that some cooling might be needed not only for summer. By comparing the summer, occupancy and no occupancy graphs, 8.1c-d, important information is obtained. Non occupancy periods (nights and midday -siesta-time) and very humid and cold, respectively. This will limit the use of night cooling, which might be too humid, and require a special control of the building at the midday, when the building is supposed to be empty (could close blinders or similar to reduce the amount of solar radiation).

Most of the data for summer occupancy time, Fig 8.1c, is encountered within the central zone, where PDEC should be capable of maintain the thermal comfort requirements.

By this quick method of analysis, very intuitive conclusions can be derived leading to a selection of the strategy to cool and ventilate the building. Even when further and more complex analysis is advised, this pre-evaluation will save time and case-studies.

Chapter

9 *Conclusions*

"But the fact that some geniuses were laughed at does not imply that all who are laughed at are geniuses. They laughed at Columbus, they laughed at Fulton, they laughed at the Wright brothers. But they also laughed at Bozo the Clown."

CARL SAGAN

9.1 Specific Conclusions

Psychrometry

The simplified psychrometric chart developed has been validated. When compared with the CIBSE equivalent chart, results showed a 99% accuracy. The combination of the CIBSE formulae together with the new method for the chart development has been found to be acceptable. The formulae used for generating the curves of the psychrometric chart are the same ones used for processing the climatic and simulation results data. This made the data as reliable as the chart itself.

Climate.

It is not easy to classify climate. Almost every location has its own particular climate. Attempts to find similarities among sites using cartesian plots failed. They are not accurate enough and they do not show the relationships between the different parameters. Plots of hourly data using the psychrometric chart were therefore used. This facilitates a study of the interaction between different elements such as dry bulb temperature and relative humidity. Some provisional boundaries to define areas that correspond to different cooling techniques were established. Two different climate files for Seville were studied using these boundaries, and notable differences were found. This could lead to the adoption of an inappropriate cooling strategy depending on the file chosen. Since climate file selection for simulation purposes is not subject to regulation, a margin of tolerance could be applied when analysing the results.

Comfort

Extended comfort envelopes have been derived for hot summer conditions in office buildings based on adaptive opportunity. The adaptive behaviour of occupants has been investigated considering changes in the clothing level, air speed and solar radiation. As a result, the new comfort envelopes extend from 22.7°C (80 % RH) to 28.8°C (~17% RH) in the absence of solar radiation. This is about 2 K wider than that obtained in a former study by Fiala et al. (1999). In the presence of diffuse solar radiation of 50 W/m^2 the comfort envelopes shift towards cooler air temperatures by about 2 K.

Increasing air speed leads to an acceptance of warmer conditions but this effect becomes less pronounced as the air speed continues to rise. It was also found that increasing air speed is more effective in the presence of solar radiation. These extended comfort envelopes were developed for PDEC buildings. However, they may also be used to examine summer comfort conditions in other types of office buildings in which thermal adaptation is possible.

Thermal simulations

The evaluation of the strategies for modelling and controlling PDEC using ESP, show the following.

For higher internal gains, the PDEC capability to achieve comfort is lower. This capacity is slightly better for the high-mass cases than for the low-mass ones. It is interesting to point out that this behaviour may follow a line parallel to the wet bulb temperature between certain dry bulb temperatures (27-35°C), and for a relative humidity lower than 70%. PDEC is capable of maintaining comfort conditions up to an external dry bulb temperature of 37°C and relative humidity of 27% (high-mass 10 W/m^2).

If the fundamentals of this thesis were made into a simple analysis program, it would reduce the need to perform a complex simulation analysis. As such, the use of PDEC in buildings would be able to be analysed by a greater number of people.

9.2 Overall conclusions

9.2.1 New guidelines for designing PDEC control systems

- The combination of higher air speed, achieved during natural ventilation operation mode, with the revealed fact that in solar irradiated areas, air speed has more influence on thermal comfort, leads to a higher set point for PDEC operation. This is also applicable when only natural ventilation techniques are studied, increasing the number of comfort hours achieved by using this technique.
- A PDEC system needs to be supported by natural ventilation until the PDEC set point is reached. Night cooling is neçessary in summer conditions for all passive techniques, with or without PDEC. Also, a set point for this strategy will allow finer tuning of the system.

- The balance between the air speeds and the air temperatures when PDEC is introduced into a naturally ventilated building needs to be investigated for each individual building to ensure that PDEC does in fact improve occupant comfort. This is because PDEC requires lower air speeds than standard natural ventilation. The move from one air speed to another must be as smooth as possible to ensure that occupant comfort remains within the comfort envelope. If the introduction of PDEC is too sudden, occupant comfort levels will move outside the comfort zone. Therefore, there needs to be a control system which regulates the use of PDEC.

9.2.2 Pre-evaluation of a site potential for natural cooling tecniques

The combination of a graphical study of climate based on the psychrometric chart, together with new extended comfort envelopes to analyse the thermal simulation results of a PDEC building, produced new and opportunistic results. Zones for operation of different systems can be defined, based on climate analysis. The boundaries of these zones vary depending on the building performance, but some generalities apply.

Bibliography

Alvarez, S. Rodriguez, E. A. and Molina, J. L. (1991), The avenue of Europe at Expo'92. Application of cooling towers, Proc. PLEA Int. Conf. Seville, Spain, 24-27 Sept, pp195-201.

Alvarez, S. Cejudo, J. M. Rodriguez, E. A. Guerra, J.(1992), Full scale experiments in EXPO'92. The bioclimatic rotonda, Proc. PLEA 91 Architecture and Urban Space, Seville Spain p209-216.

Alvarez, S. & Balaras, C. A. (1995), PASSPORT+ Final Report, PASCOOL Project, Joule II, European Commission, Contract JOU2-CT92-00131995.

Apjohn, J. (1838), Trans, Royal Irish Academy 18(i) 1.

Arens, E. Zeren, L. Gonzales, R. Berglund, L. and McNall, P. E. (1980), A new bioclimatic chart for environmental design. Proc.Bldg Energy Managment conf. (CBEM) Pergamon.

Arguiriou, A. (1999), Comparison of Methodologies for TMY generation using 20 years data for Athens, Greece. Solar Energy, Vol 66, 1, p33-45

ASHRAE (1992), Standard 55. Thermal environmental conditions for human occupancy. Atlanta, USA.

BACS (1989), British Association of Chemical Specialities. A Code of Practice. The Control of Legionella by the Safe and Effective Operation of Cooling Systems.

Bahadory, M. N. (1985), An improved design of wind towers for natural ventilation and passive cooling. Solar Energy Vol. 35, No 2, pp 119-129.

Bahadori, M. N. & Chamberlain, M. J. (1986), A simplification of weather data to evaluate daily and monthly energy needs od residential buildings. Solar Energy, 36:499-507.

Baker, N. & Standeven, M. (1996), Thermal comfort for free running buildings, Energy and Buildings 23 p175-182 ELSEVIER.

Bowman, N. T., Eppel, H., Lomas, K. L. Robinson, D. and Cook, M. J. (2000),. Passive Downdraught Evaporative Cooling – I: Review and precedents. *Building services Engineering Research and Technology.*

BSI (1992), British Standards Institute, DD 211. Draft Methods for Detection and Enumeration of Legionella Organisms in Water and Related Materials.

Brundrett, G.W. (1992), Legionella and Building Services, Butterworth.-Heinemann Oxford.

CDC (1993), Centre for Disease Control, Summary of Notifiable Diseases in the United States, Atlanta, GA.

Chaddock, J. B. (1965), Moist air properties from tabulated virial coefficients (Humidity and Moisture Measurement and Control in Science and Industry, ed. A. Wexel and W. A: Wildhack, Reinhold Publishing Corp.,New York Vol 3.

CIBSE guide C, (1975), Properties of humid air (London: Chatered Institution of Building Services) .

CIBSE guide C, (1999), London: Chatered Institution of Building Services, Internal gains, section 6.

Cunningham, W A. & Thompson, T. L. (1986), Passive cooling with natural draught cooling towers in combination with solar chimneys, Proc. PLEA 86, Pecs, Hungary.

DES (1993), Department of Environmental Services, Legionnaires' Disease. Guidelines for Control, City of Westminster.

DuBois, D. & DuBois, E. F. (1916), A formula to estimate approximate (body) surface area if weight and height are know. Archives of onternal medicine, 17:863-871.

ESRU (1998), ESP - A building and plant simulation system, User gudie, Energy Simulation Research Unit, University of Strathclyde, Glasgow.

Fanger, P. O. (1982), Thermal comfort, Kreiger, Florida. (original, technical press, 1970).

Festa, R. & Ratto, C. F. (1993), Proposal of a numerical procedure to select Reference Years. Solar Energy, 50 (1) 9-17.

Fiala, D. (1999), *Dynamic simulation of human heat transfer and thermal comfort. Ph.D. thesis*, De Montfort University, Leicester, UK.

Fiala, D., K. J. Lomas, Martinez, D. and Cook, M. J. (1999), Dynamic thermal sensation in PDEC buildings. *Proceedings PLEA* (Brisbane) 99:1, 243-248.

Ford,B. H. & Hewitt, M. G. (1996), Passive Downdraught Evaporative Cooling in non-domestic buildings, A review of the curretnt State of the Art. Procc. PLEA'96, Berlin 4pp.

Gagge, A.P. (1936), The linearity criterion applied to partitional calorimetry, Am J of Psysiology116:656-668.

Gagge, A.P. Stolwijk, J.A. and nishi, Y. (1971), An effective temperature scale based on a simple model of huma physiological regulatory response. ASHRAE, Trans.77(1) 247-262.

Giabaklou, Z. & Ballinger, J. A. (1996), A passive evaporative cooling system by natural ventilation, Building and Envirinment, 6(31), p503-507.

Givoni, B. (1992), Comfort, Climate analysis and building design guidelines. Energy and Buildings No 18 pp11-23.

Givoni, B. (1994),Passive and low cooling energy of buildings, Vamn Nostrand Reinhold, New York.

Goff, J. A. (1949), Standardisation of Thermodynamic Properties of Moist Air ASHVAE Trans. 55: 459-484).

Goff, J. A. & Gratch, S. (1945), Thermodynamic properties of moist air. Trans. ASHVE ,51, 125-164.

Grubich, V. (1961), Az idöjárás és az ember, (Climate and man), Medicina, Budapest.

Guildner, L. A, Johnson, D. P. and Jones, F. E. (1976), Vapour pressure of water at its triple point. Res. NBS 80A.

Haldane, J. S. (1905), Influence of high temperatures. Journal of Hygiene, Cambridge, 5:494.

Hassid, S. (1994), Evaluation of Passive Cooling Strategies for Israel Technion - Israel Institute of technology, 11th PLEA international, p162-169.

Hastings, S. R. (1994), Passive solar commercial and institutional buildings: A source book of examples and design insights, Wiley.

Heberden, W. (1826) An account of the heat on July 1825,...some remarks on sensible cold. Phil. Trans. 2:69.

Hewitt G. F. Delhaye J. M. and Zuber, N. (1982), Multiphase Science and Technology, Vol.1 Hemisphere Publising Corporation, New York.

Hodgson, J. M. (1998), Prevalence of Legionella bacteria in building water systems. Regional Office, New York

Hougten, F. C. & Yagloglou, C. P. (1923), Determination of the comfort zone, Trans. ASHVE, 29:336

HSC (1994), Health and Safety Commission, An Approved Code of Practice for the Prevention or Control of Legionellosis, Including Legionnaires' Disease. Second edition HMSO.

HSE (1993), Health and Safety Executive, The control of Legionellosis, Including Legionnaires' Disease Health and safety booklet HS(G) 70, Third Edition HMSO London.

Humphreys, M. A. (1978), Outdoor temperatures and comfort indoors. Building research and practice 6, 92-105.

Hyland, R. W. & Wexler, A. (1983), Formulations for the thermodynamic properties of dry air from 173.15 K to 473.15 K and of saturated moidt air from 173.15 K to 372.15 K, at pressures to 5Mpa ASHRAE Trans 89 (2A): 520-535.

ICI (1986), Working Party Report (HO/SHE/86/001) published by the Industrial Water Society, Birmingham, England.

ISO 7730 (1994), Moderate Thermal environments. Determination of the PMV and PPD Indices. International Organisation for Standardisation, Geneva.

Katsikakis, D. & Laing, A. (1993), Assesment of Ocupational Density Levels in Comercial Office Buildings (London: Stanhope Properties).

Klitsikas, N. Santamoris, M. Argiriou, A. and Asimakopoulos, D. N. (1994), Thermal Analysis of Evaporative Cooling Systems in Greece. Proceedings of the European Conference on Energy Performance, Lyon Vol. 2, pp 628-633.

Lee, D. H. K. (1980), Seventy five years for searching of a haet index, Env. Res. 22:331-356 (Academic press).

Lefebvre, A. H. (1989), Atomization and sprays. Hemisphere Publishing Corporation, New York.

Lund, H. (1995), The Design Reference Year User's Manual. Thermal Insulation Laboratory. Technical University of Denmark. Report 274.

Marion, W. & Urban, K. (1995), User's manual for TMY2s Typical Meteorological Years. National Renewable Energy Laboratoty, Golden, CO, USA.

Martinez, D. Fiala, D. Cook, M. J. and Lomas, K. L. (2000), Predicted comfort envelopes for office buildings with PDEC. ROOMVENT 2000, Proc. Int. Conf. Reading, UK. (I), p53 58

Mathews, E. H. Kleinfeld, M. Grobler, L. J. (1994), Integrated simulation of buildings and evaporatibe cooling systems, Building and Environment, 2(29) p.197-206.

McCullough, E. A. Jones B. W. and Huck J. (1985), A comprehensive data base for estimating clothing insulation. *ASHRAE Trans* 91, 29-47.

McCullough, E. A. Jones, B. W. and Tamura, T. (1989), A data base for determining the evaporative resistance of clothing. *ASHRAE Trans.* 95, p316-328.

Mollier, R & Smith, S. (1954), Physical Tables. Ninth Revised Edition, (available from the Smithtonian Institute, Washington DC).

NEL (1964), National Enigineering Laboratory, Steam Tables (London HMSO).

NBS (1955), National Bureau od Standars. Tables of Thermal Properties of Gases, Circular 564, November).

NHMC (1989), National Health and Medical Council, Guidance on Control of Legionella, Australia.

Niu, J. & van der Kooi, J. (1997), Dynamic simulation of combination of evaporative cooling with cooled ceiling system for affice room cooling, Proc. Building Simulation'97, Fifth Int. Conf. Prage, Cseck republic, p407-412.

Olgyay, V. (1963), Design with climate, Princetown, Uni. Press, Princetown, NJ.

Osbaugh, D. & Moore, T. B. (1998), Applying two stage evaporative cooling, ASHRAE Journal, 30, July, p26-30.

Passive Downdraught Evaporative Cooling, (1999), Architectural Design Guide (Task ADS7), For the European Commission.

Peterson, J. L. & Hunn, B. D. (1983), Evaporative cooling potential for office buildings, Proc 2nd Int Congress Building Energy Management, American Mechanical Engineering Society, 1A p3.31-6.40.

Petrakis, M. Lycoudis, S. and Kassomenos, P. (1996), A software tool for the creation of typical meteorological year. Environmental Software 11(4), 221-227.

Pepper, D. (1985), The roots of modern environmentalism.

Picard, P. & Millet J. R. (1993), Evaporative cooling, France, CSTB.

Rholes, F. H. & Nevins, R. G. (1971), The nature of thermal comfort for sedentary man. *ASHRAE Trans* 77:1, 239-246.

Robinson, D. Cook, M. J. Lomas, K. J. and Bowman, N. T. (1999), The design and control of buildings with passive downdraught evaporative cooling. *Proceedings PLEA* (Brisbane) 99:1, 453-458.

Rodriguez, E. A. Alvarez, S. & Martin, R. (1991), Water drops as a natural cooling resource- Physical principles, Proc. PLEA Int. Conf. Seville, Spain, 24-27 Sept, pp 619-624.

Roodman, D. M. & Lenssen, N. (1995), A building revolution. How ecology and health concerns are transforming construction, Worldwatch paper 124, MArch 1995.

Santamouris, M. (1992), Energy conservation in Office, comertial, Hotel, Schools and Health Care Buildings, Final report to the Ministry for Energy Research, Greece.

Santamouris, M. (1997), PASCOOL Programme, Natural Cooling Techniques. Design Methodology and application to Southern Europe. University of Athens, Physics Department chapter 6.

Stimson, H. F. (1969), Some precise measurements of the vapour pressure of water in the range from 25°C to 100°C Res. NBS 73A.

Williamson, T. J. (1985), The Assessment of Thermal Comfort in Dwellings with Evaporative Cooling. CLIMA 2000, Vol. 4, pp 127 -132.

Winslow, C.E.A. Herrington, L.P. Gagge, A.P. (1937), Physiological reactions to environmental temperature. Am. Journal of Phisiology, 120:1-22.

Appendix

A *Published work*

A.1 Published work

A copy of the two published papers is attached.

DYNAMIC THERMAL SENSATION IN PDEC BUILDINGS

D Fiala, K J Lomas, D Martínez, and M J Cook
Institute of Energy and Sustainable Development
De Montfort University, Leicester LE1 9BH, UK
fax: +44 (0)116 257 7449
email: dfiala@dmu.ac.uk
Internet: http://www.iesd.dmu.ac.uk

ABSTRACT In buildings with passive downdraught evaporative cooling (PDEC), occupants are subjected to environmental conditions which might be characterised by elevated relative humidities, increased air speeds, and time-varying internal conditions. A new physiological model which describes the human thermophysical system, and the active control exercised on it, has been produced. The model predicts skin and core temperatures, sweat rates, etc. on different parts of a seated, standing or exercising human. It also predicts the overall level of thermal discomfort for any set of time-varying, asymmetric environmental conditions, i.e. the dynamic thermal sensation, DTS. This paper illustrates the application of the model to the design of PDEC spaces.

1 Introduction

Passive Downdraught Evaporative Cooling (PDEC) is a means of ventilating and cooling buildings in hot, dry climates. The anatomy of a typical PDEC building comprises a ventilation tower open to the exterior air at its top and connected via openings to occupied spaces lower down. At the top of the tower a very fine mist of water particles is injected into the air using micronisers. These droplets evaporate in the warm, dry (ambient) air inside the tower raising its relative humidity (RH) and decreasing its dry bulb temperature (T_{db}). For example, during a typical southern European summer day at a state of T_{db}=35°C and RH=30%, it is possible to evaporate enough water to provide ventilation air at about a T_{db} of 27°C and an RH of 65%. This denser-than-ambient air then falls through the tower driving a ventilation flow of cool air through the occupied spaces (Robinson et al, 1999).

It is possible for small temperature depressions to induce high airflows. It is therefore likely that the micronisers will only be used to maintain a reservoir of cool air, which is then drawn off through variable sized openings into the occupied zones. During PDEC operation, the objective of the building management system is to provide air to the occupied spaces at an RH and T_{db} state that will provide thermal comfort.

2 Mathematical model of human thermoregulation and thermal comfort

In daily life people are exposed to a variety of thermal situations. Transient conditions, for instance, frequently occur due to time-varying environmental temperatures, air speeds, activity levels [met] and clothing levels [clo], etc. Exposures to thermally uncomfortable environments are associated with adjustments of the human thermoregulatory system and temporal changes in the bodily heat content can occur.

One reason for modelling the human thermal system was to extend comfort predictions to a wide range of different boundary conditions including arbitrary transients. Thereby, the model is based on the principle that any temporal change in a boundary condition (e.g. air temperature) will elicit the same change in comfort sensation as any other boundary condition (e.g. radiant temperature, or even arbitrary combinations of boundary conditions) which provoke the same dynamic change in the body's thermal state (Fiala, 1998).

The mathematical model of the thermoregulation consists of two interacting systems: the controlling active system; and the controlled passive system. The multi-segmental passive system model simulates the physical human body and the heat transfer phenomena occurring in it and at its surface. The active system predicts the regulatory responses of the central nervous system. The comfort model predicts the overall dynamic thermal sensation (DTS), and the associated percentage of dissatisfied people (Fanger, 1973).

2.1 Passive system

In the model, the human body is idealised as cylindrical and spherical elements: head, face, neck, shoulders, arms, hands, thorax, abdomen, legs, and feet - each comprising annular tissue layers of appropriate thermo-physical and -physiological properties: brain, lung, bone, muscle, viscera, fat, and two layers of skin with distinct physiological functions. Tissue layers were subdivided further into spatial sectors to allow for the treatment of lateral environmental asymmetries. The model represents an average person with respect to body weight (73.5 kg), body fat content (14%wt), Dubois-area (1.9 m^2), basal metabolic rate (87 W), basal evaporation from the skin (18 W), and basal cardiac output (4.9 l/min).

Within the human body, metabolic heat is produced which is distributed over body regions by blood circulation and heat conduction from warmer to colder tissue locations. The dynamic heat transfer model considers also the effect of heat storage in living tissues. At the body surface, heat is exchanged by free and forced convection with ambient air, long and short wave radiation, and evaporation of moisture from the skin. Part of the bodily heat is lost by respiration. Local heat and mass balances were established for each individual body element sector to account for inhomogeneities with respect to environmental conditions, clothing insulation, and regulatory responses.

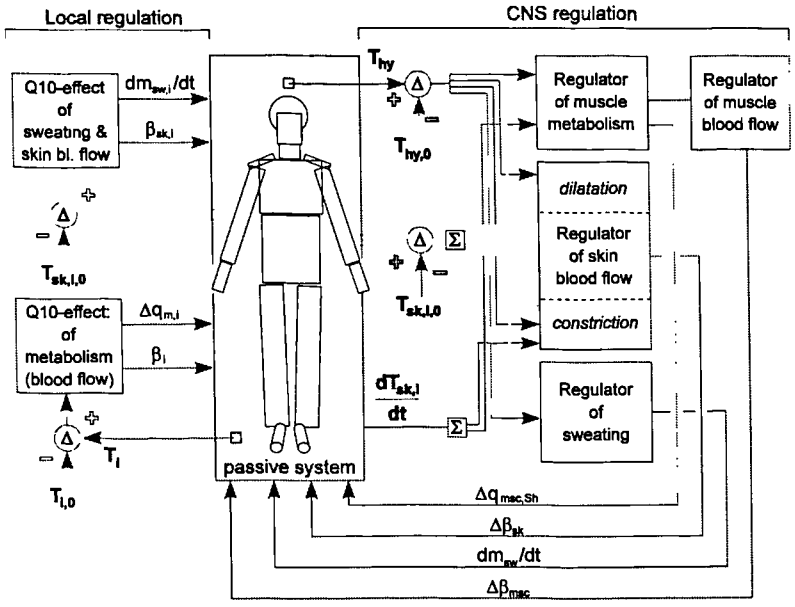

Fig. 1 Block diagram of the active system model. The central nervous system (CNS) thermoregulation accounts for overall changes in muscle metabolism $q_{msc,Sh}$ via shivering (and the corresponding changes in muscle blood flow, β_{msc}), skin blood flow β_{sk} via vasodilatation and vasoconstriction, and skin moisture extraction dm_{sw}/dt via sweating. The model uses temperatures of the skin (T_{sk}) and of the head core (hypothalamus, T_{hy}) as well as the rate of change of skin temperature ($dT_{sk,i}/dt$) as input signals into the regulatory centre. Local skin temperatures $T_{sk,i}$ are substracted (Δ) from the corresponding setpoint values $T_{sk,i,0}$ and form error signals $\Delta T_{sk,i}$. Positive difference represent 'warm' cutaneous recepetors, negative differences represent 'cold' thermoreceptors. The setpoint temperatures arise from the thermoneutral state of the (nude) body when reclining in an environment of 30°C where no thermoregulation occurs. The local afferent signals $T_{sk,i}$ are summed (Σ) to the integral signal from the skin ($\Delta T_{sk,m}$) which governs, together with ΔT_{hy}, the four responses of the CNS-regulation. The local autonomic regulation utilizes local skin and tissue temperatures, $T_{sk,i}$ and T_i, to modify local sweat rates, $dm_{sw,i}/dt$, skin blood flows, $\beta_{sk,i}$, tissue metabolic rates, $q_{m,i}$, and tissue blood flows, β_i.

2.2 Active system

Man maintains his internal temperature at a fairly constant value using four essential responses. Peripheral vasomotion, via suppression (vasoconstriction) and elevation (vasodilatation) of the skin blood flow, is activated to regulate internal temperature in moderate environments. In cold conditions, vasoconstriction is accompanied by shivering. In warm and hot conditions, vasodilatation is accompanied by sweating. A non-linear active system model has

been developed by means of regression analysis using physiological data for steady state and transient exposures obtained from numerous published experiments (Fiala, 1998). A block diagram of the active system model is shown in **Fig. 1.**

2.3 Thermal comfort

Extensive comfort experiments covering a wide range of static and transient environmental temperatures, relative humidities, and activity levels were used to derive the following equation for the overall thermal sensation by means of regression analysis (Fiala, 1998):

$$DTS = 3\ tanh\left[a_1 \Delta T_{sk,m} + g + \frac{0.11\left(\frac{dT_{sk,m}}{dt}\right)^{-} + 0.14\left(\frac{dT_{sk,m}}{dt}\right)^{+}_{max} \exp\left(-0.68\Delta t\right)}{1+g}\right]$$

$$g = 6.66 \exp\left(\frac{-0.57}{\Delta T_{hy}}\right) \exp\left(\frac{-7.63}{5-\Delta T_{sk,m}}\right)$$

where: *DTS* is the *Dynamic Thermal Sensation* according to the 7-point-ASHRAE scale running from -3 to +3; a_1=0.30K^{-1} and 1.03K^{-1} for $\Delta T_{sk,m}$<0K and $\Delta T_{sk,m}$>0K, respectively; $\Delta T_{sk,m}$ and ΔT_{hy} are given in **Fig. 1**; $(dT_{sk,m}/dt)^{-}$ [K/h] is the negative rate of change of $T_{sk,m}$, $(dT_{sk,m}/dt)^{+}_{max}$ [K/h] is the peak positive rate of change of $T_{sk,m}$; and Δt [h] is the elapsed time since the occurrence of $(dT_{sk,m}/dt)^{+}_{max}$.

2.4 Model validation

Simulation results were compared and verified using measured data for about 300 different exposures obtained from independent physiological and comfort experiments (Fiala, 1998). The model was shown to reliably predict skin and body core temperatures, regulatory responses, and the overall thermal sensation for a range of environmental temperatures between 5 and 50°C, and exercise intensities between 0.8 and 10 met.

3 Evaluation of PDEC-controlled indoor climates

3.1 Predicted human responses to PDEC conditions

Human thermal, regulatory and perceptual responses were predicted for the range of temperatures expected to occur in PDEC buildings during the summer, i.e. temperatures T_{db} between 20 and 30°C for two RH levels of 30 and 80%. The simulation series was performed as individual two-hour-exposures to steady values of T_{db} in successive steps of 0.5K.

When the PDEC system switches on, the mean radiant temperature T_r is likely to be close to T_{db} (Bowman et al, 1999). Therefore, in these simulations T_r was set to T_{db}. Furthermore, it was assumed that occupants were exposed to an air speed of 0.3 m/s and that there was no solar radiation, which is typical in the core of a PDEC building.

The analysis was performed for occupants engaged in typical office activities (activity level of *act*=1.2 met: ASHRAE, 1992) and wearing light summer clothing. This comprised briefs, socks, light long trousers, short sleeve shirt and street shoes which were applied to individual elements of the passive system. The summer dress was extended by modelling the chair which covers parts of the posterior leg segments. The *overall* resistance for this extended clothing ensemble was calculated by the model and resulted in a value of I_{cl}=0.55clo.

Predicted components of the environmental heat exchange and the physiological and comfort reactions are plotted in **Fig. 2.** The dry heat loss of the human body, Qc+Qr, falls with increasing T_{db} from 130 W at 20°C to about 50 W at 30°C. In 'warm' conditions this reduction is accomplished by increased skin moisture generation (dmsk/dt) due to regulatory sweating which evaporates (Esk) keeping the resultant, total heat loss from the skin surface (Qsk) almost constant at about 110W over a temperature range of 26°C<T_{db}<30°C. The mean skin temperature (Tsk,m) varies in line with Qsk. The skin heat loss, and the dry and latent heat loss by respiration (Qrsp), is generally capable of balancing the heat gain by metabolism as-

sociated with the activity performed. As a result, the body core temperature (Tcore) is maintained within 0.2K over the whole range of T_{db}. In these thermal processes, changes in the skin blood flow (SBF), accompanied by the coupling effect of sweating in the warmth, are the governing thermoregulatory mechanisms. The dynamic thermal sensation (DTS) varies between 'cool' and 'warm', i.e. $-2<DTS\lesssim+1.5$. Thermal neutrality, ($DTS\rightarrow\pm0$) appears to be associated with a narrow range of temperature between about $25°C<T_{db}<27°C$ for subjects at *act*=1.2 met exposed to va=0.3 m/s, and clad in summer clothing. The percentage of dissatisfied varies according to changes in the thermal sensation (Fanger, 1973).

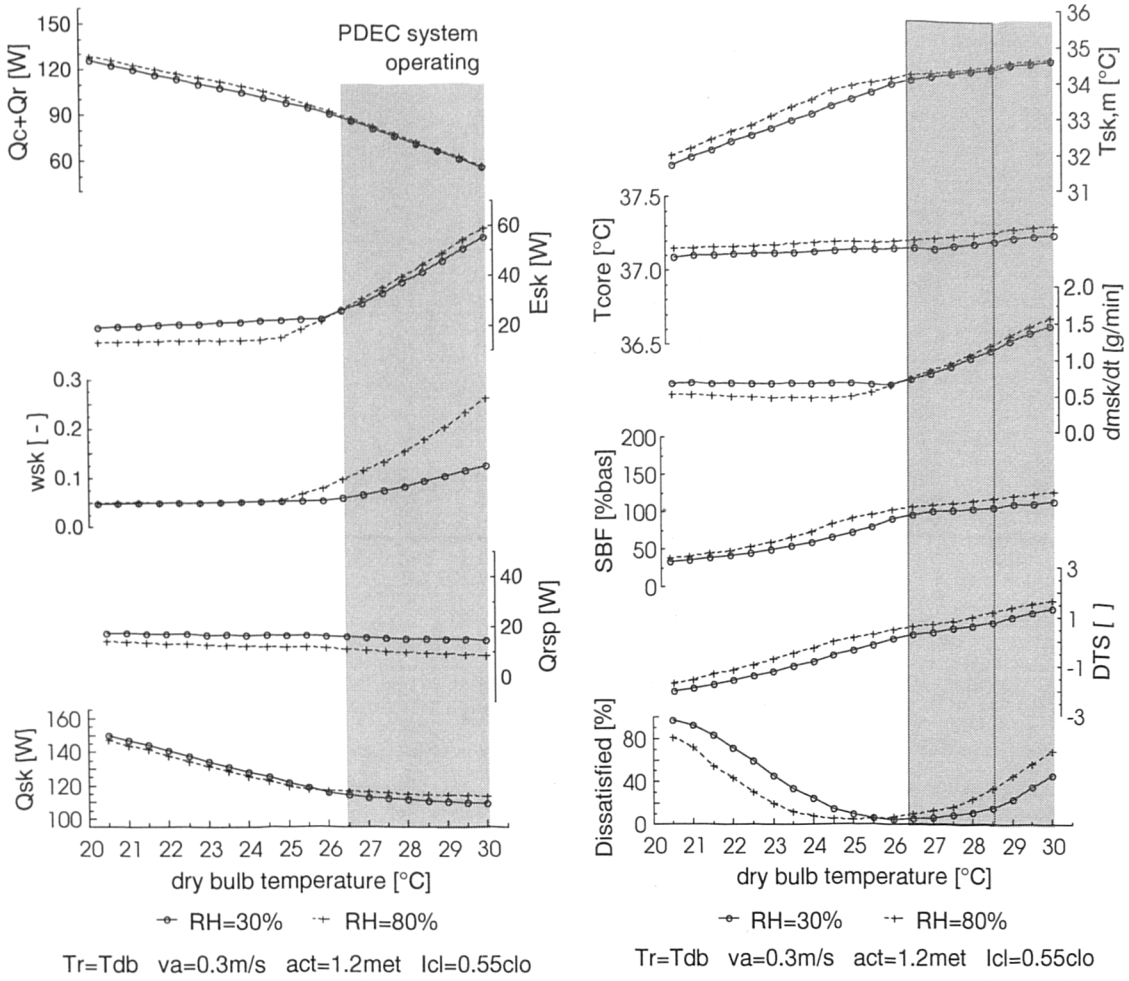

Fig. 2 Components of the environmental heat exchange (left) and physiological and comfort responses (right) predicted for occupants exposed to indoor climates of PDEC buildings.

There is generally no pronounced effect of relative humidity, when RH≤80%, on human responses for these moderate dry bulb temperatures. Nevertheless, the wetted skin area ratio (wsk) (ASHRAE, 1993) rises more rapidly with T_{db} in the warmth when the evaporation of sweat is inhibited by the elevated water vapour pressure of air at high RH. It is apparent, however, that even RH's of 80% are acceptable for occupants within a range of about $24°C<T_{db}<28°C$ (the impact of RH within the comfort zone is described in more detail in the next section). Outside this range of environmental temperatures, a rise in RH from 30% to 80% causes an average change in percentage of people dissatisfied of about 20%.

3.2 Comfort envelopes for PDEC-buildings

A series of simulations were carried out to establish zones of thermal comfort for PDEC buildings. In these buildings, ceiling fans might be used to enhance air movements, so air speeds from 0.3 to 0.8 m/s were studied. This assumes that occupants will accept increased air velocities in *warm* conditions without suffering from draught (see Fanger et al, 1988). This was shown experimentally for air speeds of up to 1.5 m/s (for references see e.g. Givoni, 1992) even though there was no subjective control of air speed.

PDEC is a method of ventilating and cooling buildings in hot, dry climates. These climates are naturally accompanied by increased solar radiation which influences, as a radiant heat gain factor, the sensation of thermal comfort, so it was considered in the analysis.

In **Fig. 3**, comfort envelopes are plotted onto the psychrometric chart for air speeds of 0.3m/s and 0.8m/s. The impact of diffuse solar radiation at 25W/m² is also included. The remaining boundary conditions applied to the simulations are noted in section 3.1. Here, successive steps in RH of 5% between 10%<RH<90% were used. The assessment of comfort envelopes is based on a 10%-dissatisfaction-criterion (ASHRAE, 1992).

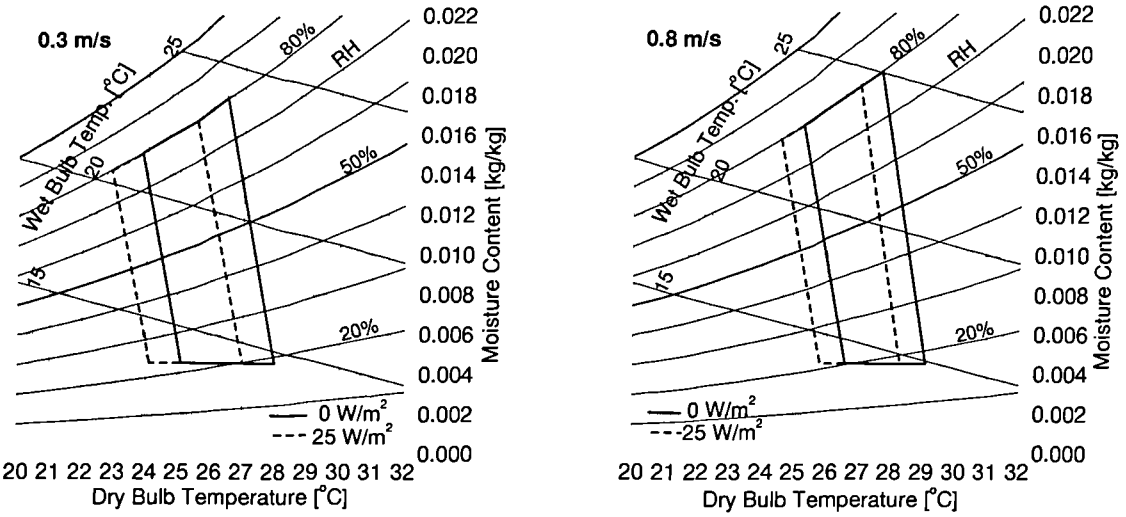

Fig. 3 Comfort envelopes for air velocities of 0.3m/s (left) and 0.8m/s (right). In both diagrams the shift of the comfort zone due to diffuse solar radiation of 25 W/m² is also indicated.

The comfort zone was found to range between 24°C<T_{db}<27°C for va=0.3 m/s, and 25.5°C< T_{db}<28°C for va=0.8 m/s, both at RH=70% (which might be appropriate under PDEC operation). Diffuse solar radiation of only 25 W/m² was sufficient to cause a shift of these comfort envelopes toward lower dry bulb temperatures by 1K. The variation of RH with temperature was found to be linear at a rate of 2.5×10^{-2} K/RH% which agrees well with published data obtained from comprehensive experiments (Rohles et al, 1971).

The above results refer to exposures in which environmental parameters are held constant. However, in PDEC buildings environmental parameters may vary with time and affect the comfort of the occupants. This is demonstrated by a comparison of exposures to T_{db}=26°C with: (i) a constant air speed of va=0.5 m/s; and (ii) an air speed which fluctuates periodically around its average of 0.5 m/s by ±0.4 m/s at a rate of 9×10^{-2} m/s per min (**Fig. 4**).

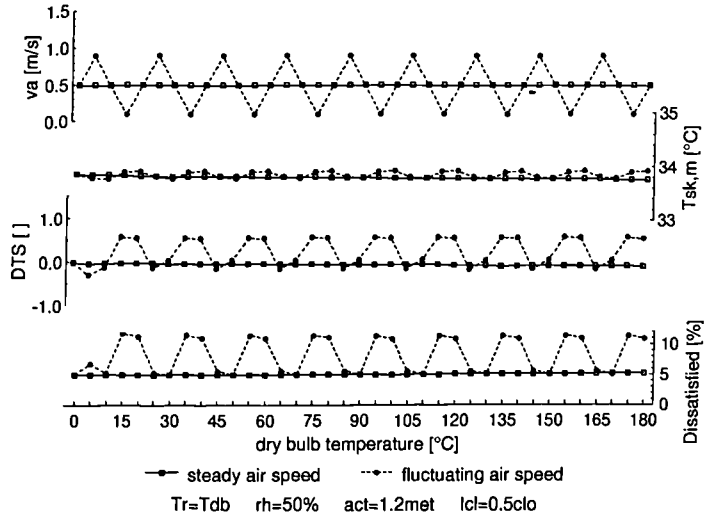

Fig. 4 Physiological and comfort responses to dry bulb temperature of 26°C predicted for steady and fluctuating air speed.

In addition to local thermal discomfort which might be invoked (Fanger et al, 1988) fluctuating airflow appears to have an additional, specifically dynamic, effect on overall human thermal comfort which is associated with temporal changes of the mean skin temperature. Even though $T_{sk,m}$ is held within comfortable limits 33.8-34.0°C, positive and negative rates of change of the mean skin temperature ($dT_{sk,m}/dt$) caused by fluctuating air speed, elicit, as punitive signals into the human thermal system, discomfort and reduce the acceptability of environmental conditions as shown in **Fig. 4.**

4 Summary and concluding remarks

The method of low energy cooling of indoor spaces by PDEC generates indoor environments which are characterised by relative humidities of up to 80% at temperatures of about 27°C. Air velocities could be up to about 0.8 m/s, and close to windows there will be short wave solar gains. It is also anticipated that there will be temporal changes in the environmental parameters, in particular, air speeds.

A dynamic model of human thermoregulation and thermal comfort has been developed to predict physiological and comfort responses for a wide range of steady-states and arbitrary transients including conditions where adjustments of the human thermoregulatory system and dynamic changes in the bodily heat content occur. The model has been used to study responses of occupants exposed to PDEC controlled environments.

PDEC seems to produce moderate conditions whereby thermal stress reactions of occupants are avoided. There was also no profound effect of relative humidities up to 80% on the thermal state of the human body, comfort perception and thermal acceptability for temperatures (T_{db}) in the range of 24°C to 28°C. Outside this temperature range a rise in RH from 30 to 80% caused an average change of people dissatisfied of about 20%.

Zones of comfort were assessed for PDEC buildings which extend the traditional comfort envelopes (ASHRAE, 1992) to environments with increased air velocities in which there is a moderate solar gain. Diffuse solar radiation of only 25 W/m² caused a shift of the comfort envelope toward lower dry bulb temperatures by about 1°C. Rapid changes in air speed were found to have a detrimental effect on the overall comfort perception and the associated percentage of dissatisfied building occupants. Thus, rapidly changing air speeds should be avoided.

5 References

ASHRAE Handbook (1993) Fundamentals. American Society of Heating, Refrigerating and Air-Conditioning Engineers, chap. 8: Physiological Principles and Thermal Comfort, Atlanta.

ASHRAE Standard 55 (1992). Thermal environmental conditions for human occupancy. American Society of Heating, Refrigerating and Air-Conditioning Engineers, Atlanta.

Bowman N.T. et al. (1999) Application of passive downdraught evaporative cooling to non-domestic buildings. Final Report to EU Commission under Joule contract JOR3CT950078, 16-pp.

Fanger P.O. (1973) Thermal Comfort - Analysis and Applications in Environmental Engineering. McGraw-Hill, New York - London - Sidney - Toronto, pp. 28-30.

Fanger P.O., A.K. Melikov, H. Hanzawa, and J. Ring (1988) Air turbulence and sensation of draught. Energy and Buildings 12, pp. 21-39.

Fiala D. (1998) Dynamic simulation of human heat transfer and thermal comfort. PhD Thesis, De Montfort University Leicester, UK.

Givoni B. (1992) Comfort, climate analysis and building design guidelines. Energy and Builidngs 18, pp. 11-23.

Robinson D., M.J. Cook, K.J. Lomas, and N.T. Bowman (1999) The design and control of buildings with passive downdraught evaporative cooling. Proceedings of The 16th International Conference on Passive and Low Energy Architecture (PLEA'99), Queensland, Australia.

Rohles F.H., and R.G. Nevins (1971) The nature of thermal comfort for sedentary man. ASHRAE Trans. 77:1, pp. 239-246.

ROOMVENT 2000 7th INTERNATIONAL CONFERENCE

READING, UK 9-12 July 2000

PAPER 196

PREDICTED COMFORT ENVELOPES FOR OFFICE BUILDINGS WITH PASSIVE DOWNDRAUGHT EVAPORATIVE COOLING

D. Martinez , D. Fiala, M. J. Cook and K. J. Lomas

Institute of Energy and Sustainable Development, Scraptoft Campus, De Montfort University, Scraptoft, Leicester, LE7 9SU, UK

ABSTRACT

Passive Downdraught Evaporative Cooling is a low energy strategy for maintaining thermal comfort in buildings located in hot dry climates. The thermal performance of such buildings can be predicted using simulation models. The temperatures predicted can be compared with standard comfort envelopes which show the range of temperatures and relative humidities within which occupants will be thermally comfortable. Standard comfort envelopes do not account for the adaptive opportunity which is important in free-floating buildings. Such adaptation could include changing clothing levels, local air speed (e.g. by using of fans) and solar radiation (by use of shading devices). A state of the art dynamic heat transfer and thermal comfort simulation model has been used to develop new comfort envelopes based on the adaptive behaviour theory. These "adaptive comfort envelopes" indicate occupants will be satisfied over a wider range of environmental conditions. The work indicates that increasing local air speeds is particularly effective in improving comfort when occupants are exposed to solar radiation.

KEYWORDS

Comfort envelope, adaptive behaviour, thermal sensation, PDEC, low energy buildings

INTRODUCTION

In hot dry climates, thermal mass together with night venting may keep office building comfortable without resorting to air conditioning. Active or passive evaporative cooling can assist by further reducing air temperatures. In a recent European project, Robinson et al. (1999), Bowman et al. (2000) Passive Downdraught Evaporative Cooling (PDEC) was explored as a novel way of cooling office buildings. PDEC combines the benefits of a natural ventilation strategy with a passive cooling technique. This is achieved by injecting microscopic drops of water into a hot, dry airstream using micronisers. Due to the evaporation of the water drops by the air, the relative humidity and density of the air increase and the dry-bulb temperature is reduced. Thus PDEC environments are characterised by high relative humidities, increased air speeds and, due to the free running nature of passively controlled buildings, a range of temperature fluctuations. In order to determine whether a building with PDEC will be comfortable, four issues need to be considered: (i) the local climate conditions, (ii) the thermal behaviour of the building and system, (iii) the resultant effect on indoor climate conditions, and (iv) the behaviour of the occupants.

In a former study, Fiala et. al. (1999), comfort envelopes were developed. However, these envelopes did not incorporate the adaptive behaviour of occupants in response to changes in environmental conditions that occur e.g. free-running buildings, Humphreys (1978). In this paper the comfort envelopes have been extended to account for adaptive changes in clothing, local air speed and diffuse solar radiation. The work is based on analysis of occupants' physiological and comfort responses, as predicted for combinations of relative humidity, dry-bulb temperature and solar radiation. This analysis was undertaken using a detailed dynamic model of human heat transfer and thermal comfort developed by Fiala (1998). The model predicts skin and core temperatures, sweat rates and the overall Dynamic Thermal Sensation (DTS) for any type of time-varying, asymmetric environmental conditions, clothing and activity levels. DTS is predicted according to the 7-point-ASHRAE scale running from –3 (cold) to +3 (hot) with 0 representing thermal neutrality.

EXISTING COMFORT ENVELOPES FOR PDEC BUILDINGS

In the former study, Fiala et. al. (1999), the effect of PDEC-environments on predicted thermal, regulatory and perceptual responses of occupants was studied for summer conditions in office buildings. The subjects were assumed to be wearing typical summer clothing (0.55 clo) and be engaged in typical office activities (1.2 met). Based on that analysis, zones of comfort were defined for PDEC office buildings, considering two levels of air velocity (0.3 m/s and 0.8m/s). Also included was the impact of varying solar radiation on subjects' responses (0 W/m^2 and 25 W/m^2). The analysis showed that even relative humidities of 80% were predicted to be thermally acceptable for the PDEC-building occupants. Thus the comfort envelopes (dashed lines in Figure 2), established a new upper limit for relative humidity, which allows PDEC systems to operate above the traditional 60% limit, ASHRAE 55 (1992). However, the envelopes did not indicate the tolerance to higher temperatures which adaptive behaviour might enable.

STRATEGY FOR EXTENDING THE EXISTING COMFORT ENVELOPES

In order to quantify the impact of thermal adaptation in the existing comfort envelopes, the three most influential adaptive reactions were investigated: (i) changes in clothing insulation (ii) variation in local air speed (using fans) and (iii) the manipulation the amount of diffuse solar radiation (using blinds). In principle, these adaptive actions should enable occupants to feel comfortable in a wider range of environmental conditions.

Different summer clothing ensembles for men and women, and for different ranges of operative temperatures, (light ensemble for 20°C $<T_o<$25°C and a very-light ensemble for 25°C $<T_o<$32°C) have been considered. These differences considered both the use of lighter garment fabrics and the selection of different garment items i.e. long/short sleeve, lighter shoes, dress instead of a skirt and blouse, etc. An occidental office dress-code, however, has been respected in all cases. The clothing was modelled in detail by applying individual items of an ensemble to the corresponding body elements of the multi-segmental model. The Fiala model was fed with the measured overall values of clothing insulation I_{cl} [clo], clothing area factor f_{cl} [-], and the evaporative resistance of the fabric R_{Ef} [m^{2}kPa/W], obtained from literature, McCullough et al. (1985) and (1989).

The effect of the chair was also considered. It was modelled as an item, which covers a part of the posterior leg segments. Back contact was considered but without any force. The individual clothing ensembles considered in the study were as follows:

- *Women-light outfit*: bra, pantyhose, panties, skirt knee length, blouse long sleeve, open lady shoes and chair, I_{cl}=0.63clo, i_{cl} =0.34 [1],
- *Women-very-light outfit*: bra, panties, long thin dress with short sleeves, open ladies shoes and chair, I_{cl}=0.42clo, i_{cl} =0.28,
- *Men-light outfit*: briefs, socks, light long trousers, long sleeve shirt, street shoes and chair, I_{cl}=0.69clo, i_{cl} =0.30,
- *Men-very-light outfit*: briefs, socks, light long trousers, short sleeve shirt, sandals and chair, I_{cl}=0.43clo, i_{cl} =0.29,

Air movement affects the evaporation of moisture from the skin and thus of the comfort perception. If occupants start feeling warmer, thermal neutrality might be maintained by switching on ceiling, desktop or floor mounted fans thus increasing the local air speed. When a PDEC system is operating (warm conditions assumed), the air speed in occupied spaces would be about 0.3 m/s whereas the air speed value may reach about 1.5 m/s when fans are switched on. For "cool" conditions, (PDEC system off), the typical air speed may be just 0.2 m/s which ensures the required ventilation levels.

The "adaptive opportunity" also includes the interaction of occupants with the building fabrics. One of the most influential effects is the use of shading devices. Operating shading devices such as blinds or louvres, will modify the diffuse solar radiation on the body. Likewise, occupants, if permitted to by the management regime may move to work in more shaded areas (away from windows). Direct solar radiation should be eliminated by the building's own external shading devices. The investigated values were zero and 50 W/m^2 (the latter ensures high natural lighting level).

PROCESS OF DEVELOPMENT

The upper and lower limits of the new extended comfort envelopes were obtained from the former study, Fiala (1999) i.e. relative humidity of 80% and a moisture content of 0.0045 kg/kg, respectively. The right and left boundaries of the new comfort zones, were defined by the operative temperature (T_o) and relative humidity at which 10% of the people will be thermally uncomfortable, ASHRAE 55,(1992)

A file matrix with combinations of operative temperatures and relative humidities was created, along with the different clothing ensembles, air speeds and solar radiation values. These were used as the input data to the simulation program. Indoor operative temperatures were investigated for a range between 20°C<T_o<32°C in successive steps of ΔT_o = 0.5K. The relative humidities investigated ranged between 10%<RH<90% in steps of 2%. The diffuse solar intensities subjected to analysis were 0 W/m^2 and 50 W/m^2. The considered air velocities were 0.2 m/s (for the range 20°C<T_o<25°C) and 0.3, 0.6, 0.9, 1.2 and 1.5 m/s (for the range 25°C<T_o<32°C). Clothing levels were studied separately for men and women, resulting in values of I_{cl}=0.69clo/0.43clo (for men light/very light ensembles) and I_{cl}=0.63clo/0.42clo (for women light/very light ensembles). A metabolic rate of 1.2 met, was used as the office activity level, ISO 7730 (1994). So, a total of nearly 26,000 different combinations of boundary conditions emerged.

The simulation series were conducted as individual two-hour-exposures to the steady environmental and personal conditions. Simulation results for which 8%<PPD<12% applies were filtered out for further data processing. This data is plotted onto a psychrometric chart, Figures 1a and 1b. The required comfort limits of PPD=10% were obtained by linear regression through the filtered data for both the right-hand side boundary, i.e. DTS>0, and the left-hand side boundary, i.e. DTS<0. A good general correlation (0.85<|r|<0.93) for the linear regressions was achieved.

---

[1] The overall values of I_{cl} and i_{cl}, were calculated by the Fiala model from the individual clothing items.

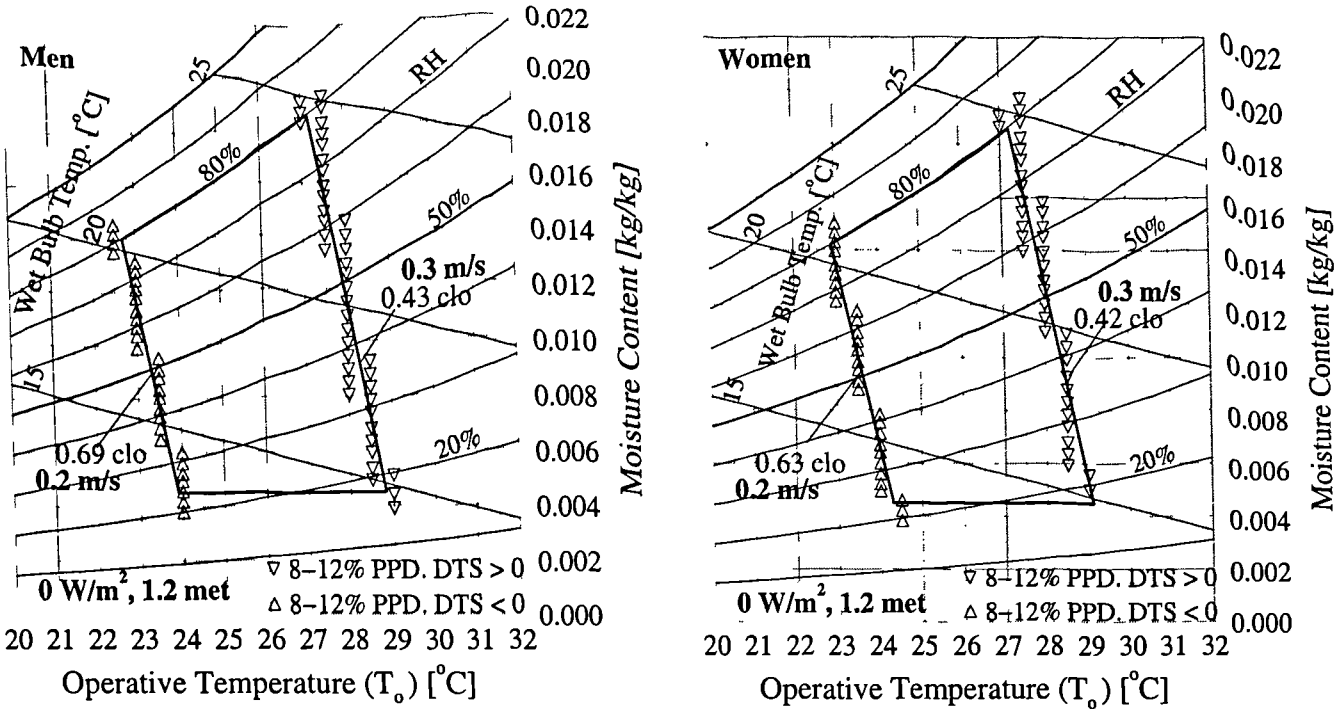

Figure 1a and 1b: Predicted comfort envelopes for men (left) and women (right) at 0 W/m^2 solar radiation and the corresponding minimum air speeds.

The analysis of the comfort boundaries indicated that there were no significance differences between men and women (see Figure 1a and 1b). For this reason only the results obtained for one sex (men) were considered in the further analysis.

RESULTS

In absence of solar radiation, Figure 2, the new comfort envelope ranges between 22.7°C (80 % RH) and 28.8°C (~17%RH) for minimum air speeds. This represents an enlargement of the tolerated temperature range of about 2 K when compared with the former comfort envelope (dashed lines in Figure 2) which was developed using a constant clothing level. A further extension of about 0.7 K towards warmer temperatures was achieved by increasing the air speed from 0.3 m/s to 0.6 m/s. However, further increases in the air speed produced successively less increase in tolerance to high temperatures. This is because at increased air velocities, the air temperature perceived as comfortable approaches the temperature of the body surface.

To counter the thermal effect of diffuse solar radiation of intensity 50W/m^2, the operative temperature must be reduced. This is indicated by the shift of the comfort envelope by about 2 K, indicating a strong effect of solar radiation on thermal comfort. It can be seen in Figure 3 that the effect of air speed on comfort is more pronounced when solar radiation enters the space than when it is excluded. This is because elevated air speeds are capable of removing more heat from the irradiated body surface. So, an increase of air speed from 0.3 m/s to 1.5 m/s extends the acceptable comfort conditions in the presence of solar radiation by 2.4 K, but only by 1.7 K in the absence of solar radiation. In both cases the variation of RH with temperature was found to be linear at a rate of about 2.5x10^{-2} K/RH% which agrees well with published data obtained from comprehensive experiments, Rohles et. al. (1971).

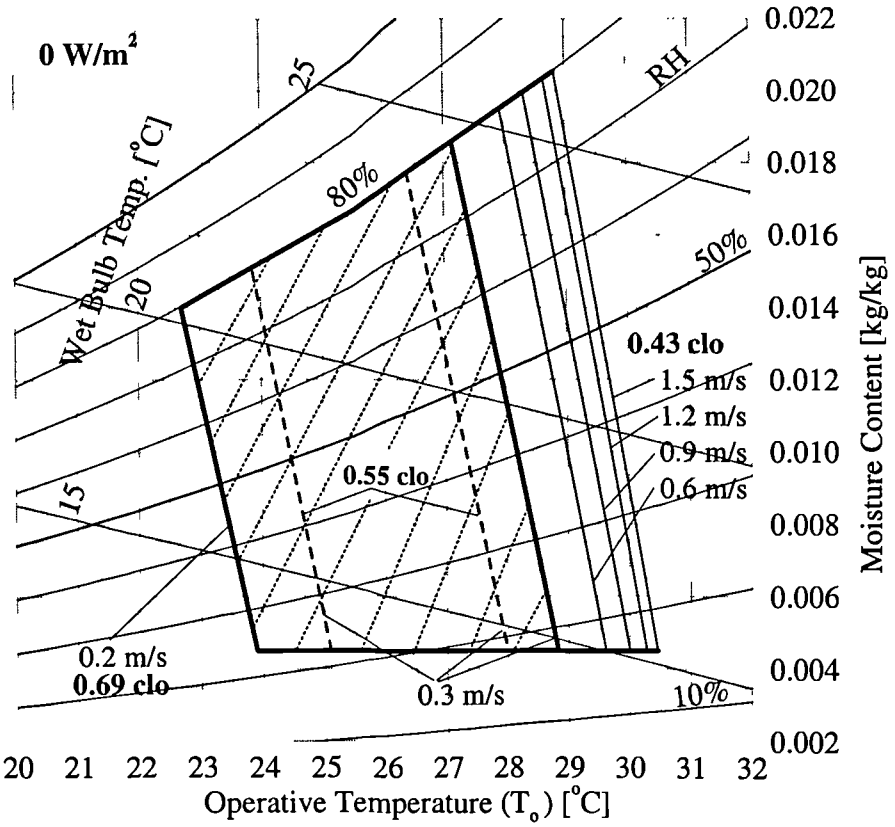

Figure 2: Predicted comfort envelopes for 0 W/m^2 of solar radiation and different air speeds. The former comfort envelope for 0.55clo and 0.3m/s is also included (dashed lines).

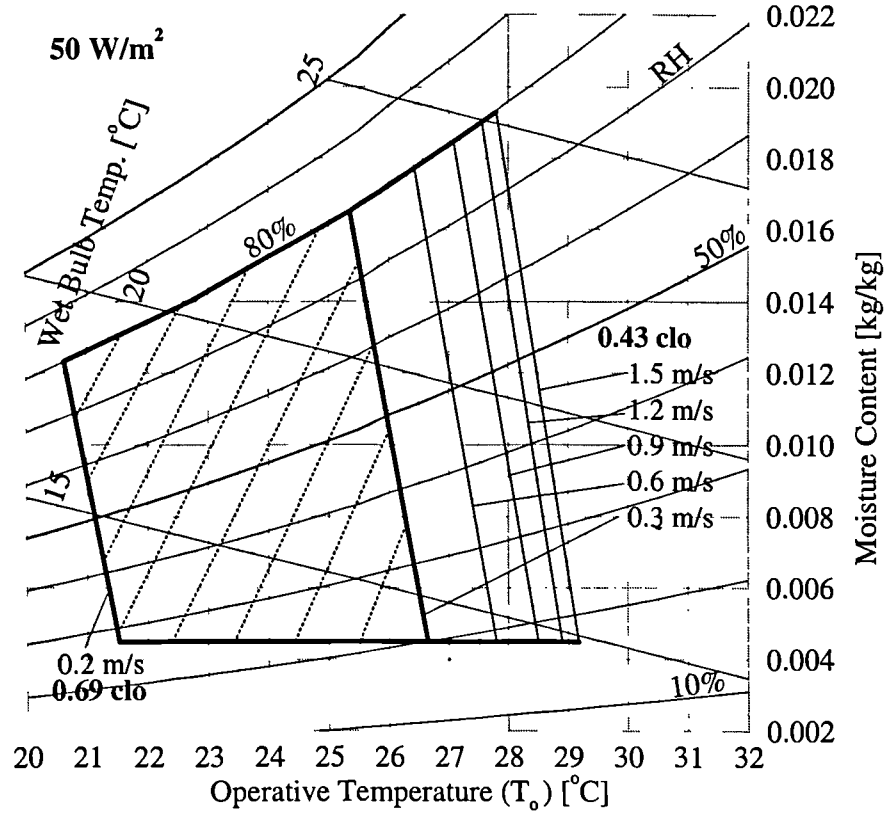

Figure 3: Predicted comfort envelopes for 50 W/m^2 of diffuse solar radiation and different air speeds.

CONCLUSIONS

In this study, extended comfort envelopes have been derived for hot summer conditions in office buildings. The adaptive behaviour of occupants has been investigated considering changes in the clothing level, air speed and solar radiation. As a results, the new comfort envelopes extend from 22.7°C (80 % RH) to 28.8°C (~17% RH) in absence of solar radiation. This is about 2 K wider than that obtained in the former study, Fiala et al. (1999). In the presence of diffuse solar radiation of 50 W/m^2 the comfort envelopes shift towards cooler air temperatures by about 2 K.

Increasing air speed leads to an acceptance of warmer conditions but this effect becomes less efficient as the air speed continues to rise. It was also found that increasing air speed is more effective in the presence of solar radiation.

These extended comfort envelopes were developed for PDEC buildings. However, they also may be used to examine summer comfort conditions in other types of office buildings in which thermal adaptation is possible.

REFERENCES

ASHRAE Standard 55 (1992). Thermal environmental conditions for human occupancy. ASHRAE, Atlanta, USA.

Bowman N. T., Eppel H., Lomas K. L., Robinson D. and Cook M. J. (2000). Passive Downdraught Evaporative Cooling – I: Review and precedents. *Building services Engineering Research and Technology* **(in press)**.

Fiala D. (1998). *Dynamic simulation of human heat transfer and thermal comfort. Ph.D. thesis*, De Montfort University, Leicester, UK.

Fiala D, K J Lomas, D Martinez, and M J Cook. (1999). Dynamic thermal sensation in PDEC buildings. *Proceedings PLEA* (Brisbane) **99:1**, 243-248.

Humphreys M. A. (1978). Outdoor temperatures and comfort indoors. *Building research and practice* **6**, 92-105.

ISO 7730 (1994). Moderate Thermal environments. Determination of the PMV and PPD Indices. International Organisation for Standardisation, Geneva.

McCullough E.A., Jones B. W. Huck J. (1985). A comprehensive data base for estimating clothing insulation. *ASHRAE Trans* **91**, 29-47.

McCullough E. A., Jones B. W. Tamura T. (1989). A data base for determining the evaporative resistance of clothing. *ASHRAE Trans* **95**, 316-328.

Rholes F. H. and Nevins R.G. (1971). The nature of thermal comfort for sedentary man. *ASHRAE Trans* **77:1**, 239-246.

Robinson D., M. J. Cook, K.J. Lomas, and N. T. Bowman (1999) The design and control of buildings with passive downdraught evaporative cooling. *Proceedings PLEA* (Brisbane) **99:1**, 453-458.